UNIVERSITY OF SOUTHAMPTON

FACULTY OF ENGINEERING, SCIENCE AND MATHEMATICS

National Oceanography Centre, Southampton

School of Ocean and Earth Science

The marine biogeochemistry of dissolved organic carbon and dissolved organic nutrients in the Atlantic Ocean

By

Xi Pan

Thesis for the degree of Doctor of Philosophy

June 2007

Graduate School of the

National Oceanography Centre, Southampton

This PhD dissertation by

Xi Pan

Has been produced under the supervision of the following persons:

Supervisors:

Prof. Eric P. Achterberg

Dr. Richard Sanders

Chair of Advisory Panel:

Dr. Duncan A. Purdie

Declaration of Authorship

I, Xi Pan, declare that the thesis entitled “The marine biogeochemistry of dissolved organic carbon and dissolved organic nitrogen and phosphorus” and the work presented in it are my own. I confirm that:

- this work was done wholly or mainly while in candidature for a research degree at this University;
- where any part of this thesis has previously been submitted for a degree or any other qualification at this University or any other institution, this has been clearly stated;
- where I have consulted the published work of others, this is always clearly attributed;
- where I have quoted from the work of others, the source is always given. With the exception of such quotations, this thesis is entirely my own work;
- I have acknowledged all main sources of help;
- where the thesis is based on work done by myself jointly with others, I have made clear exactly what was done by others and what I have contributed myself;

Signed: …….

Date: …….

UNIVERSITY OF SOUTHAMPTON

ABSTRACT

FACULTY OF ENGINEERING, SCIENCE AND MATHEMATICS

NATIONAL OCEANOGRAPHY CENTRE, SOUTHAMPTON

SCHOOL OF OCEAN AND EARTH SCIENCE

Doctor of Philosophy

THE BIOGEOCHEMISTRY OF DISSOLVED ORGANIC CARBON AND DISSOLVED ORGANIC NUTRIENTS IN THE ATLANTIC OCEAN

By Xi Pan

The marine biogeochemistry of dissolved organic carbon (DOC) has come under increased scrutiny because of its involvement in the global carbon cycle and consequently climate change. Dissolved organic nitrogen (DON) and phosphorus (DOP), which have historically been ignored because of their suggested "biological unavailability", have now received greater attention due to their importance in nutrient cycling, particularly in oligotrophic ecosystems. DOM, a byproduct of photosynthetic production, has important ecological significance as a substrate that supports heterotrophic bacterial growth, thereby causing oxygen consumption and regenerating inorganic nutrients. In the open ocean the net production of DOC is ultimately due to the decoupling of biological production and consumption processes. Concentrations of DOM in the surface oceans, therefore, are controlled by both physical and biological processes. This research investigates the biological factors that control the distributions of DOC, DON and DOP in surface waters, the importance of DOC degradation to oxygen consumption, the importance of DON and DOP degradation to remineralised dissolved inorganic nitrogen (DIN) and dissolved inorganic phosphorus (DIP), and the C:N:P stoichiometry of DOM pool in the Atlantic Ocean. Samples were collected on

Atlantic Meridional Transects (AMT) cruise 16 and 17, which crossed the southern temperate region, the southern subtropical gyre, the equatorial region, the northern subtropical gyre, and the northern temperate region. This work described here was performed as a component of the AMT programme.

Concentrations of DOC and TDN were determined using a high-temperature catalytic combustion technique, and TDP concentrations were determined using a UV oxidation method. Concentrations of DON and DOP were estimated as the difference between the independent measurements of TDN and TDP. The results showed that the highest DOM concentrations were found in surface (0-30 m) waters, ranging from 70-80 μM DOC, 4.8-6.5 μM DON and 0.2-0.3 μM DOP, and decreased with increasing water depth to 45-55 μM DOC, 2.6-4.0 μM DON and 0.04-0.05 μM DOP at 300 m. The lowest DOM concentrations were observed in the deep (>1000 m) ocean, averaging 44 μM DOC, 2.3 μM DON and 0.02 μM DOP. In the upper 300 m, the concentrations of semilabile (and labile) DOC decreased by 45-95% from the surface values. DON and DOP were the dominant components of the total dissolved nutrient pools in the upper 50 m, accounting for up to 99% and 80% of the TDN and TDP pools, respectively. In the upper 300 m, semilabile (and labile) DON and DOP decreased by 50-65% and 90-95% from the surface values, respectively.

The decoupled correlations between DOC/DON/DOP and chlorophyll-a and rates of carbon fixation suggested that phytoplankton biomass and rates of primary production were not the important controls of the cumulative DOC, DON and DOP. Zooplankton grazing was hypothesised to be an important factor in regulating the distributions of DOC, DON and DOP in surface waters. Poor correlations between DOC/DON/DOP and DIN/DIP suggested that inorganic nutrients were not the significant controls in DOC, DON and DOP distributions. N and P were probably retained mainly in the organic pool in the surface waters due to a hypothesised insufficient functioning of the

microbial degradation. If the vertical migration of zooplankton was significant in bringing new nutrients into the surface waters, strong correlations between dissolved organic and inorganic nutrients should not be anticipated. *Prochlorococcus* spp. abundance was statistically linked with the concentrations of DOC, DON and DOP. The significant correlations may reflect the ability of *Prochlorococcus* to assimilate the labile forms of dissolved organic nutrients (including DOC), which may be quantitatively significant in surface waters of the Atlantic Ocean.

The C:N, N:P and C:P stoichiometry of the bulk DOM pool deviated from the Redfield ratio of 6:1, 16:1 and 106:1, ranging from 12-18, 20-100 and 300-1400, respectively, in the upper 300 m, suggesting that the cumulative DOM was rich in C relative to N and P, and N relative to P compared to the Redfield trajectories. The offsets of the C:N:P stoichiometry relatively to the Redfield ratio were due to nutrient limitations that imposed on prokaryotic and eukaryotic microbial populations. The C:N:P stoichiometry of the bulk DOM pool showed an increased trend, with C:N = 12-16, N:P = 20-25, and C:P = 300-350 in the upper 30 m, C:N = 12-18, N:P = 50-100, and C:P = 700-1400 at 300 m, and C:N = 17-24, N:P = 79-132; C:P = 1791-2442 at 1000 m. The differences in the C:N:P stoichiometry of the bulk DOM pool between the upper and deep waters suggested preferential remineralisation of P relative to C and N, and N relative to C. A greater remineralisation length scale for DOC relative to DON and DOP produced a long-term, steady flux of C from the surface to the deep ocean. Therefore, CO_2 fixed in the upper ocean during planktonic photosynthesis was continuously “pumped” into the ocean interior, and stored in the deep ocean up to thousands of years. The C:N, N:P and C:P stoichiometry of the semilabile (and labile) DOM pool generally agreed with the Redfield ratio (C:N = 6; N:P = 16; C:P = 106) in the upper 30 m. At 100 m C:N ratio was 5-12, C:P ratio was 20-30, and C:P ratio was 100-150. At 300 m, C:N ratio was 5-12, N:P ratio was 25-100, and C:P ratio was 150-500. The findings suggested that in the upper 300 m, there was no preferential

remineralisation between the semilabile (and labile) DOC and DON, however, the semilabile (and labile) DOP seemed to be preferentially remineralised relative to the semilabile (and labile) DOC and DON.

In the upper thermocline (*i.e.* above 300 m), DOC degradation was important with respect to oxygen consumption, contributing to as much as 25% of the apparent oxygen utilization (AOU). The remaining of 75% was attributable to POC decomposition. However, the AOU contributable to DOC showed a function of latitude, with 15-55% found in the central subtropical Atlantic gyres and 15-25% in the equatorial region. The most likely explanation for the variation of DOC relative to POC degradation with respect to AOU was the regional variability in the export of POC, which was suggested to be highest in the high nutrient regions of the equator and at the poleward margins of the subtropical gyres. As a result, DOC formed an important contribution to AOU in oligotrophic regions, while POC was the dominant control of AOU in upwelling regions.

Some freshly-produced fractions of DON and DOP with turnover times of months to years were capable of escaping rapid microbial degradation in surface waters and became entrained into deep waters via diffusive mixing. Subsequent microbial degradation of these DON and DOP took place in the thermocline, regenerating inorganic nutrients. Statistically significant correlations were observed between the DON-to-DIN and DOP-to-DIP relationships. Calculations of the fluxes of dissolved organic nutrients relative to inorganic nutrients suggested that in the upper thermocline (*i.e.* above 300 m), the downward fluxes of DON and DOP contributed to a total of 4% and 5% of the upward fluxes of DIN and DIP, respectively, into the euphotic zone. The remaining of 95% of the upward dissolved inorganic nutrients fell out of the euphotic zone as particles in order to prevent nutrient accumulation and to maintain nutrient integrity of the pelagic ecosystem.

Acknowledgements

I would like to thank my supervisors Prof. Eric Achterberg and Dr. Richard Sanders for their tremendous support throughout this research. I would like to express my gratitude to Prof. Robert Upstill-Goddard and Dr. Mark Moore for their great advice on this work. Thank you to my parents Dr. Bei Zheng and Mr. Hongda Pan for the continuous encouragement and motivation. I also acknowledge the financial support by the University of Southampton.

Table of Contents

List of Figures

List of Tables

1. Introduction

1.1. The role of DOM in biogeochemical cycles

Marine dissolved organic matter (DOM), operationally defined as organic matter that can pass a filter of 0.2-0.7 μm (Carlson 2002), forms one of the largest exchangeable carbon (C) reservoirs on earth (Hansell and Carlson 2002). The amount of C in the oceanic DOM pool is estimated to be ~700 x 10^{15} g C (Hansell and Carlson 1998), similar to that of the atmospheric CO_2 pool (~750 x 10^{15} g C; Siegenthaler and Sarmiento 1993). Net oceanic uptake of CO_2 is approximately 2.1 x 10^{15} g C per year (Quay *et al.* 1992; Takahashi *et al.* 1999), which is a small percentage of the oceanic dissolved organic carbon (DOC) pool (Carlson 2002). Thus, a net oxidation of merely 1% of the oceanic DOC will be sufficient to generate a CO_2 flux which is greater than that produced annually by fossil fuel combustion (Hedges 2002), and strongly impact the balance between oceanic and atmospheric CO_2 (Carlson 2002). Both the size and potential dynamics of the oceanic DOC pool have brought it within the focus of global C cycle research (Williams and Druffel 1988; Toggweiler 1989; Hedges 1992; Hedges 2002).

Another growing interest in marine DOM over the past 3 decades has been the recognition of its important ecological significance, that is, DOM serves as a food substrate in support of heterotrophic bacterial growth (Williams 1970; Pomeroy 1974; Williams 1981a; Azam *et al.* 1983; Ducklow and Carlson 1992; Carlson 2002). A portion of the photosynthetically fixed C is lost from the planktonic food web as DOC (discussed in section 1.3). The bioavailable fraction is taken up by heterotrophic bacterioplankton and then passed to protists and zooplankton (Azam and Fuhrman 1984), or remineralised back into its inorganic constituents (Ducklow *et al.* 1986) via the microbial loop (Azam *et al.* 1983). As an important process in biogeochemical cycling of the bioactive elements (*e.g.,* nitrogen and phosphorus) within the ocean (Pomeroy 1974; Azam and Hodson 1977), remineralisation of dissolved organic

nitrogen (DON) and phosphorus (DOP) regenerates dissolved inorganic nutrients (Smith *et al.* 1986; Vidal *et al.* 1999). These inorganic nutrients are regenerated from dissolved organic nutrients, together with those derived from particulate organic matter (POM), and are responsible for maintaining the nutrient integrity of the pelagic ecosystem (Christian *et al.* 1997).

1.2. Composition of the DOM pool

The DOM pool is composed of a great variety of organic molecules ranging from simple monomers to complex polyers that are exchanged biogeochemically within the marine environment (Benner 2002). Due to the analytical difficulties, *i.e.,* a lack of suitable chromatographic methods with sufficient sensitivity for the characterisation of DOM (Benner 2002), there is a paucity of data on the molecular composition of DOM. Hence, the chemical composition of marine DOM is still poorly described. However, in a broad sense, oceanic DOM is considered to contain hydrocarbons, carbohydrates, lipids, fatty acids, amino acids, nucleic acids and humics (Benner 2002).

1.3. Sources of DOM

The euphotic zone is the principal site of organic matter production in the open ocean (Carlson 2002). Production of DOM is most evident in ocean regions that experience annual phytoplankton blooms, such as Arctic and Antarctic waters. The magnitude and quality of DOM produced during these bloom events varies considerably and is controlled by a number of biological, chemical and physical parameters (Carlson 2002). While DOM production is ultimately constrained by the magnitude of primary production (*e.g.* Carlson 2002), there are several main mechanisms responsible for DOM production, including extracellular release by phytoplankton (*e.g.* Collos *et al.* 1992), grazing-induced DOM production (Daly and Smith 1993), release via cell lysis (both viral and bacterial) (*e.g.* Proctor and Fuhrman), solubilisation of particles (*e.g.* Smith *et al.* 1992), bacterial release (e.g. Smith *et al.* 1992), terrestrial inputs (*e.g.*

Cauwet 2002) and atmospheric deposition (*e.g.* Seitinger and Kroeze 1998), and release from sediments (*e.g.* Burdige and Zheng 1998).

1.3.1. Extracellular phytoplankton production

Extracellular release of DOM by phytoplankton is an important source of DOM (Collos *et al.* 1992). Substantial observations have been undertaken in order to investigate DOM release by phytoplankton assemblages. One of the most widely used approaches is a measure of percent extracellular release (PER), which determines the ^{14}C (Carlson 2002), ^{15}N (Bronk 2002) and ^{32}P (or ^{33}P) (Karl and Björkman 2002) accumulation in DOC, DON and DOP relative to the particle form through the primary production process. Recently reported PER values have shown that the proportion of photosynthetically fixed ^{14}C that is released as DOC via this phytoplankton exudation ranges from 3-32% of total carbon fixation (Baines and Pace 1991; Lee and Henrichs 1993; Vernet *et al.* 1998; Carlson 2002), and that the proportion of photosynthetically fixed ^{15}N that is released as DON ranges from 4-100% (Slawyk and Raimbault 1995; Slawy *et al.* 1998; Raimbault *et al.* 1999; Bronk *et al.* 1998; Diaz and Raimbault 2000; Hasegaw *et al.* 2000; Ward and Bronk 2001; Bronk 2002). Clearly, phytoplankton release can be an important source of DOM release. The reported large range probably results from temporal and spatial variabilities (Carlson 2002; Bronk 2002). Unfortunately, investigation on PER of DOP lags far behind similar research on DOC and DON. Hudson and Taylor (1996) have developed a technique to measure the release of DOP from size-fractionated plankton communities, however, the technique is only suitable for evaluating the release rates from the combined processes of phytoplankton exudation, zooplankton excretion, sloppy feeding and cell lysis (Karl and Björkman 2002). Insight into DOP release relative to total gross ^{32}P (or ^{33}P) uptake therefore still remains elusive.

1.3.2. Grazing-induced DOM production

Zooplankton grazing is another important mechanism that is responsible for the control of phytoplankton populations in the oceans (Daly and Smith 1993), and this process is considered to be the principal pathway of DOM from phytoplankton to bacteria (Jumars *et al.* 1989). Phytoplankton grazing by zooplankton via sloppy feeding will result in breakage of phytoplankton cells, releasing DOC (Strom *et al.* 1997; Steinberg *et al.* 2000), DON (Miller and Glibert 1998; Conover and Hustavson 1999; Puddu *et al.* 2000) and DOP (Puddu *et al.* 2000; Björkman *et al.* 2000) into the water column. Carlson (2002) reviewed the published percent of DOM released by macro- and microzooplankton, and the reported values ranged from 0.2-10% of total body C, 1-14% of total body N, and ~28% of total P released. Some studies have shown evidence that microzooplankton tend to ingest whole cells, leading to a minor release of DOM during feeding (*e.g.,* Strom *et al.* 1997), and that macrozooplankton tend to break down phytoplankton cells during feeding, resulting in significant amounts of DOM released (*e.g.,* Urban-Rich 1999). These literature data suggest that macro-, micro- and mesozooplankton (Thibault *et al.* 1999) grazers can potentially play an active role in transforming particulate carbon back to the dissolved phase via the feeding process, and egestion and excretion (Carlson 2002).

1.3.3. DOM production via cell lysis

Viral infection can be responsible for 10-50% of bacterial mortality (Proctor and Fuhrman 1990; Fuhrman 1992; Steward *et al.* 1996; Fuhrman 1999). This process has also been linked to the decline of primary production and mortality of eukaryotic cells in the water column (Suttle *et al.* 1990; Bratbak *et al.* 1992; Gobler *et al.* 1997). Suttle (1994) estimated that approximately 3% of global primary production is lost due to viral lysis. Through lytic infection, viruses attached to the host cell produce numerous progeny viruses. The progeny then burst the host cell, releasing viruses, proteins, nucleic acids, monomers, oligomers, polymers, and cell fragments (Fuhrman 1999).

Although the potential importance of viral lysis on prokaryotic and eukaryotic phytoplankton assemblages in the water column has been widely acknowledged (Gobler *et al.* 1997; Fuhrman 1999), there are extremely limited quantitative assessments of this phenomenon (Gobler *et al.* 1997). Bacteria can also be important producers of DOM (Imai *et al.* 1993), evidenced by the observations of Berman *et al.* (1999) in Lake Kinneret, Israel and in the Charente Estuary, France. However, this bacterial-induced cell lysis has received little attention as a potential mechanism of DOM production (Carlson 2002). Work is required to quantify this process to determine if the production of DOM from viral and bacterial lysis is an important mechanism.

1.3.4. Solubilisation of particles

The sinking particles (including fecal materials, zooplankton excretions and detrital substances; Carlson 2002; Bronk 2002) are continuously subject to dissolution, desorption and solublisation because of the presence of a large variety of the ectoenzymes secreted from marine eukaryotes and prokaryotes. The sinking particles are colonised by bacteria (Smith *et al.* 1992). Due to their inability to directly utilise POM, these attached bacteria secrete a large variety of enzymes forming a hydrolytic, enzymatic reactor (Smith *et al.* 1992) to dissolve these particles and release DOM (Azam and Cho 1987; Cho and Azam 1988; Karner and Herndl 1992; Smith *et al.* 1992, 1995). However, the absence of knowledge of particle hydrolysis in marine systems has hampered our understanding of organic matter released as DOM due to solubilisation of particles.

1.3.5. Bacterial release

Recent studies (Smith *et al.* 1992; Carlsson and Granéli 1993; Carlsson *et al.* 1993; Tanoue *et al.* 1995; McCarthy *et al.* 1998; Jørgensen *et al.* 1999; Berman *et al.* 1999) have indicated that heterotrophic bacterioplankton can also be a source of DOM. These

studies have shown that DOM compounds that have chemical characteristics of bacterial origin are distributed ubiquitously in the oceanic basins. To be able to hydrolyse the sinking particles and high molecular weight DOM, bacterioplankton directly release a large variety of hydrolytic enzymes (Bronk 2002; Carlson 2002). However, there is lack of quantitative evaluation of DOM production associated with this bacterial release.

1.3.6. Terrestrial inputs and atmospheric deposition

River water is rich in DOM (ranging from 83 to 2000 μM C; Libes 1992) originated from terrestrial run-off, sewage, industrial effluents, and agricultural and urban run-off. On a global scale, the riverine DOM discharge into the ocean is approximately 0.25-0.38 Gt C (1 Gt = 10^{15} g) yr^{-1} (Dafner and Wangersky 2002a; Cauwet 2002).

Atmospheric inputs of DOM are important for both freshwater and the marine environment (Seitinger and Kroeze 1998; Boyer *et al.* 2002; Berman and Bronk 2003). Atmospheric inputs include dry (*i.e.,* aerosols) and wet precipitation (*i.e.,* rainwater). Aerosols are a suspension of solid and liquid materials in a gaseous medium (Chester 1990). They originate from vegetation, soils, forest burning and industrial activities, and can be transported over several thousand kilometres (Blank *et al.* 1985). This long-range transport can be a significant organic matter input to the open oceans. Global rainwater DOM inputs (0.43±0.15 Gt C yr^{-1}; Willey *et al.* 2000) also have an important role in the DOM flux from land to ocean. Recent studies have shown that on a global scale oceans receive ~0.09 Gt C yr^{-1} from rainwater (Willey *et al.* 2000).

1.3.7. Release from sediment

DOM can be released into the water column from sediments during resuspension and diffusion of porewater DOM (Burdige and Zheng 1998), and diagenetic processes (Burdige 2002). It has been reported that DOM concentrations in pore waters of

surface sediments are higher than those in the overlying water column (Burdige and Homstead 1994; Bauer and Druffel 1998), especially in estuarine and coastal environments (Burdige 2002; Dafner and Wangersky 2002a, b). Burdige and Homstead (1994) suggested that diffusion of porewater DOM into overlying waters may occur as a result of resuspension events caused by bioturbation from macrofauna and/or episodic winter storms. Burdige *et al.* (1992) made a lower-limit estimate of the globally integrated benthic DOC flux from marine sediments (0.1-0.9 x 10^{14} g C), which is comparable in magnitude to riverine inputs. Clearly, sediments play an important role in the storage of DOM (Dafner and Wangersky 2002b). But the processes involved in the production and consumption of DOM in sediments are not well understood.

1.4. Sinks for DOM

Despite a high variability of 30-8,543 mg C m^{-2} day^{-1} (285-fold range) in depth integrated primary production in the world's oceans (Behrenfeld and Falkowski 1997), DOM concentrations are maintained in a remarkably narrow range of 40-80 μM C (2-fold range) in the upper 1000 m of the open ocean (Hansell 2002). Given that DOM production can be a significant fraction of the total primary production, this striking offset between the range in primary production rates and DOC concentrations indicates that several biotic and abiotic DOM removal processes are at work (Carlson 2002), including heterotrophic bacterial uptake (*e.g.* Williams 2000), direct phytoplankton assimilation (*e.g.* Palenik and Morel 1990 a, b), photochemical decomposition (*e.g.* Mopper *et al.* 1991), and sorption onto sinking particles (*e.g.* Keil and Kirchman 1994). The magnitude of these removal processes is not well understood (Carlson 2002).

1.4.1. Heterotrophic bacterial uptake

Heterotrophic bacterioplankton are recognised as the dominant consumers of DOM in the ocean (Azam and Hodson 1977). It has been estimated that total bacterial C

utilisation could amount to as much as 50% of plankton production (Williams 2000; Søndergarrd *et al*. 2000; Becquevort *et al.* 2000). Low molecular weight (LMW) DOM (<1000 Da) compounds can be directly transported through bacterial cell membranes via permeases (Carlson 2002) and be converted into biomass. High molecular weight (HMW) DOM (>1000 Da) compounds must be hydrolysed to LMW DOM via hydrolytic enzymes (Hoppe 1991; Smith *et al.* 1992; Christian and Karl 1995) before they can pass across the cell membrane and be utilised by bacterioplankton (Amon and Benner 1994, 1996).

Bacterial uptake rates of DOM can be influenced by several factors. The main control is thought to be bacterial mortality caused by viral lysis (*e.g.,* Steward *et al.* 1996; Fuhrman 1999), protozoan grazing (*e.g.,* Christian 1995; Rønn *et al.* 2002), and nutrient limitation (*e.g.,* Pomeroy *et al.* 1995; Thingstad *et al.* 1998). Predatory control by bacterivorous flagellate grazing and viral lysis are the main processes keeping bacterial abundance in check (Kirchman 2000). Some other studies have suggested that in the surface ocean, bacteria are in competition with phytoplankton for nutrients (*e.g.,* Pomeroy *et al.* 1995; Thingstad *et al.* 1998).

1.4.2. Direct phytoplankton assimilation

Many phytoplankton species have cell surface amine oxidases, which can assimilate amino groups from amino acids (*e.g.,* Palenik and Morel 1990 a, b; Bronk 2002). Recent culture experiments have shown that *Prochlorococcus* can take up ~25% of amino acids in surface waters of the southern subtropical Atlantic (Zubkov *et al.* 2004), ~5% in the southern Atlantic subtropical Front (Zubkov and Tarran 2005), and ~33% in the oligotrophic and mesotrophic Arabian Sea (Zubkov *et al.* 2003), and that ~3% of total bacterioplankton consumption of amino acids could be assigned to *Synechococcus* cells in the oligotrophic and mesotrophic Arabian Sea (Zubkov *et al.* 2003).

1.4.3. Photochemical decomposition

Photochemical processes in the marine environment are currently a topic of intense investigation because of the potentially detrimental effects of increasing UV radiation reaching the ocean surface as a result of the depletion of the ozone layer. Photodegradation of DOC is estimated to be at a rate of 20 nM hr^{-1} (Mopper *et al.* 1991). Moran and Zepp (1997) estimated the annual loss of DOC via photochemical degradation to be 12-16 Gt C yr^{-1} or 2-3% of the oceanic DOC pool per year. In the mixed layer of coastal and shelf waters, ~10% per year of the DOC pool can be directly converted photochemically to dissolved inorganic carbon (DIC) (Vodacek *et al.* 1997).

1.4.4. Sorption onto sinking particles

Sorption of DOM onto surfaces such as sinking particles has been proposed as an abiotic removal mechanism (Keil and Kirchman 1994; Druffel *et al.* 1996; Nagata and Kirchman 1996; Druffel *et al.* 1998). Druffel *et al.* (1996) hypothesised that abiotic sorption or incorporation of DOC onto POC may be a mechanism to explain suspended POC observed in the oceans interior. Unfortunately, the magnitude of the importance of this abiotic removal mechanism of DOC (also DON and DOP) is not well known due to insufficient data (Druffel *et al.* 1998).

1.5. Lability and vertical profile of DOM

The bulk DOM pool represents a continuum of biological lability, from refractory compounds turning over on time scales of centuries to millennia (Williams and Druffel 1987; Bauer *et al.* 1992; Hansell and Carlson 2001a), to very labile compounds turning over on time scales of minutes to days (Fuhrman and Ferguson 1986; Keil and Kirchman 1991; Carlson and Ducklow 1996; Cherrier *et al.* 1996; Rich *et al.* 1997; Carlson *et al.* 1999). The refractory pool forms the largest fraction of the bulk DOC (Benner *et al.* 1992; Amon and Benner 1996; Skoog and Benner 1997; Carlson 2002),

which can be best represented by the deep ocean DOC stocks (>1000 m), with an average age of 4000 to 6000 years old in the north Atlantic and the north Pacific Oceans, respectively (Williams and Druffel 1987; Bauer *et al.* 1992). Based on mass balance calculations and natural $\delta^{14}C$ estimates, Druffel *et al.* (1992) suggested that the refractory component of the bulk DOM pool is uniformly distributed throughout the water column and represents approximately 70% of surface DOC in thermally stratified systems (Carlson and Ducklow 1995, 1996; Cherrier *et al.* 1996; Carlson 2002).

Rapid turnover maintains the most biologically reactive organic components at nanomolar concentrations in the open ocean (Fuhrman and Ferguson 1986; Rich *et al.* 1997; Keil and Kirchman 1999; Skoog *et al.* 1999; Carlson 2002). Due to this rapid biological turnover, the labile pool can not be reliably quantified using the current analytical methods (Carlson 2002). Ogura (1972) used remineralisation experiments to identify a third type of DOC, one that was utilised by microbes but turned over on time scales of months to years. Other field studies have shown that a portion of the DOC pool present in excess of deep-water concentrations is resistant to rapid microbial degradation (*e.g.,* Kirchman *et al.* 1993; Carlson and Ducklow 1995). This fraction of DOC is termed the semilabile DOC pool (Kirchman *et al.* 1993; Carlson and Ducklow 1995).

A conceptual model is shown in Figure 1.1, which describes partitioning of the bulk DOC pool into fractions of varying lability, and this conceptual schematic clearly shows a vertical variability of DOC concentrations.

A summary of concentrations of DOC, DON and DOP in the surface and deep-ocean is presented in Table 1.1. In the open ocean the net production of DOM is attributable to the decoupling of biological production and consumption processes (Carlson 2002).

The highest concentrations are observed in surface (typically 0-100 m) waters, where the DOM pool is composed of fractions with different turnover times and lability (Anderson and Williams 1999; Carlson *et al.* 2000; Carlson 2002), typically ranging from 60-90 μM C, 3.5-7.5 μM N and 0.1-0.4 μM P (Tab. 1.1). Concentrations of the refractory DOM pool range from 35-45 μM C, 1.5-3.0 μM N and 0.02-0.15 μM P (Tab. 1.1). The semilabile component with a relatively long turnover time is degraded slowly from the upper ocean towards greater depths during mixing processes, with this degradation being responsible for generating the concentration gradients observed in the thermocline (Fig. 1.1).

DOM	Surface ocean	Deep ocean	Reference
DOC (μM)	60-90	35-45	1-6, 9-10
DON (μM)	3.5-7.5	1.5-3.0	6-11
DOP (μM)	0.1-0.4	0.02-0.15	6-12

Table 1.1 A summary of concentrations of DOC, DON and DOP in the surface (0-100 m) and deep (>1000 m) ocean. Reproduced from Benner (2002).

References. 1, Williams and Druffel (1987); 2, Carlson *et al.* (1994); 3, Sharp *et al.* (1995); 4, Peltzer and Hayward (1996); 5, Hansell and Carlson (1998); 6, Holm-Hansen *et al.* (1966); 7, Jackson and Wiliiams (1985); 8, Smith *et al.* (1986); 9, Walsh (1989); 10, Abell *et al.* (2000); 11, Loh and Bauer (2000); 12, Ridal and Moore (1992).

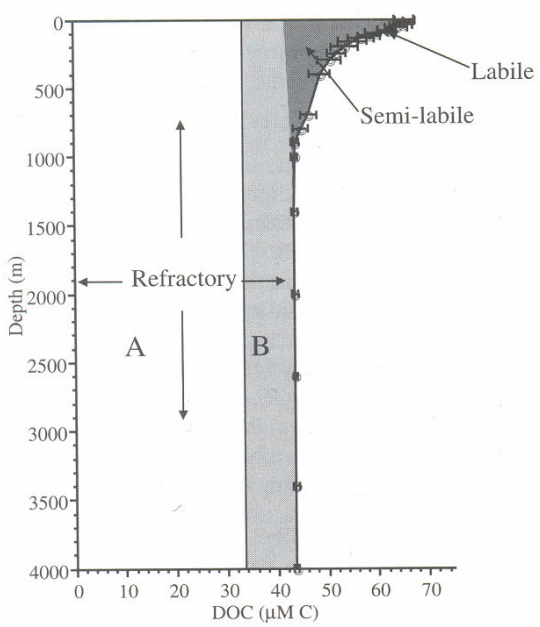

Figure 1.1 Conceptual model of the various pools of refractory, semilabile and labile DOC in the open ocean. Reproduced from Carlson (2002). The refractory pool is divided into two broad pools based on the deep ocean gradient observed by Hansell and Carlson (1998). The authors observed the lowest concentration of DOC (34 μM C) in the North Pacific and used this concentration to represent refractory DOC which turns over on time scales of greater than ocean mixing (A, white box). The deep DOC concentrations in excess of the 34 μM C represents the fraction of the biologically refractory pool that turns over on time scales of ocean mixing (B, light gray box).

1.6. DOM export

The export of DOM in the ocean is a consequence of its accumulation in the surface ocean, redistribution with the wind-driven circulation, and diffusive mixing via the thermohaline circulation (Hansell 2002). The wind-driven circulation refers to winter-time overturning (Hansell and Carlson 2001), Ekman transport (Mahaffey et al. 2004), and eddy activities (Williams and Follows, 1998). Thermohaline circulation refers to the vertical movement of water that takes place when its density increases by a significant change of temperature or salinity (Hansell 2002). After a long debate for

several decades, the export of DOC, DON and DOP has now been understood to play an important role in the biogeochemistry of the ocean carbon, nitrogen and phosphorus cycles via their contribution to the marine biological pump (Copin-Montégut and Avril 1993; Carlson *et al.* 1994; Ducklow *et al.* 1995). The export of DOM, together with POM, drives respiration in the ocean interior, causes oxygen consumption, and helps maintain the ocean's strong vertical gradient of inorganic carbon and inorganic nutrients (Hansell 2002).

1.7. Aim, objectives and hypotheses

The aim of this research is to investigate the biogeochemical cycling of DOC, DON and DOP in surface waters (0-300 m) of the tropical and subtropical Atlantic Ocean.

Based on Atlantic Meridional Transect (AMT) 16 and 17 cruises, the objectives of this research are

(1) To determine the concentrations of DOC, DON and DOP in the upper 300 m,
(2) To investigate the spatial and temporal variability of the concentrations of DOC, DON and DOP in the upper 300 m,
(3) To investigate the vertical variability of the concentrations of DOC, DON and DOP in the upper 300 m,
(4) To explore the biological controls over the distributions of DOC, DON and DOP in euphotic waters,
(5) To explore the C:N:P stoichiometry of DOM pool in the upper 300 m,
(6) To evaluate the importance of DOC degradation in the thermocline in terms of oxygen consumption, and
(7) To evaluate the importance of DON and DOP degradation in the thermocline in terms of regenerated DIN and DIP.

The hypotheses of this research are

(1) That biological processes are important in controlling the distributions of DOC, DON and DOP in surface waters,

(2) That DOC degradation forms an important contribution with respect to oxygen consumption,

(3) That there is regional variability of DOC degradation relative to oxygen utilisation, which is due to regional variability of the export of POC, and

(4) That downward diffusion of DON and DOP in the thermocline is important to the upward DIN and DIP supply to the microbial community in surface waters.

2. Methods

2.1. Sampling

This work on the biogeochemistry of DOM was performed as a component of the Atlantic Meridonal Transect (AMT) programme on cruises AMT-16 and -17 on the Royal Research Ship (RRS) *Discovery*. Cruise AMT-16 (D294) from Cape Town, South Africa to Falmouth, UK took place between 19 May and 29 June 2005; cruise AMT-17 (D299) from Govan, UK to Port Elizabeth, South Africa, was undertaken between 15 October and 28 November 2005. Cruise tracks and sampling locations for these cruises are shown in Figure 2.1. Summaries of the CTD number, station positions, sampling dates and sampled *Niskin* bottle numbers are given in Table 2.1 and 2.2. The two AMT cruise tracks are identical apart from some deviations between ~30^{o}N and ~40^{o}N. These deviations are not significant in terms of intercruise comparisons of DOC concentrations, which are to be discussed in Section 3.3.

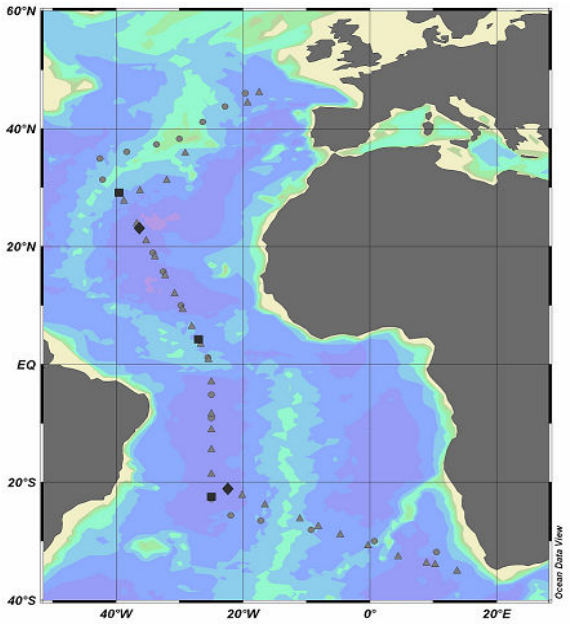

Figure 2.1. Cruise tracks and station positions for the Atlantic Meridional Transect (AMT) programme. Cruises are AMT-16 (circles; 19 May and 29 June 2005) and AMT-17 (triangles; 15 October and 28 November 2005). The whole water column (~5 km) was sampled at 3 stations (indicated by squares) on AMT-16 and 2 stations (indicated by diamonds) on AMT-17.

CTD No.	Sampling Date	Coordinates Longitude (°E)	Coordinates Latitude (°N)	Sampled *Niskin* bottle No.
3	24/05/05	10.50	-31.83	23, 19, 13, 11, 10, 9, 4, 3, 2, 1
6	26/05/05	0.70	-29.97	23, 19, 13, 11, 10, 9, 4, 2, 1
8	28/05/05	-9.25	-28.07	23, 19, 13, 11, 10, 9, 6, 4, 3, 2, 1
11	29/05/05	-13.44	-27.23	23, 19, 15, 13, 11, 10, 9, 6, 4, 3, 2
13	30/05/05	-17.23	-26.53	23, 19, 15, 13, 11, 10, 7, 5, 3, 2, 1
15	31/05/05	-21.93	-25.60	23, 19, 13, 11, 10, 9, 8, 5, 3, 2, 1
17	01/06/05	-25.01	-22.88	23, 19, 15, 13, 12, 11, 8, 5, 3, 2, 1
18	01/06/05	-25.00	-22.45	23, 21, 20, 18, 16, 15, 12, 11, 10, 9, 8, 7, 6, 4, 3, 2, 1
21	03/06/05	-25.00	-16.28	23, 19, 13, 11, 10, 9, 8, 5, 3, 2, 1
23	04/06/05	-25.00	-12.41	23, 19, 13, 11, 10, 9, 8, 5, 3, 2, 1
25	05/06/05	-25.00	-9.08	23, 19, 16, 13, 12, 11, 10, 7, 5, 4, 3, 2, 1
26	06/06/05	-25.00	-5.16	23, 19, 13, 11, 10, 9, 8, 5, 3, 2, 1
28	07/06/05	-24.99	-1.63	23, 19, 13, 11, 10, 9, 8, 5, 3, 2, 1
29	08/06/05	-25.56	1.17	23, 19, 15, 13, 11, 10, 7, 5, 4, 3, 2, 1
31	09/06/05	-27.03	4.27	23, 19, 13, 11, 10, 9, 8, 5, 3, 2, 1
32	09/06/05	-27.45	5.15	23, 21, 19, 18, 16, 15, 14, 11, 10, 9, 8, 7, 6, 5, 4, 3, 2, 1
35	11/06/05	-29.79	10.01	23, 19, 15, 13, 12, 11, 10, 7, 5, 4, 3, 2
38	13/06/05	-32.60	15.76	23, 19, 13, 11, 10, 9, 8, 5, 3, 2, 1
40	14/06/05	-34.21	18.96	23, 19, 15, 13, 12, 11, 10, 7, 6, 4, 3, 2, 1
42	15/06/05	-36.16	22.81	23, 19, 13, 11, 10, 9, 8, 5, 3, 2, 1
43	15/06/05	-36.46	23.36	23, 21, 20, 18, 16, 15, 14, 12, 11, 10, 9, 8, 7, 6, 5, 4, 3, 2, 1
46	17/06/05	-39.54	29.16	23, 20, 16, 14, 13, 12, 11, 8, 6, 5, 4, 3, 2
48	18/06/05	-42.14	31.38	23, 19, 13, 11, 9, 8, 5, 3, 2
50	19/06/05	-45.54	33.58	23, 19, 13, 11, 10, 9, 8, 5, 3, 2, 1
52	20/06/05	-42.56	34.90	23, 19, 15, 13, 12, 11, 9, 7, 5, 4, 3, 2, 1
54	21/06/05	-38.34	36.07	23, 19, 13, 11, 10, 9, 8, 5, 4, 2, 1
56	22/06/05	-33.66	37.35	23, 19, 13, 11, 10, 9, 8, 5, 3, 2, 1
58	23/06/05	-30.06	38.31	23, 19, 13, 11, 10, 9, 8, 5, 3, 2, 1
60	24/06/05	-26.38	41.14	23, 19, 15, 13, 12, 11, 10, 7, 5, 4, 3, 2, 1
62	25/06/05	-22.87	43.74	23, 19, 13, 11, 9, 8, 5, 3, 2, 1
64	26/06/05	-19.67	46.03	24, 22, 20, 18, 15, 14, 13, 10, 9, 6, 3

Table 2.1 Summaries of the CTD number, station positions, sampling dates and sampled *Niskin* bottle numbers on AMT-16.

CTD No.	Sampling Date	Coordinates Longitude (°E)	Coordinates Latitude (°N)	Sampled *Niskin* bottle No.
3	19/10/05	-17.44	46.23	24, 19, 17, 14, 11, 8, 7, 3, 2, 1
4	20/10/05	-19.32	44.45	24, 21, 18, 15, 12, 11, 9, 6, 5, 3, 2, 1
7	28/10/05	-29.13	35.92	24, 20, 17, 14, 11, 10, 8, 5, 4, 2, 1
9	30/10/05	-32.05	31.30	24, 21, 18, 15, 12, 11,10, 8, 5, 4, 2, 1
11	31/10/05	-36.27	29.53	24, 20, 17, 14, 11, 10, 8, 5, 4, 2, 1
13	01/11/05	-38.81	27.78	24, 21, 18, 15, 12, 11, 8, 5, 4, 2, 1
15	02/11/05	-36.78	23.96	24, 18, 17, 14, 11, 10, 9, 8, 5, 4, 2, 1
17	02/11/05	-36.35	23.14	24, 22, 20, 19, 18, 17, 16, 15, 14, 11, 12, 10, 9, 8, 7, 6, 5, 4, 3, 2, 1
18	03/11/05	-35.28	21.05	22, 19, 16, 13, 10, 9, 8, 7, 4, 3, 1
20	04/11/05	-33.92	18.38	24, 20, 17, 14, 11, 10, 9, 7, 4, 3, 1
22	05/11/05	-32.30	15.13	24, 21, 18, 15, 12, 11, 8, 5, 4, 2, 1
24	06/11/05	-30.80	12.07	24, 20, 17, 14, 11, 10, 9, 6, 5, 3, 2, 1
26	07/11/05	-29.52	9.43	22, 19, 16, 13, 10, 9, 8, 5, 4, 2, 1
29	08/11/05	-28.11	6.51	24, 18, 17, 14, 14, 11, 10, 8, 5, 4, 2, 1
32	09/11/05	-26.66	3.48	24, 18, 17, 14, 11, 10, 9, 6, 5, 4, 2, 1
34	10/11/05	-25.44	0.89	24, 21, 18, 15, 12, 11, 8, 5, 4, 2, 1
36	11/11/05	-25.00	-2.89	24, 20, 17, 14, 11, 9, 6, 5, 4, 2, 1
37	12/11/05	-25.00	-8.28	24, 22, 21, 20, 19, 18, 17, 16, 14, 12, 9, 7, 6, 5, 3, 1
38	13/11/05	-25.00	-11.00	24, 20, 15, 14, 11, 10, 9, 6, 5, 4, 3, 1
40	14/11/05	-25.00	-14.38	24, 21, 18, 15, 12, 11, 8, 5, 4, 3, 1
42	15/13/05	-25.00	-18.56	24, 21, 18, 15, 12, 11, 8, 5, 4, 3, 1
44	16/11/05	-22.44	-21.13	24, 20, 17, 14, 11, 10, 8, 5, 4, 3, 1
46	16/11/05	-22.38	-21.10	24, 23, 21, 20, 19, 18, 17, 16, 15, 13, 12, 11, 10, 9, 8, 7, 6, 5, 4, 3, 2, 1
47	17/11/05	-20.16	-22.16	24, 20, 17, 14, 11, 10, 8, 6, 5, 4, 3, 1
49	18/11/05	-16.53	-23.76	24, 21, 18, 15, 13, 12, 10, 6, 5, 4, 2
50	19/11/05	-11.05	-26.14	24, 22, 20, 18, 16, 15, 14, 10, 7, 5, 4, 3, 2, 1
51	20/11/05	-8.12	-27.40	24, 20, 17, 14, 11, 10, 9, 6, 5, 4, 2, 1
53	21/11/05	-4.69	-28.85	24, 21, 18, 15, 13, 12, 11, 6, 5, 4, 1
55	22/11/05	-0.30	-30.67	24, 20, 17, 15, 13, 12, 10, 7, 6, 5, 3, 1
57	23/11/05	4.44	-32.53	24, 21, 18, 15, 12, 11, 9, 7, 6, 56, 4, 1
59	24/11/05	8.92	-33.65	24, 21, 18, 15, 12, 11, 9, 6, 5, 3, 2, 1
61	24/11/05	10.30	-33.91	21, 17, 15, 13, 11, 9, 7, 6, 5, 4, 3, 2, 1
62	25/11/05	13.78	-34.98	23, 22, 20, 18, 16, 15, 14, 13, 12, 10, 9, 8, 7, 6, 5, 4, 3, 2, 1

Table 2.2 Summaries of the CTD number, station positions, sampling dates and sampled *Niskin* bottle numbers on AMT-17.

Seawater samples were obtained from the upper 300 m of the water column at 11 or 12 depths during daily predawn (0200-0400 h, local time) deployments of a rosette sampler equipped with 24 x 20 litre Niskin bottles and a Sea-Bird 9/11 CTD mounted with a Seabird 43 oxygen sensor. During AMT-16, the sampling depth increased to 1 km on every third day. At 3 stations (indicated by squares on Fig. 2.1), the whole water column was sampled during mid-day (1400-1600 h, local time) CTD casts, with 10 depths sampled in the upper 300 m and 12 from 300 to ~5000 m. During AMT-17 there were 2 stations (indicated by diamonds on Fig. 2.1) where the whole water column was sampled during mid-day (1500-1700 h, local time) CTD casts, with 10 depths sampled in the upper 300 m and 12 from 300 to ~5000 m.

2.2. Sample preservation

Water samples were siphoned from Niskin sampling bottles into 250 ml sample-rinsed high-density polyethylene (HDPE) bottles (Nalgene), following gas and inorganic nutrient sampling. To remove particulate matter, subsamples were filtered immediately through ashed (450^{o}C, 6 h) glass fibre filters (0.7 μM nominal pore size, 47mm diameter, Whatman GF/F, England) using an ashed (450^{o}C, 6 h) glass filtration unit (Nalgene, US) under gentle vacuum (<15 kPa) to avoid plankton cell breakage, which can lead to a considerable increase in DOM concentrations. The HDPE bottles and the glass filtration unit were soaked in HCl (10% v/v, Analar grade, VWR Ltd, England) between stations for more than 12 hours, followed by a thorough rinse using de-ionised water (Milli-Q, Millipore Inc, England).

Approximately 15 ml of the filtrates were collected in 20 ml precombusted (450^{o}C, 6 h) glass ampoules (Adelphi Ltd, England), followed by acidification to pH 2 using HCl (50% v/v, Analar grade, VWR Ltd, England). These ampoules were flame-sealed using a butane-propane mixture gas torch (VWR Ltd, England), and stored in a refrigerator (4^{o}C) for DOC and total dissolved nitrogen (TDN) analyses. The analyses were

performed in the shore-based laboratory at the National Oceanography Centre, Southampton (NOCS), UK, within 3 months of sample collection. Total dissolved phosphorus (TDP) concentrations were determined by shipboard measurements, with details to be described in Section 2.5.

2.3. Determination of DOC and TDN

Full methodological details are published in Pan *et al.* (2005). This section summarises key features of the method. The determination of DOC and total dissolved nitrogen (TDN) was based on a high-temperature catalytic (HTC) combustion technique using a commercial TOC-5000A total organic carbon analyser (Shimadzu Corp., Japan) (after Spyres *et al.* 2000) coupled with a Model NCD 705E nitrogen chemiluminescence detector (Antek Instrument Inc., US) (after Kähler *et al.* 1997). Ancillary instrumentation included an autosampler ASI 5000A (Shimadzu Corp., Japan), a low mass horizontal furnace LMS/100101/A (Stanton Redcroft Ltd., England) and a membrane vacuum pump (Werthelm, Germany). Carbon-free, high purity (99.995%) oxygen (BOC gas, England) was used as carrier gas. Figure 2.2 shows a schematic diagram of the coupled HTC TOC-NCD system. A full analytical measurement cycle consists of two steps (Pan *et al.* 2005).

Step 1 DOC analysis. Acidified samples were sparged using pure oxygen for a period of 8 minutes (100 ml min^{-1}) to remove inorganic carbon compounds and then injected (100 μl) into the furnace of the TOC instrument. The carrier gas pushed the sample into the combustion column, which was heated to 680^{o}C and filled with a catalyst (aluminum oxide coated by 0.5% of platinum; Shimadzu Corp., Japan). Organic carbon and nitrogen compounds, and ammonia in the sample were oxidised to CO_2, NO and H_2O, whereas nitrate and nitrite were reduced to NO as well as H_2O. The resulting gas stream was pushed in turn through an electronic dehumidifier to remove water vapour, and a Cu-based halogen scrubber for gas purification. Then the dried, purified gas

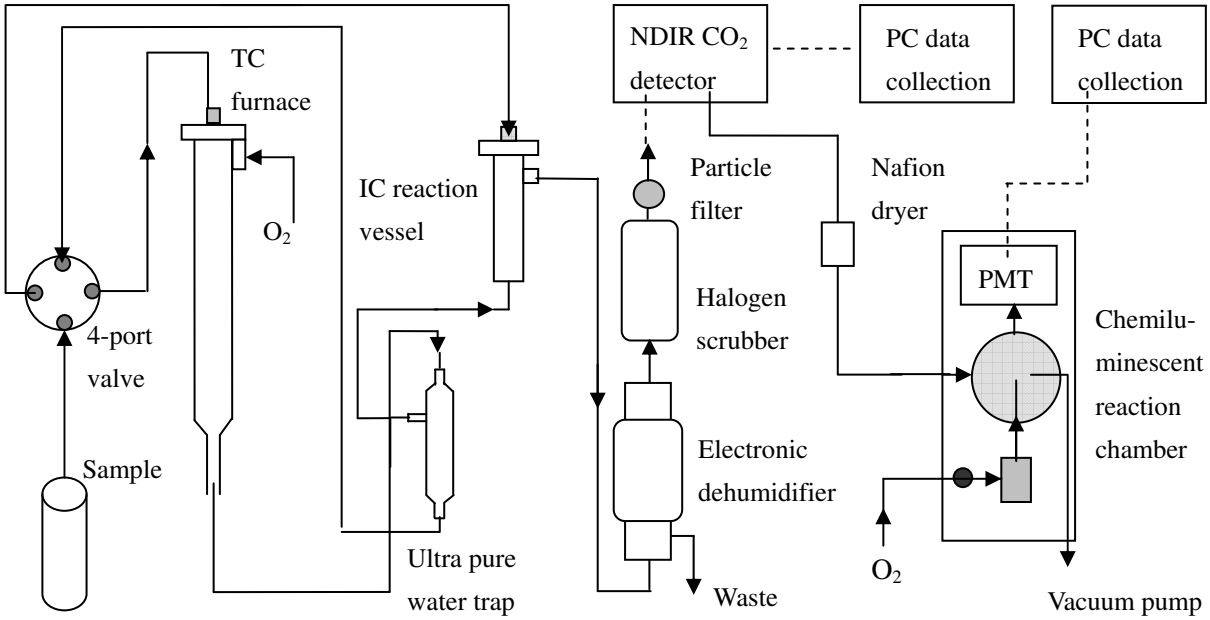

Figure 2.2. Schematic diagram of the Shimadzu TOC 5000A total organic carbon analyser coupled with an Antek NCD 705E nitrogen chemiluminescence detector using high temperature catalytic (HTC) combustion (modified from Badr *et al.* (2003)).

stream was drawn into the sample cell housed in a nondispersive infrared (NDIR) gas analyser, where CO_2 in the gas stream was detected. The produced analogue signals were amplified by the amplifier and converted to pulse frequency by the V/F converter. Pulse frequency was recorded by an RS-232 board (PC-15N) (Shimadzu Corp., Japan) placed in the rear of the Shimadzu TOC instrument. A desktop computer was linked to the RS-232 board via an AWM E101344 style 2464 28AWG cable. A TOC control (5000/5000A & 5050/5050A) software (version 1.05.01, Shimadzu Corp., Japan) was used to quantify pulse frequency as peak area. This software was also capable of instrument control.

Step 2 TDN analysis. The gas stream was drawn out of the TOC instrument with the aid of the vacuum pump, passed through a Nafion membrane dryer (Perma Pure Inc.,

US) in order to remove any remaining water vapour, and then routed to the NCD reaction chamber. The additional drying step using the Nafion dryer is important as moisture quenches the chemiluminescence reaction and leads to tailing of the peak (Walsh 1989). The vacuum pump produced an operating pressure of 2-10 torr in the reaction cell. The TDN determination relies on the chemiluminescent reaction of NO and O_3. NO generated from Step 1 reacted with O_3 produced by the ozone generator housed in the NCD instrument to give rise to the radical species NO_2^*, which emitted quantifiable energy (light) upon decay to its ground state:

$$NO + O_3 \rightarrow O_2 + NO_2^* \rightarrow NO_2 + h\nu$$

The reaction of NO and O_3 occurred in front of the photo-multiplier tube (PMT). The emitted light ($h\nu$) was collected by the PMT and converted to a voltage signal that was stoichiometrically proportional to the total nitrogen concentrations in the sample. The analogue signals from the Antek NCD instrument were collected by a CIO-DAS08/JR16 A/D card (Talisman Electronic Ltd., England) installed in a desktop computer through a female 37-pin, D-type connector (Talisman Electronic Lt., England). An interface box was built to link the analogue output of the NCD to the A/D card. A TCIO-MINI37 screw terminal board (Talisman Electronic Ltd., England) was placed in the interface box. A one metre long TC37FF-5 cable (Talisman Electronics Ltd., England) linked the terminal board and the D-type connector on the A/D card. A virtual instrument (VI) designed using a Class-VP graphical programming in collaboration with Antek Instrument Inc. was used to acquire the digital signals from the A/D card and quantify the signals as peak area. DON concentration was calculated as the difference between the measured concentrations of TDN and DIN.

2.4. Optimisation of DOC and TDN analyses

2.4.1. Stock and standard solution

The coupled HTC TOC-NCD system was calibrated using a mixture of potassium hydrogen phthalate and glycine (both Analar Grade, VWR Ltd., England), with a C:N ratio of 6:1, dissolved in de-ionised water (Milli-Q, Millipore Inc, England). Examples of standard solution graphs for DOC and TDN determinations are presented in Figure 2.3, both of which show excellent linearity between 8-600 μM C and 0.3-100 μM N, respectively. Given low background concentrations of DOC and DON in the Atlantic Ocean, the standard solution set was prepared in a range of 0-240 μM C (i.e., 0, 30, 60, 120, and 240 μM C) and 0-40 μM N (i.e., 0, 5, 10, 20, 40 μM N), with de-ionised water serving as the matrix. The limit of detection, estimated as 3 times background noise was ~8.0 μM C and ~1.0 μM N.

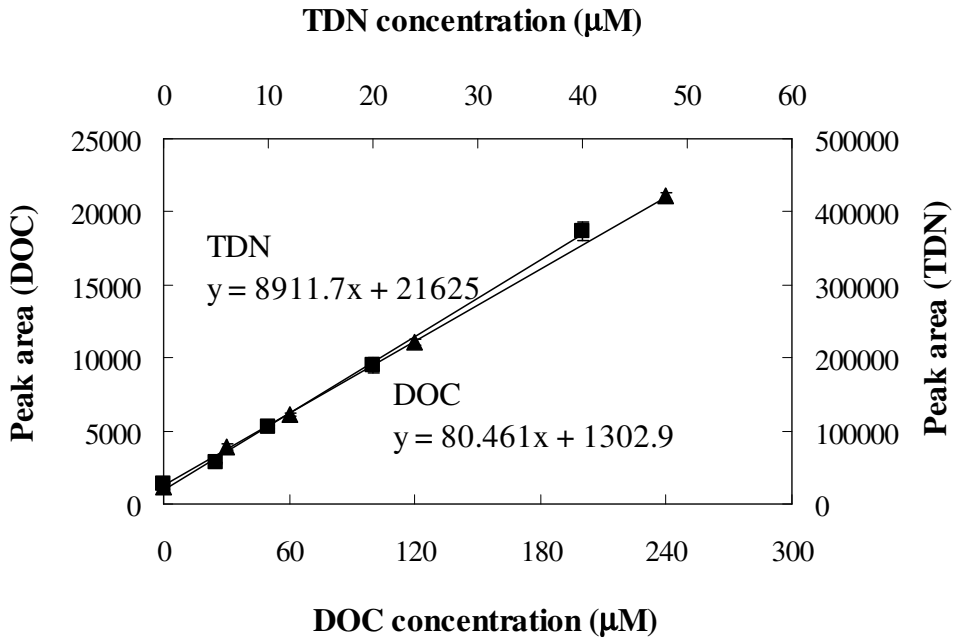

Figure 2.3. Example of calibration graphs for DOC (indicated by triangles) and TDN (indicated by squares) analyses using a mixture of standards of potassium hydrogen phthalate and glycine (with a C:N ratio of 6:1).

2.4.2. Instrument blank

In order to accurately measure DOC and TDN concentrations, one needs to carefully evaluate the source and magnitude of the analytical blank of instruments. Systematic assessments of the system blank of the HTC method (e.g., Benner and Strom 1993, Spyres *et al.* 2000) have suggested that the instrument blank is the predominant contributor to the total system blank, and that the catalyst is the major source of C contamination in the instrument. As much as 500 μM C was found with a new catalyst packed into a combustion tube (Benner and Strom 1993). However, the equivalent to 2500 injections of 200 μl of de-ionised water passing through the catalyst bed can bring the instrument blank down to less than 25 μM C (Benner and Strom 1993). The Shimadzu platinised-alumina catalyst was experimented with the HTC TOC-NCD system; a well-conditioned catalyst (injections of greater than 1 litre of de-ionised water through the catalyst bed) generated a consistent system blank of ~10 μM C and ~0.5 μM N, in good agreement with Alvarez-Salgado and Miller (1998) and Spyres *et al.* (2000) who reported total blanks of 0.3-0.6 μM N and ~10 μM C, respectively.

2.4.3. Oxidation efficiency

Naturally-occurring DON and DOC are comprised of a spectrum of compounds with various resistance to degradation, and the chemical characteristics of DOC and DON compounds still remain poorly understood. Hence, none of the available standard compounds can be assumed to be representatives of natural DOC and DON. In order to investigate the ability of the HTC TOC-NCD system to degrade naturally occurring organic compounds, the recovery efficiency was tested using a wide range of synthetic compounds with different refractivities. A comparison with other findings (Tab. 2.3) suggests that the HTC approach is a robust tool for the determination of DOC and TDN in natural waters.

(In)organic compounds	Matrix	Concentration (μM)	Recovery (%) HTC	HT[a]	UV	WCO[b]	Reference
C compounds							
APDC[c]	UV-DW[f]	100	90				this study
Antipyrine	UV-DW	100	95				this study
	DW[g]	250				95	Raimbault *et al.* 1999
Caffeine	UV-DW	100	100				this study
	DW	250				99	Raimbault *et al.* 1999
EDTA[d]	UV-DW	100	99				this study
Glycine	UV-DW	100	102				this study
	DW	250				100	Raimbault *et al.* 1999
NEDA[e]	UV-DW	100	96				this study
Thiourea	UV-DW	100	100				this study
	DW	250				97	Raimbault *et al.* 1999
Urea	UV-DW	100	101				this study
	DW	250				100	Raimbault *et al.* 1999
N compounds							
APDC	UV-DW	15	95				this study
Antipyrine	DW[5]	2				45	Nydahl 1978
	DW	5		88	61	52	Bronk *et al.* 2000
	DW	10		94	55		Walsh 1989
	UV-DW	15	98				this study
	DW	24.6	85				Alvarez-Salgado and Miller 1998
	DW	40		101	51		Walsh 1989
	DW	40		70	47	68	Bronk *et al.* 2000
	DW	45.5				50	Raimbault *et al.* 1999
Caffeine	DDW[h]	2.14		102			Koike and Tupas, 1993
	UV-DW	15	97				this study
	DW	20.8				96	Raimbault *et al.* 1999
	DW	25.3	97				Alvarez-Salgado and Miller, 1998
EDTA	DW	2				99	Nydahl 1978
	DW	5		104	88	87	Bronk *et al.* 2000
	DW	10		102	103		Walsh 1989
	UV-DW	15	100				this study
	DW	20		87	77	89	Bronk *et al.* 2000
	DW	24.8	102	87	77	89	Alvarez-Salgado and Miller 1998

(*Continues*)

(*Continued*)

(In)organic compounds	Matrix	Concentration (μM)	Recovery (%) HTC	HT[a]	UV	WCO[b]	Reference
N compounds							
EDTA	DW	40		101	96		Walsh 1989
	DW	50		97			Le Poupon *et al.* 1997
	DW	N/A		101			Hopkinson *et al.* 1993
Glycine	DW	2				93	Nydahl 1978
	DW	5		104	96	97	Bronk *et al.* 2000
	DW	10			100		Collos and Mornet 1993
	UV-DW	15	100				this study
	DW	20		100			Walsh 1989
	DW	20.8		100		100	Raimbault *et al.* 1999
	DW	40			100		Walsh 1989
	DW	40		96	55	97	Bronk *et al.* 2000
NEDA	UV-DW	15	97.5				this study
	DW	40		96	84		Walsh 1989
Thiourea	DDW	2.14		94			Koike and Tupas 1993
	UV-DW	15	98				this study
	DW	23.9	96				Alvarez-Salgado and Miller 1998
	DW	83.3				78	Raimbault *et al,* 1999
Urea	DW	2				100	Nydahl 1978
	DDW	2.14		100			Koike and Tupas 1993
	DW	5		97	101	99	Bronk *et al.* 2000
	DW	10		100	83		Walsh 1989
	DW	10			100		Collos and Mornet 1993
	UV-DW	15	101				this study
	DW	25		96	96	106	Bronk *et al.* 2000
	DW	25.2	101				Alvarez-Salgado and Miller 1998
	DW	40		102	73		Walsh 1989
	DW	50		84			Le Poupon *et al.* 1997
	DW	75		97	76	100	Bronk *et al.* 2000
	DW	83.3				100	Raimbault *et al.* 1999
	DW	N/A		101			Hopkinson *et al.* 1993

(*Continues*)

(*Continued*)

(In)organic compounds	Matrix	Concentration (μM)	Recovery (%) HTC	HT[a]	UV	WCO[b]	Reference
N compounds							
NH4Cl or (NH4)2SO4	DW	2				100	Nydahl 1978
	DW	5		94	78	96	Bronk *et al.* 2000
	UV-DW	15	99				this study
	DW	25		94	35	99	Bronk *et al.* 2000
	DW	25.3	97				Miller 1998
	DW	40		100	100		Walsh 1989
	DW	75		99	29	104	Bronk *et al.* 2000
	DW	N/A		100			Hopkinson *et al.* 1993
KNO_3	UV-DW	15	102				this study
	DW	40		100	100		Walsh 1989
	DW	N/A		100	100	100	Bronk *et al.* 2000
$NaNO_3$	UV-DW	15	101				this study
	DW	24.7	101				Miller 1998
	DW	40		101	100		Walsh 1989
	DW	N/A		100			Hopkinson *et al.* 1993

[a] High temperature combustion

[b] Wet chemical oxidation

[c] Ethylenediaminetetraacetate

[d] Ammonium pyrrolidine-dithiocarbamate

[e] N-1-Naphthylethylenediamine

[f] UV irradiated de-ionised water

[g] De-ionised water

[h] Double de-ionised water

Table 2.3. A comparison of oxidation efficiency of selected synthetic DOC and DON compounds using different analytical approaches.

2.4.4. Accuracy, precision, errors and sensitivity

In my laboratory, certified reference (CRM) deep ocean water was analysed frequently, provided by D.A. Hansell, Rosenstiel School of Marine and Atmospheric Science (RSMAS), the University of Miami, to help monitor the analytical accuracy. This CRM, collected from a depth of 2600 m in the Sargasso Sea without filtration, was acidified and preserved in 10 ml glass ampoules. I found that it can be stored at room temperature for at least 2 years without significant changes in DOC and TDN concentrations (Tab. 2.4). My analysis of the reference material yielded mean

Dates	n	DOC concentration (μM)	TDN concentration (μM)
December 2004	6	45.8 ± 0.4	22.0 ± 0.2
February 2005	8	46.1 ± 0.2	21.8 ± 0.3
April 2005	4	45.5 ± 0.3	21.5 ± 0.3
May 2005	4	45.1 ± 0.2	21.4 ± 0.2
July 2005	18	44.3 ± 0.3	21.6 ± 0.8
August 2005	20	45.1 ± 0.7	21.3 ± 0.3
September 2005	16	46.1 ± 0.2	21.4 ± 0.1
December 2005	16	44.5 ± 0.2	21.6 ± 0.3
January 2006	18	45.8 ± 0.6	21.5 ± 0.4
February 2006	8	45.1 ±0.3	21.2 ± 0.3
March 2006	4	44.6 ± 0.2	21.6 ± 0.3
July 2006	2	45.2 ± 0.3	21.5 ± 0.2
September 2006	8	46.0 ± 0.3	21.8 ± 0.4
December 2006	6	44.5 ± 0.4	20.8 ± 0.2
April 2007	12	45.0 ± 0.4	21.5 ±0.6
Summary	150	Mean 45.2 ± 1.2	Mean 21.6 ± 1.0

Table. 2.4. Results of the measurements of CRMs (deep Sargasso Sea water).

concentrations of 45.2±1.2 µM DOC and 21.6±1.0 µM TN (n=150), which were in good agreement with the certified values of 44-46 µM DOC and 21.5 µM TN (Hansell and Carlson 2001b).

To evaluate analytical precision, the coefficient of variation (CV), which was calculated as the ratio of the standard deviation (σ) of replicate experiments to the arithmetic mean, was evaluated. The CV was typically better than 1% for DOC analysis and better than 5% for TDN analysis with 3-5 replicate injections. Table 2.5 summarises the optimisation of the HTC TOC-NCD system. However, it should be noticed that DON concentration is estimated as the difference in the measured TDN and DIN concentrations. Therefore, the DON concentrations incorporate the combined errors of the independent measurements of TDN and DIN, with the standard deviation of the DON measurement estimated from $(\sigma^2_{TDN} + \sigma^2_{DIN})^{1/2}$. A small error in TDN or DIN measurements can lead to a large error in the estimate of DON, especially when the DON is a small fraction of the TDN. Hence, quality-assurance protocols and an excellent analytical precision are required for the TDN+DIN measurements.

Instrument conditions	Analytical details
Standards	Potassium hydrogen phthalate and glycine
Carrier and sparge gas	Oxygen (99.995%)
Carrier gas flow	150 ml min^{-1}
Sparge gas flow	100 ml min-1, 8 minutes
Injection volume	100 µl
Sample through-put	4 samples per hour involving 3-5 repeat injections
Recording	Peak area
Shimadzu TOC 5000A	
Gas flow rate	150 ml min^{-1}
Catalyst	Aluminum oxide coated by 0.5% of platinum
Furnace temperature	680°C
Oxidation products	CO_2 and H_2O
Detection	Non-dispersive infrared gas analyser

(*Continues*)

(*Continued*)

Instrument conditions	Analytical details
Shimadzu TOC 5000A	
Linear range	8-600 μM C
Limit of detection	8 μM C
CRM	45.2 ± 1.2 μM DOC
Precision	Less than 1.0 %
Total blank	~10 μM DOC
Antek NCD 705E	
Gas flow rate	30 ml min^{-1}
Operation pressure	2-10 torr
Oxidation product	NO and H_2O
Detection	Nitrogen chemiluminescence detector
Linear range	0.3-100 μM N
Limit of detection	~1.0 μM N
CRM	21.6 ± 1.0 μM TN
Precision	Less than 5%
Total blank	~0.5 μM N

Table. 2.5. Optimisation of high temperature catalytic (HTC) combustion based on a Shimadzu TOC 5000A total organic carbon analyser coupled with an Antek NCD 705E nitrogen chemiluminescence detector.

Instrument sensitivity, as ascertained from the slope of the standard calibration, forms an important characteristic of the HTC analysis of DOC and TDN. A low instrument sensitivity increases the limit of detection of the analysis, and also provides an indication of poor catalyst or detector performance (Watanabe *et al.* 2007). The slope of the linear regression for the DOC standard calibration was 84.26 ± 4.55 (n = 150), and for TDN standard calibration was 8900 ± 100 (n = 150), both of which indicated the stable and reliable performance of the HTC TOC-NCD instruments.

2.5. Determination of TDP

TDP concentrations were measured using the standard phosphomolybdenum blue colorimetric approach following sample exposure to high-intensity ultraviolet (UV) irradiation in order to convert organically-bound phosphorus into inorganic (*i.e.* SRP) form. UV treatment was conducted using a Metrohm 705 UV digestion (Metrohm Ltd., England) system, following Sanders and Jickells (2000). In this method, the filtrates were transferred in a 10 ml fused quartz tube equipped with a graphite stopper, and irradiated for 2 h at a temperature of ~85^{o}C under high-intensity UV light (500 w). This photooxidation time and the reaction temperature were well documented and widely accepted by nutrient chemists (*e.g.* Karl *et al.* 1993). No catalysts or oxidants were added during this photochemical reaction, as this test had been undertaken by Sanders and Jickells (2000), who found no increase in oxidation efficiency. The difference between the measured concentrations of TDP and DIP was taken as DOP concentration.

2.6. Optimisation of TDP analysis

2.6.1. Oxidation efficiency

The oxidation efficiency of this UV irradiation system was examined by Torres *et al.* (in prep) in a laboratory in NOCS using a variety of synthetic compounds with different refractivities. The results suggest that this method is sufficient to oxidise ~70% of DOP to DIP, which was in agreement with Ormaza-Gonzalez and Statham (1996) and Sanders and Jickells (2000). Hence, the estimates only represent lower limits of DOP concentrations.

2.6.2. Accuracy, precision and errors

Unlike DOC and TDN, there is no TDP CRM available for intercomparison of methods and results. So far, analytical accuracy of TDP determination remains a challenge for nutrient analysis. The analytical precision was better than 10% based on

the CV of the results of the analysis of individual water samples from multiple Niskin bottles fired at the same nominal depth.

Similarly, DOP concentration is estimated as the difference in the measured TDP and DIP concentrations. Therefore, the DOP concentrations combine the errors of the independent measurements of TDP and DIP, with the standard deviation of the DOP measurement estimated from $(\sigma^2_{TDP} + \sigma^2_{DIP})^{1/2}$. Again, a small error in TDP or DIP measurements can lead to a large error in the estimate of DOP, especially when the DOP is a small fraction of the TDP. Hence, quality-assurance protocols and an excellent analytical precision are required for the TDP+DIP measurements.

The slope of the linear regression for the TDP standard calibration was assessed by E.M.S. Woodward and K. Chamberlain (Plymouth Marine Laboratory; PML) during the shipboard measurements to monitor the performance of the instrument. However, the variation in slope was not available by the time this work has been done.

2.7. Determination of other hydrographic, biological and chemical properties

Micromolar and nanomolar concentrations of nitrate plus nitrite and phosphate were measured by M. Woodward and K. Chamberlain (PML). Carbon fixation, chlorophyll a concentrations, and particulate organic carbon (POC) and nitrogen (PON) concentrations were determined by P. Holligan, A. Poulton, T. Andy and A. Hickman (NOCS). Nanophytoplankton, picophytoplankton, *Prochlorococcus*, *Synechococcus*, and heterotrophic bacterioplankton abundance were measured by M. Zubkov and I. Mary (NOCS) and G. Tarran (PML). Alkaline phosphatase and amino acids were determined by S. Reynolds and R. Mather (University of Liverpool; UOL). Table 2.6 lists the measurements of selected hydrographic, biological and chemical properties as well as plankton community structures for AMT-16 and -17 cruises.

Measurements	Protocol	Personal
AMT-16		
Attenuation, temperature, salinity	CTD, SBE oxygen sensor	UKORS[a]
Micromolar nitrate + nitrite	Auoanalyser	K. Chamberlain, PML[b]
Micromolar phosphate	Auoanalyser	K. Chamberlain, PML
Nanomolar nitrate + nitrite	Chemiluminescence	K. Chamberlain, PML
Nanomolar phosphate	Chemiluminescence	K. Chamberlain, PML
Dissolved organic carbon	High temperature combustion	X. Pan, NOCS[c]
Dissolved organic nitrogen	High temperature combustion	X. Pan, NOCS
Dissolved organic phosphorus	UV oxidation	X. Pan, NOCS
Dissolved oxygen	Winkler titration	N. Gist, PML
Carbon fixation	Incorporation of ^{14}C into particulate organic carbon	A. Poulton, NOCS and I. Cook, PML
Chlorophyll a	Fluorometer	A. Poulton, NOCS and I. Cook, PML
Suspended organic carbon and nitrogen	CHN analyser	A. Poulton, NOCS and I. Cook, PML
Prochlorococcus	Flow cytometry	G. Tarran, PML
Synechococcus	Flow cytometry	G. Tarran, PML
picophytoplankton	Flow cytometry	G. Tarran, PML
nanophytoplankton	Flow cytometry	G. Tarran, PML
heterotrophic bacterioplankton	Flow cytometry	G. Tarran, PML
amino acids	High performance liquid chromatography	S. Reynolds, UOL[d]
Alkaline phosphatase	Incorporation of the fluorogenic substrate MUF-P[e] in cold sterile artificial seawater	S. Reynolds, UOL
AMT-17		
Attenuation, temperature, salinity	CTD, SBE oxygen sensor	UKORS[a]
Micromolar nitrate + nitrite	Auoanalyser	M. Woodward and K. Chamberlain, PML
Micromolar phosphate	Auoanalyser	M. Woodward and K. Chamberlain, PML
Nanomolar nitrate + nitrite	Chemiluminescence	M. Woodward and K. Chamberlain, PML
Nanomolar phosphate	Chemiluminescence	M. Woodward and K. Chamberlain, PML

(*Continues*)

(*Continued*)

Measurements	Protocol	Personal
AMT-17		
Dissolved organic carbon	High temperature combustion	X. Pan, NOCS
Dissolved organic nitrogen	High temperature combustion	X. Pan, NOCS
Dissolved organic phosphorus	UV oxidation	X. Pan, NOCS
Dissolved oxygen	Winkler titration	N. Gist, PML
Carbon fixation	Incorporation of ^{14}C into particulate organic carbon	T. Andy, NOCS
Chlorophyll a	Fluorometer	P. Holligan and A. Hickman, NOCS
Suspended organic carbon and nitrogen	CHN analyser	T. Andy, NOCS
Prochlorococcus	Flow cytometry	M. Zubkov and I. Mary, NOCS
Synechococcus	Flow cytometry	M. Zubkov and I. Mary, NOCS
picophytoplankton	Flow cytometry	M. Zubkov and I. Mary, NOCS
nanophytoplankton	Flow cytometry	M. Zubkov and I. Mary, NOCS
heterotrophic bacterioplankton	Flow cytometry	M. Zubkov and I. Mary, NOCS
amino acids	High performance liquid chromatography	R. Mather, UOL
Alkaline phosphatase	Incorporation of the fluorogenic substrate MUF-P[d] in cold sterile artificial seawater	R. Mather, UOL

[a] UK Ocean Research Services, UK

[b] Plymouth Marine Laboratory, UK

[c] National Oceanography Centre, Southampton, UK

[c] the University of Liverpool, UK

[e] Methyl-umbelliferyl phosphate

Table. 2.6. List of selected measurements and protocols during AMT-16 and -17 cruises.

Accuracy of automated nutrient analyses was not assessed on the shipboard measurements. The detection limits were 0.1 μM for micromolar measurements and 2 nM for nanomolar measurements, respectively. The precision was better than 0.5%. Further details can be found in Rees *et al.* (2006) and Krom *et al.* (2005).

The precision for dissolved oxygen analyses was to be discussed in Section 2.8, whilst analytical accuracy, precision and detection limits were not available for other supporting measurements by the time this work has been done.

2.8. Calculation of AOU

To calibrate the Seabird 43 oxygen sensor on the CTD rosette, during each CTD cast water samples were drawn from 4-6 randomly selected Niskin bottles into 125 ml volume calibrated borosilicate glass bottles and fixed immediately on deck using manganous chloride and alkaline iodide solutions following Robinson *et al.* (2006). Samples were then acidified using sulphuric acid (5 M), and the liberated iodine was titrated against sodium thiosulphate using a semi-automated spectrophotometric oxygen analyser similar to that described by Williams and Jenkinson (1982). Oxygen concentration dissolved in seawater was calculated by N. Gist (PML) following Benson and Krause (1984). The precision (CV) for this oxygen analysis, determined by analysing dissolved oxygen concentrations from 4 Niskin bottles fired at the same depth, was better than 0.03%. A linear regression was then performed between the calculated oxygen concentrations and the Seabird generated concentrations for each sampled Niskin bottle to generate a regression equation. This equation was applied to compute dissolved oxygen concentrations for the remaining Niskin bottles sampled for DOC, which had not been sampled for dissolved oxygen. This has been done for each CTD cast for AMT-16 and -17. Oxygen saturation and AOU concentration were calculated using the calibrated CTD data using the solubility equations of Garcia and Gordon (1992) and solubility coefficients of Benson and Krause (1984).

3. Results

3.1. General hydrography

3.1.1. Temperature, salinity and density

Details of the broad-scale hydrographic features observed in AMT transects (AMT1-17) have been provided by Aiken *et al.* (2000) and Robinson *et al.* (2006). The following results and discussion only focuses on AMT-16 and -17 transects for which the maximum sampling depth was 300 m. The warmest (>27°C) waters were observed in the upper 50 m between ~10°S and ~15°N due to intensive irradiance in the equatorial region (Fig. 3.1). Cold water tongues were formed in subsurface waters of the equator in response to equatorial upwelling. As a consequence, cold deep ocean water was brought up to a shallower depth. In the subtropical regions, tongues of warm waters can be observed as a result of subtropical downwelling, bringing warm surface waters down to a greater depth. At higher latitudes (>40°N and >35°S), no remarkable changes in water temperature were observed with increasing water depth in the upper 300 m. This phenomenon can be explained by a weakened thermal stratification of the water column in these temperate regions.

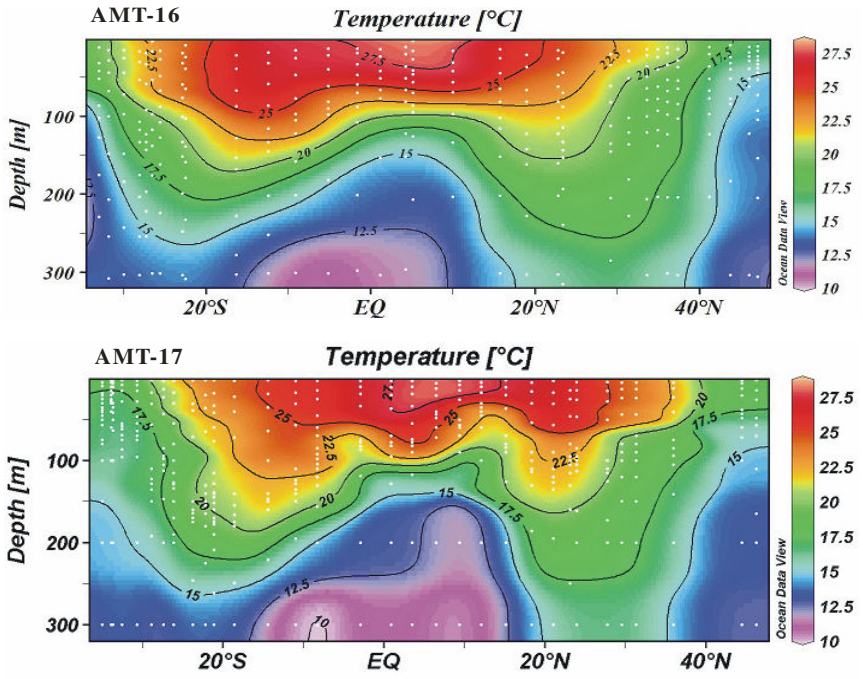

Figure 3.1. Latitudinal-depth contours of temperature in the upper 300 m for AMT-16 and -17.

In surface waters, low salinity (<35.5) was observed in the region north of the equator between ~0 and ~10°N due to local rainfall, and at ~35°S caused largely by an intrusion of upwelled deep Benguela Coastal waters (Fig. 3.2). On AMT-17, this coastal upwelling effect was more pronounced most likely due to a close proximity of the sampling location to the west coast of South Africa. As a result of equatorial upwelling, the tongues of low salinity (<35.5) waters upwelled from the deep ocean and reached ~160 m in the section. The subtropical regions were characteristic of an enhanced salinity of 36.5-37.5, extending down to ~150 m. The latitudinal-depth contours of salinity suggested that the Equatorial Undercurrent (EUC), the source of equatorial upwelling, was centred at ~2°N at a depth of ~70 m. Similar to the temperature profiles, a minor variability in salinity was observed with increasing water depth at higher latitudes (>40°N and >35°S).

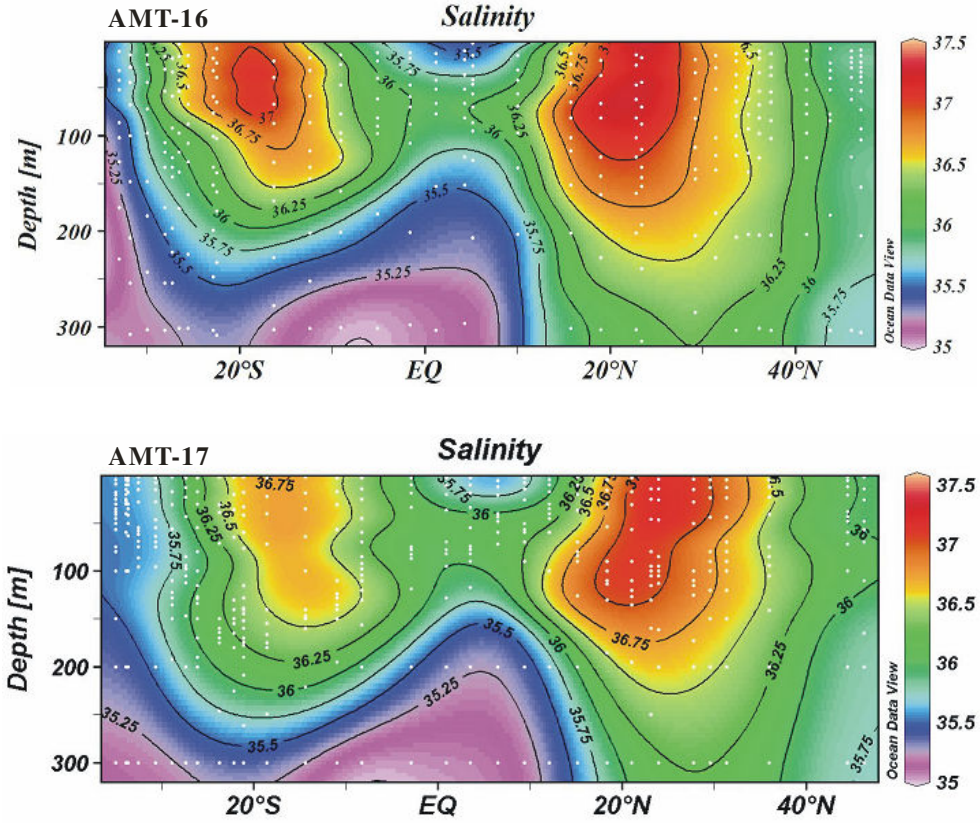

Figure 3.2. Latitudinal-depth contours of salinity in the upper 300 m for AMT-16 and -17.

The profiles of potential density, calculated using *in situ* temperature and salinity data by the British Oceanographic Data Centre suggested that less dense (<26.0 kg m^{-3}) water masses generally resided in the upper 100 m of the tropical and subtropical Atlantic (Fig. 3.3), with a penetration down to ~200 m in the southern subtropical Atlantic. The least dense (<23.5 kg m^{-3}) surface (0-50 m) waters resided in the equator between ~8°S and ~15°N. Within the tropical and subtropical regions where the water column was highly stratified, an evident variability in potential density was observed with increasing water depth, while attenuating thermal stability of the water column at higher latitudes (>40°N and >35°S) led to a lower variability.

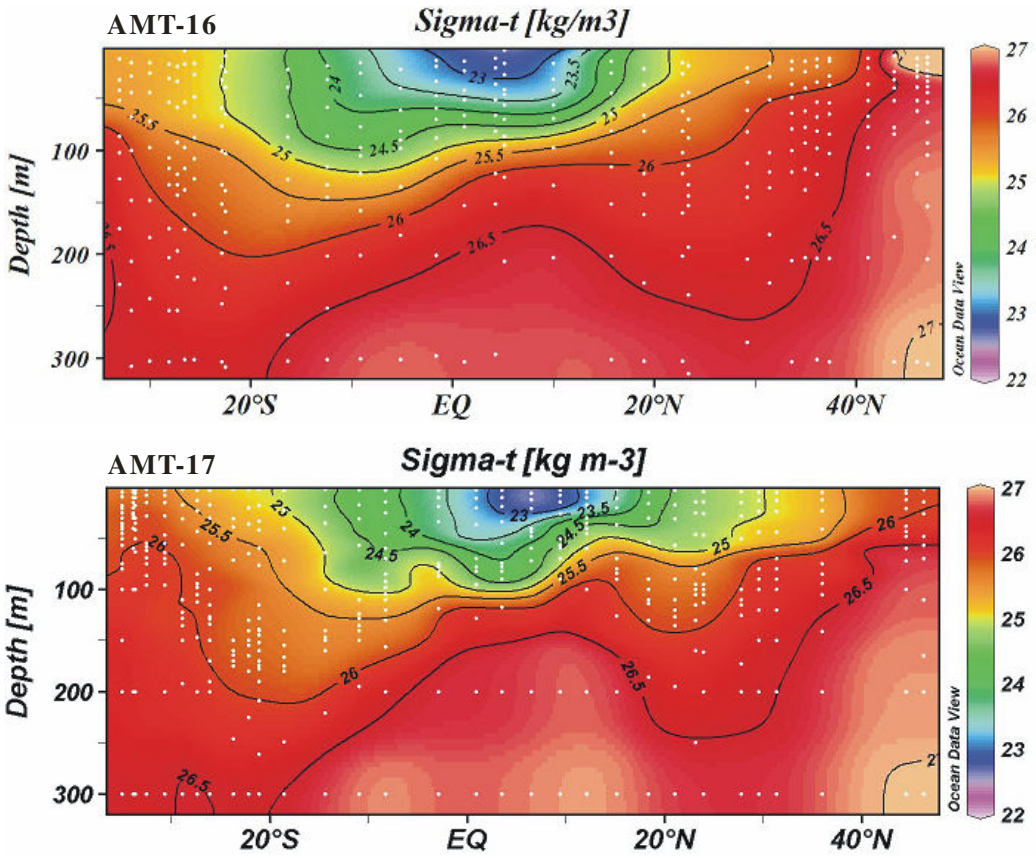

Figure 3.3. Latitudinal-depth contours of density in the upper 300 m for AMT-16 and -17.

3.1.2. Mixed layer depth, seasonal thermocline and euphotic zone

On AMT-16, the mixed layer depth (MLD), with its bottom boundary defined by a

density (sigma-t) increase of 0.125 kg m^{-3} from the surface value following Williams *et al.* (2000), was 30-90 m in equatorial waters, 80-100 m in the southern subtropical Atlantic, and 30-60 m in the northern subtropical Atlantic (Fig. 3.4a). On AMT-17, the MLD was 30-90 m in the equatorial Atlantic, 20-50 m in the southern subtropical Atlantic, and 30-70 m in the northern subtropical Atlantic. The latitudinal-depth contours for AMT-16 and -17 suggested an important intercruise variability of the MLD in the southern subtropical Atlantic, but not in the equatorial and northern subtropical regions.

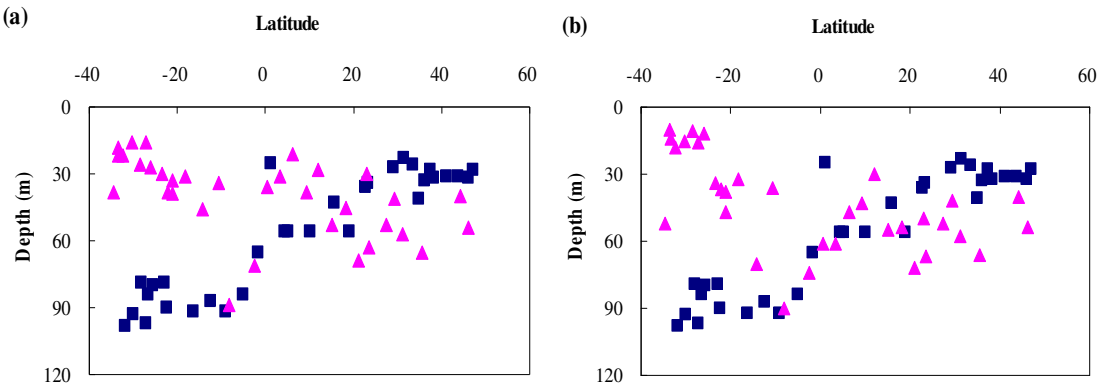

Figure 3.4. Latitudinal-depth contours of (a) the mixed layer depth (MDL) and (b) seasonal thermocline for AMT-16 (indicated by squares) and -17 (indicated by triangles).

The thermocline is the transition layer between the mixed layer at the surface and the deep water layer, where the temperature changes rapidly with increasing depth (Pinet 2003). The top of the thermocline, therefore, reflects the bottom of the mixed layer. On AMT-16, the seasonal thermocline, defined by an *in situ* temperature decrease of 0.5°C from the surface value following Sprintall and Tomczak (1992), was 30-90 m in the equatorial region, 80-100 m in the southern subtropical Atlantic, and 30-60 m in the northern subtropical Atlantic (Fig. 3.4b). On AMT-17, the seasonal thermocline was 40-90 m in the equatorial region, 10-75 m in the southern subtropical Atlantic, and

30-75 m in the northern subtropical Atlantic. The plots showed an intercruise variability of seasonal thermocline in the subtropical Atlantic, particularly in the southern subtropical region.

Pronounced seasonal variations in the MLD are shown in Figure 3.4a. This is largely due to variations in wind strength and surface heat fluxes. Wind plays a vital role in the development of the mixed layer because of the vertical shear resulting from wind-induced surface currents (Pinet 2003). Stronger heating leads to greater stratification, stability and lower potential energy; on the other hand, cooling destabilises the water column in the winter, allowing mixing to occur even in the absence of winds (Soloviev and Lukas 2006). For this reason, winds and surface heat fluxes combine to affect formation and seasonal variation of the mixed layer. Figure 3.4a shows a poleward increase in seasonal variation in MLD. This is a result of increased winds and cooling towards higher latitudes. Mixed layers were deeper in the Southern Hemisphere winter than in the Northern Hemisphere winter. This may reflect the fact that winds are generally stronger in the Southern Hemisphere and that there is a greater input of heat in the Northern Hemisphere (Soloviev and Lukas 2006).

During AMT-16 and -17, thickness of the euphotic zone (Fig. 3.5), defined as a depth where light intensity falls to 1% of that at the surface (Poulton *et al.* 2006), was shallowest at 40-90 m in equatorial waters due to enhanced photosynthetic primary production sourced by upwelled nutrients, deepest at 90-160 m in the subtropical Atlantic because of a reduced production caused by nutrient limitation, and 40-80 m in temperate waters due to an improved production sourced by augmented nutrients possibly caused by Ekman transport along the poleward flanks of the subtropical gyres (Mahaffey *et al.* 2004) and coastal upwelling effects at the Benguela Coast, South Africa (Robinson *et al.* 2006).

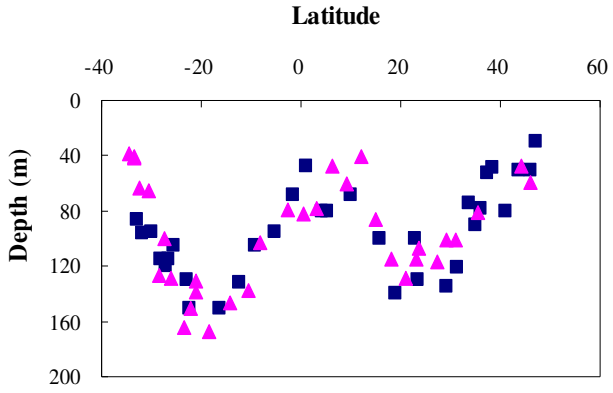

Figure 3.5. Latitudinal-depth contours of the thickness of euphotic zone for AMT-16 (indicated by squares) and -17 (indicated by triangles).

3.2. Distribution of DIN and DIP

Latitudinal-depth contours of DIN concentrations are plotted in Figure 3.6. DIN (NO_3^- + NO_2^-) distributions generally showed reduced concentrations (<0.1 μM) in surface waters, with substantial increases with increasing depth. At 300 m, the concentrations increased to >10 μM. The nitracline, defined as the depth below which N+N concentrations exceeded 1 μM within this study, was relatively deep (>150 m) in the subtropical Atlantic gyres (SAG: southern Atlantic subtropical gyre (SASG) between ~35°S and ~10°S; northern Atlantic subtropical gyre (NASG) between ~15°N and ~40°N) and relatively shallow (>50 m) in the equatorial Atlantic region (EQA between ~10°S and ~15°N). In the EQA, DIN concentrations in near-surface (30 m) waters were below the detection limit of the standard colorimetric method, but rapidly increased to >1 μM in the EUC, and further increased to >5 μM at 100 m and >25 μM at 300 m. In the SAG, DIN concentrations in the upper 30 m were also below the detection limit of 0.1 μM. These DIN-depleted surface waters penetrated down to ~100 m in the central gyres, but rapidly increased to ~5 μM at 200 m. At 300 m, DIN concentrations were ~10 μM.

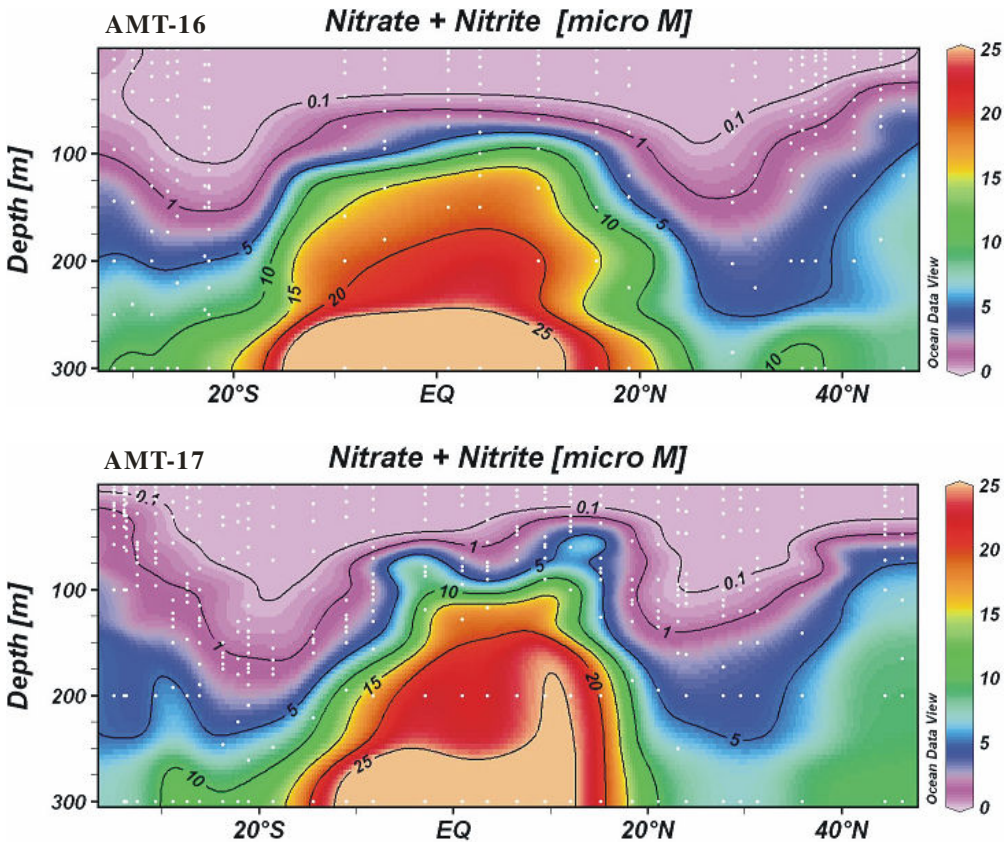

Figure 3.6. Latitudinal-depth contours of DIN in the upper 300 m for AMT-16 and -17.

DIN concentrations in the upper 30 m are shown in Figure 3.7. Broadly, there were no pronounced spatial variations, with the concentrations ranging from 5 nM to 30 nM, albeit the highest concentrations (>100 nM) were observed at the southeast flank (~30^{o} S) of the SASG, likely due to coastal upwelling. On AMT-16, relatively higher concentrations (>50 nM) were observed between the equator and ~25^{o}N. This may be caused by strengthened nitrogen fixation in boreal spring. On AMT-17, enhanced concentrations of DIN were absent within this region, likely due to a weakening of nitrogen fixation in boreal autumn. Comparing the concentrations of DIN in the upper 30 m on two AMT cruises, there were no pronounced seasonal variations. DIN is likely to be the limited nutrient throughout the year in the tropical and subtropical Atlantic regions. Interestingly, relatively elevated concentrations (>50 nM) were present at >40^{o}N on AMT-16. This may be linked with a short-term biological activity or a

regional semiscale upwelling event.

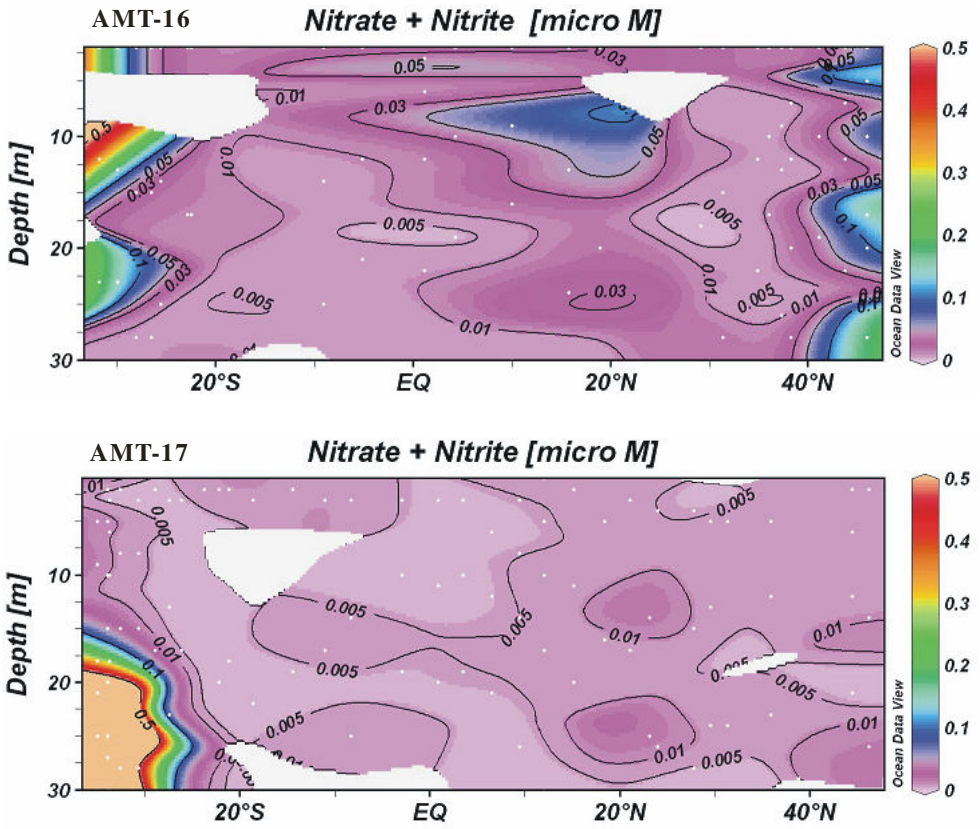

Figure 3.7. Latitudinal-depth contours of DIN in the upper 30 m for AMT-16 and -17.

The latitudinal-depth profiles of DIP in the upper 300 m are shown in Figure 3.8. Similar to DIN concentrations, there was a general pattern of low concentrations in surface waters and high values at depth. In the EQA, DIP concentrations in surface waters were below the detection limit of 0.1 µM, but rapidly increased to >0.3 µM at 100 m. At 300 m, the concentrations were >1.5 µM. In the SAG, DIP concentrations were generally <0.2 µM in the upper 100 m, and increased to >0.3 µM at 300 m. DIP (PO_4^{3-}) distributions showed relatively higher concentrations in the SASG than in the NASG. This might be attributed to the absence of nitrogen fixation and limited iron availability in the SASG, both of which can favour the DIP accumulation in the water

column. On AMT-16, the 0.1 μM DIP contour was ~60 m in the equatorial and southern subtropical regions, and penetrated down to ~250 m in the northern subtropical gyre. On AMT-17, the 0.1 μM contour reached ~180 m in the northern subtropical gyre, shallowed to ~60 m in the equatorial region, and outcropped at ~5°S.

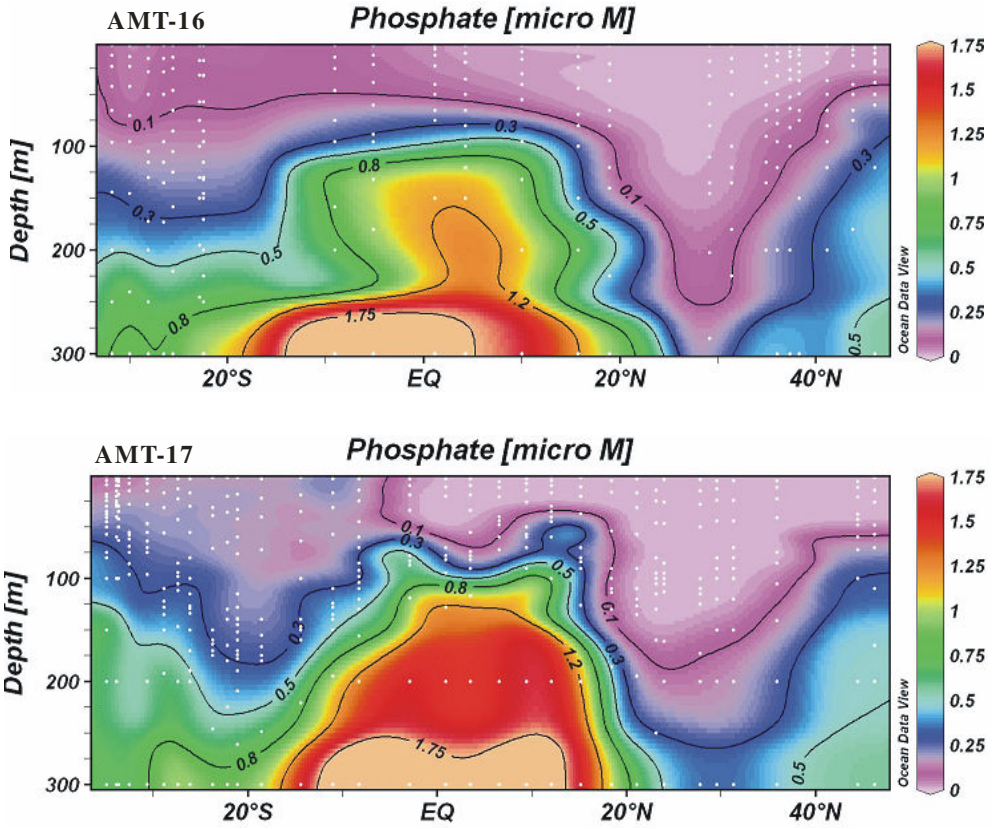

Figure 3.8. Latitudinal-depth contours of DIP in the upper 300 m for AMT-16 and -17.

DIP concentrations in the upper 30 m are plotted in Figure 3.9, showing clear spatial variations. The lowest concentrations (<30 nM) were generally present in the north equatorial and the northern subtropical regions. In the south equatorial and the southern subtropical regions, the concentration were generally >50 nM. Comparing two AMT cruises, there were no evident seasonal variations in DIP concentrations in the EQA; but the seasonal variations were rather pronounced in the SAG, especially in

the NASG, showing a seasonal decrease with the onset of autumn. This is the result of strengthened primary production during spring and summer.

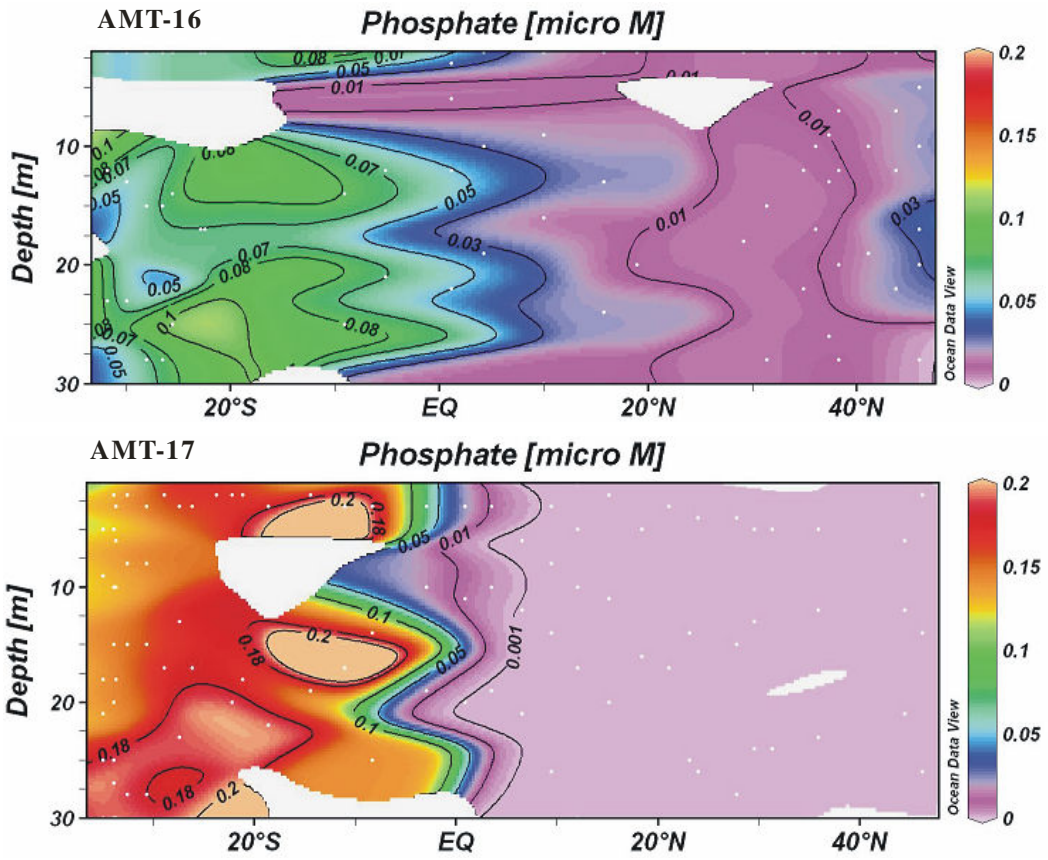

Figure 3.9. Latitudinal-depth contours of DIP in the upper 30 m for AMT-16 and -17.

3.3. Distribution of DOC, DON and DOP

DOC analyses on both cruises have generated a total of 794 discrete data points. The latitudinal-depth profiles of DOC in the upper 300 m are plotted in Figure 3.10, showing a general pattern of high concentrations in surface waters and low values at depth, with a vertical gradient in DOC present throughout the section. The highest concentrations (>78 µM) of DOC were found in surface (30 m) equatorial waters between ~15°S and ~15°N, with an extension to ~25°S on AMT-16. On AMT-16, the enhanced concentrations of DOC decreased to ~70 µM at 100 m, compared with ~60

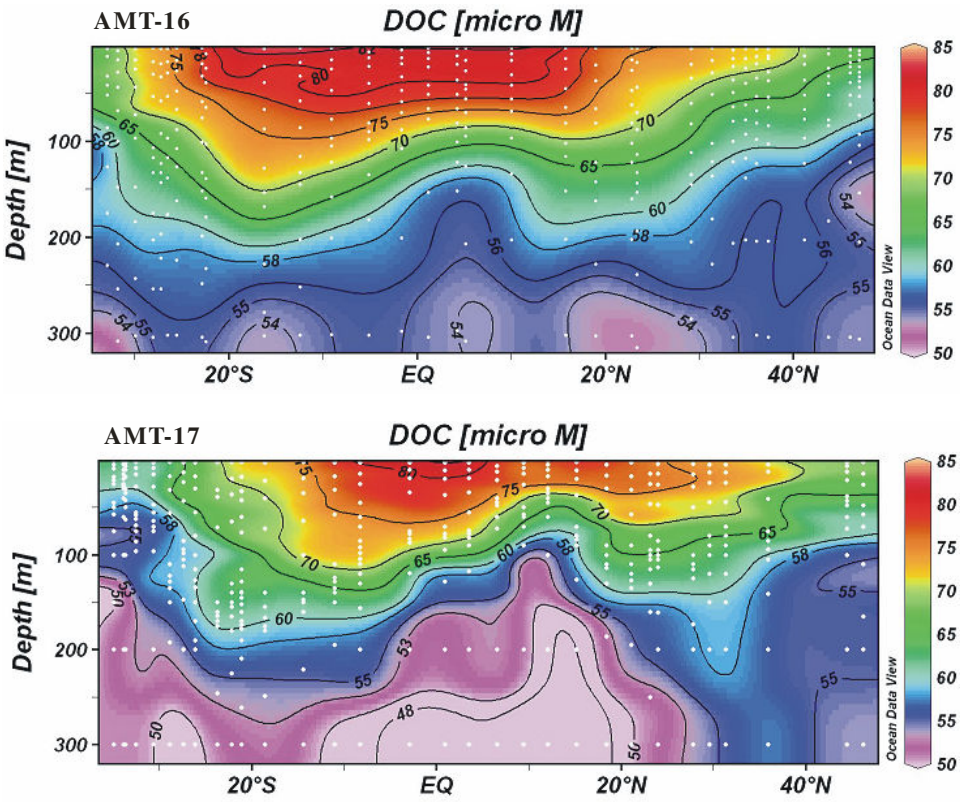

Figure 3.10. Latitudinal-depth contours of DOC in the upper 300 m for AMT-16 and -17.

µM on AMT-17. At 300 m, the concentrations further decreased to ~55 µM on AMT-16, compared to ~48 µM on AMT-17. The differences in DOC concentrations in subsurface waters may be caused by different magnitude of equatorial upwelling. This different strength of upwelling is to be discussed in Section 4.2. In the NASG, DOC concentrations ranged from 68 µM to 78 µM in surface (30 m) waters. The concentrations decreased to <65 µM at 100 m, and further reduced to <56 µM at 300 m. In the SASG, DOC concentrations varied from 65 µM to 80 µM in surface (30 m) waters, with a decrease to 56 µM to 70 µM at 100 m. At 300 m, the concentrations of DOC were <55 µM. There were no evident seasonal variations in DOC concentrations in the equatorial and northern subtropical regions. However, in the southern subtropical gyre, the seasonal variations were rather pronounced. In the upper 100 m, relatively higher concentrations were shown in austral autumn on AMT-16, compared to those in

austral spring on AMT-17. Further research could focus on the seasonality of DOC in the southern Atlantic subtropical region. The two AMT cruise tracks are identical apart from some deviations between ~30°N and ~40°N. These deviations are not significant in terms of intercruise comparisons of DOC concentrations.

DON analyses on both cruises have generated a total of 749 discrete data points. Unfortunately, the whole dataset for AMT-16 cannot be used because the subtraction of DIN from TDN concentrations consistently yielded negative values of DON concentrations. This may be due to the errors generated from the separated TDN and DIN analyses. Hence, I only present DON results for AMT-17 transect, and the following data discussion will be based on these results. The latitudinal-depth contours

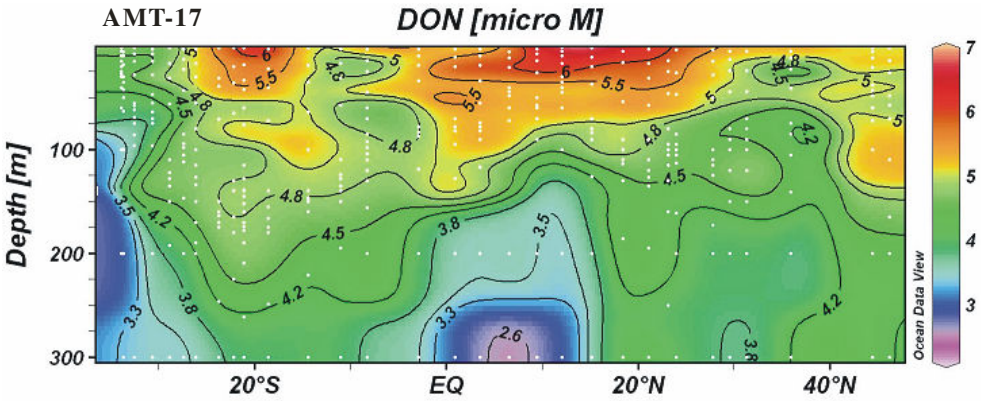

Figure 3.11. Latitudinal-depth contours of DON in the upper 300 m for AMT-17.

of DON for AMT-17 showed that DON concentrations were elevated (>4.8 μM) in surface (30 m) waters, with the highest values (>6.0 μM) observed at ~20°S and between ~10°N and ~25°N (Fig. 3.11). The enhanced DON concentrations in surface waters decreased consistently with increasing water depth to <5.0 μM at 10 m and <4.0 μM at 300 m. Owning to equatorial upwelling, DON-depleted (< 3.8 μM) deep ocean water entered into the subsurface waters, reaching ~150 m. Furthermore, strong coastal upwelling brought DON-poor (<3.8 μM) water up to ~150 m at ~35°S, further

affecting the DON inventories in these surface waters.

DOP analyses on both cruises have generated a total of 732 discrete data points. However, the subtraction of DIP from TDP concentrations for AMT-16 transect consistently gave rise to negative DOP concentrations. This may be caused by the errors during either the separated DIP and TDP analyses or incomplete UV oxidation prior to TDP analysis. Thus, the results from AMT-16 were excluded in the following discussion chapter. The latitudinal-depth contours of DOP for AMT-17 showed a general pattern of high concentrations in surface waters and low values at depth (Fig. 3.12). The highest concentrations (>0.25 μM) of DOP were found in surface (30 m) waters of the tropical and southern subtropical Atlantic regions (~28°S-~8°N), the central northern subtropical region (~25°N-~35°N), and at the northeast flank of the northern subtropical Atlantic (>40°N). Within these regions where enhanced DOP concentrations were observed, I found no concomitant elevation of DON concentrations. A vertical gradient was present throughout the section, suggesting that DOP concentrations rapidly decreased with increasing water depth. At 100 m, DOP concentrations decreased to ~0.12 μM, and further decreased to ~0.07 μM and ~0.05 μM at 200 m and 300 m, respectively.

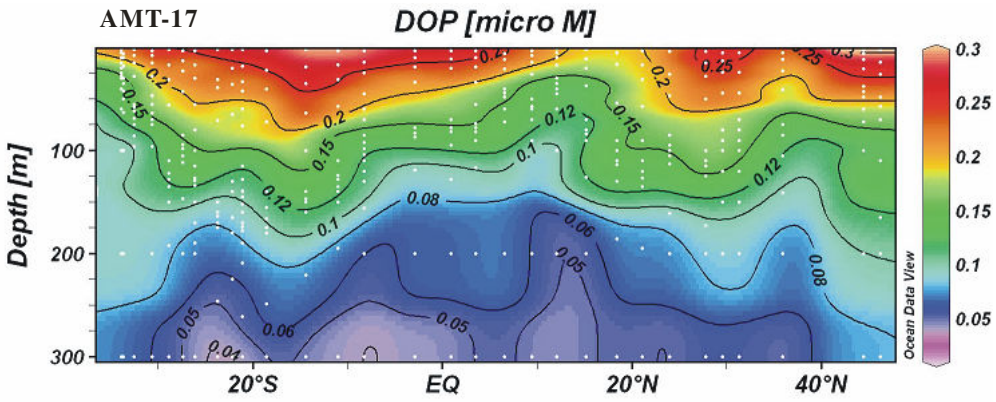

Figure 3.12. Latitudinal-depth contours of DOP in the upper 300 m for AMT-17.

3.4. Distribution of chlorophyll-a and carbon fixation

In surface (30 m) waters, total chlorophyll-a concentrations were generally <0.2 mg m^{-3} in the EQA and <0.1 mg m^{-3} in the SAG, and increased at depth to form a basin-scale subsurface chlorophyll-a maximum (Fig. 3.13). The deep chlorophyll-a maximum occurred over the section at depths averaging 75 m in the EQA, 60 m in the temperate region, and 120 m in the SAG. The highest concentrations in surface waters were found at >30°S, indicating high phytoplankton abundance and biomass in this region. The elevated concentrations of chlorophyll-a reflected an increase in nutrient loads that were likely sourced by coastal upwelling, evidenced by relatively high concentrations of DIN and DIP observed within this region. The latitudinal-depth profiles suggested that there was no considerable variability in the concentrations of chlorophyll-a between AMT-16 and -17 cruises, both in surface waters and in the subsurface chlorophyll-a maximum.

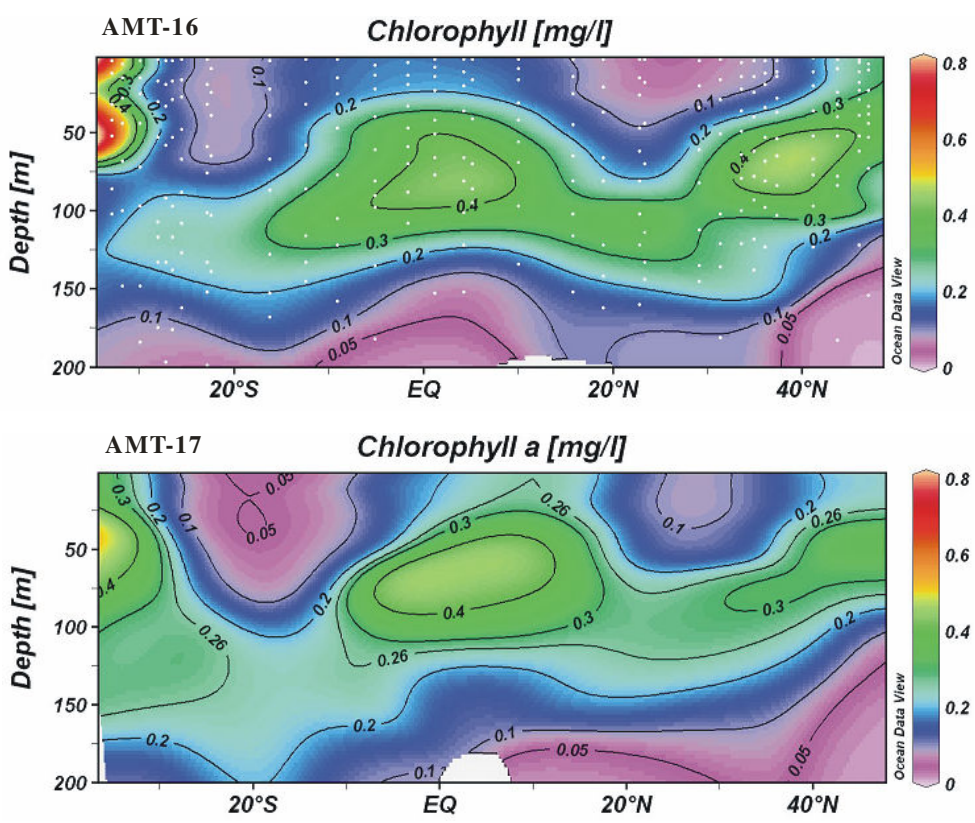

Figure 3.13. Latitudinal-depth contours of chlorophyll-a in the upper 200 m for AMT-16 and -17.

The Latitudinal-depth contours of carbon fixation rates on AMT-16 are shown in Figure 3.14. The latitudinal-depth contours of carbon fixation for AMT17 were not plotted as the rates were determined only at 55% light depth during this cruise. The profiles for AMT-16 suggested that daily production rates were generally highest in surface waters and decreased with depth as irradiance decreased. The subsurface chlorophyll maximum made merely a small contribution to water-column carbon fixation, in agreement with Marañón *et al.* (2000), except where it shallowed in the equatorial and temperate Atlantic regions (Poulton *et al.* 2006). In surface waters of the SASG and NASG, rates of carbon fixation were 0.15-0.45 mmol C m^{-3} d^{-1} compared to 0.45-0.55 mmol C m^{-3} d^{-1} in surface waters of the EQA and the temperate regions.

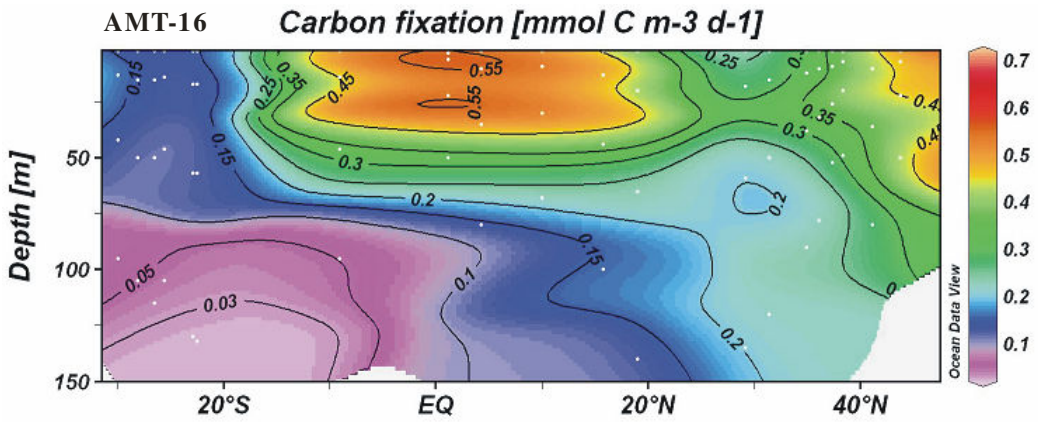

Figure 3.14. Latitudinal-depth contours of carbon fixation rates for AMT-16.

3.5. Distribution of POC and PON

The Latitudinal-depth contours of POC concentrations are plotted in Figure 3.15, generally showing elevated concentrations in surface waters and low values at depth. On AMT-16, the highest concentrations (>6.0 mmol C m^{-3}) of POC were found at the southeast flank (~30°S) of the SASG, in the northern north Atlantic subtropical region (~25°N-~40°N), and at the northeast flank (>40°N) of the NASG. The lowest concentrations (<2.3 mmol C m^{-3}) were present in subsurface waters of the equatorial

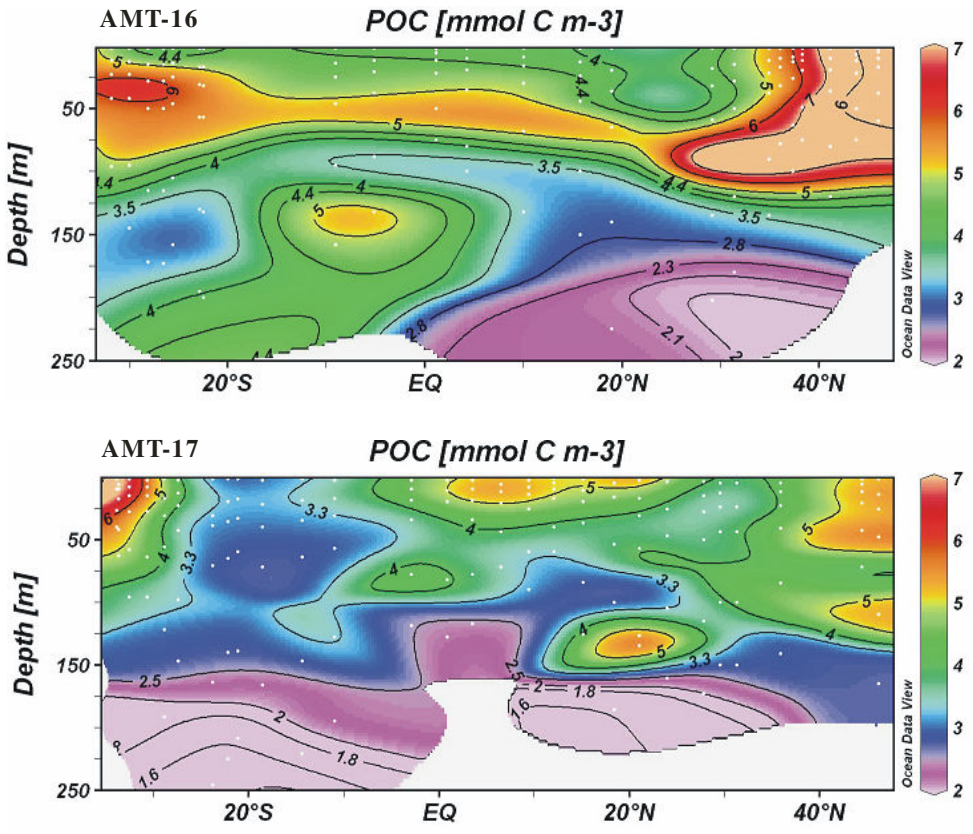

Figure 3.15. Latitudinal-depth contours of POC in the upper 250 m for AMT-16 and -17.

and northern subtropical regions. The high concentrations (>5 mmol C m^{-3}) present between ~25°N and ~50°N may be attributed to the enhanced carbon fixation rates (Fig. 3.11) found in this region. On AMT-17, the highest concentration (>5 mmol C m^{-3}) of POC were found at the southeast flank of the SASG and the northeast flank of the NASG, as well as in the north equatorial and northern subtropical regions. The lowest concentrations (<2.3 mmol C m^{-3}) were found at below 150 m across the whole Atlantic Ocean. Furthermore, high concentrations (>4.5 mmol C m^{-3}) were observed at ~150 m centered at ~8°S on AMT-16 and at ~20°N on AMT-17. The profiles of POC concentrations did not show clear seasonal variations, although relatively higher concentrations observed in the SASG for AMT-16 compare to AMT-17, which may be caused by horizontal stretching of the plot due to insufficient data points on AMT-16.

If the SASG for AMT-16 is excluded, in the upper 250 m of the water column POC concentrations decreased by 49-73%; when taking the SASG into account, POC concentrations decreased by 11-73% within this depth range.

The Latitudinal-depth contours of PON concentrations are plotted in Figure 3.16, generally showing elevated concentrations in surface waters and low values at depth. On AMT-16, the highest concentrations (>0.65 mmol N m^{-3}) of PON were found between ~25°N and ~50°N. In this region, a concomitant enhancement of POC concentrations (Fig. 3.12) was observed. Again, the elevated concentrations of POC and PON were likely the result of enhanced carbon fixation within this region. High

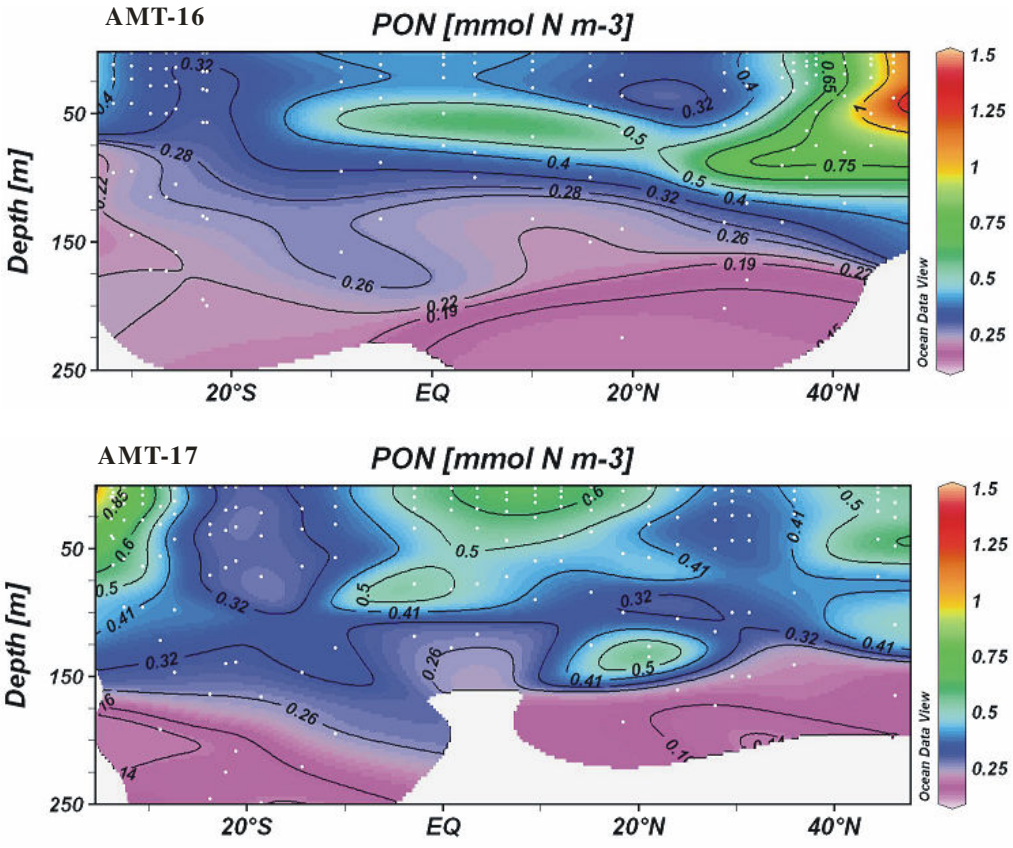

Figure 3.16. Latitudinal-depth contours of PON in the upper 250 m for AMT-16 and -17.

concentrations (>0.6 mmol N m^{-3}) were also observed in surface waters of the equatorial region between ~10°S and ~15°N, as the result of enhanced carbon fixation. The lowest concentrations (<0.15 mmol N m^{-3}) were found in subsurface waters of the north equatorial and northern subtropical regions. On AMT-17, the highest concentrations (>0.6 mmol N m^{-3}) were found in the north equatorial region, at the southeast flank of the SASG, and at the northeast flank of the NASG. Within these regions, concomitant enhanced concentrations of POC were observed, resulted from relatively high primary production. High concentrations (>5 mmol N m^{-3}) also presented at ~150 m at ~20°N. The lowest concentrations (<0.16 mmol N m^{-3}) dominated the subsurface waters across the whole Atlantic Ocean. PON concentrations decreased consistently with increasing water depth to <0.15-0.20 mmol N m^{-3} at 250 m. Over the upper 250 m of the water column, PON concentrations decreased by 53-80% when excluding the SASG for AMT-16 and 45-80% when this region was included. The profiles of PON concentrations did not show pronounced seasonal variations in the EQA and SAG.

3.6. Distribution of dissolved oxygen and AOU

The latitudinal-depth contours of dissolved oxygen concentrations are plotted in Figure 3.17, showing no significant seasonal variations. There was a clear concentration gradient present in the equatorial region that was characterised by equatorial upwelling, with relatively high concentrations (>180 μmol kg^{-1}) found in the surface (30 m) waters and relatively low values (<100 μmol kg^{-1}) in the subsurface (300 m) waters. In the subtropical gyres, there was absent of a pronounced vertical gradient in dissolved oxygen concentrations. The concentrations ranged from ~175 μmol kg^{-1} to ~200 μmol kg^{-1} in the upper 300 m.

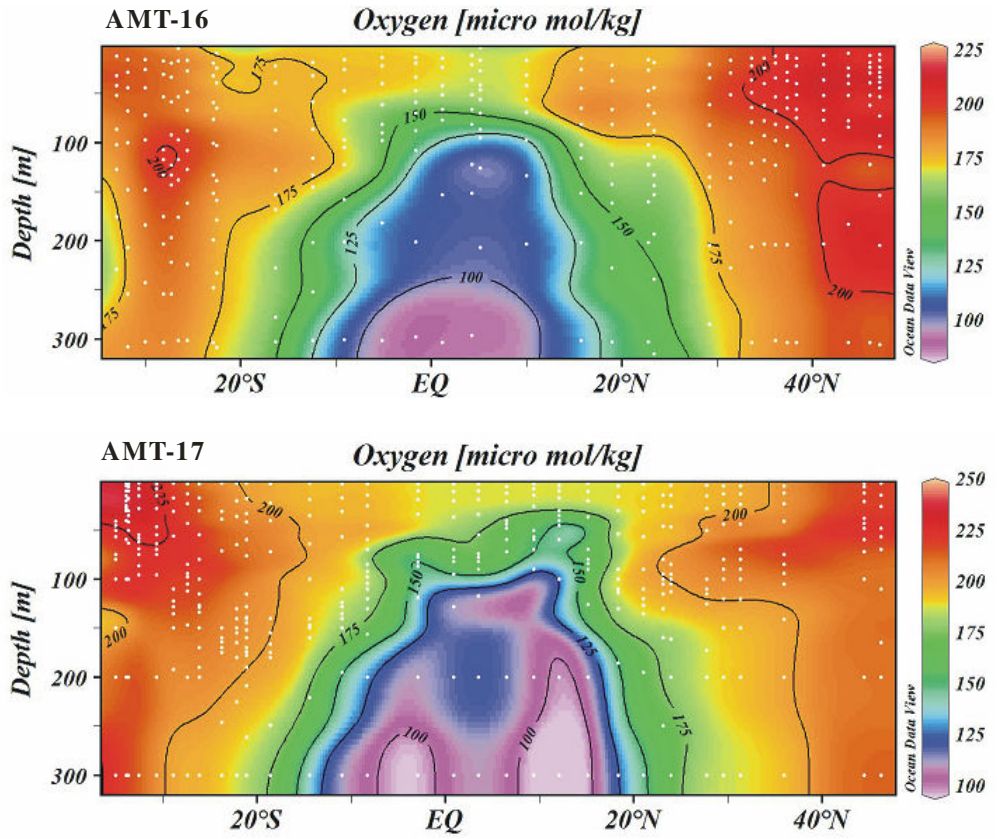

Figure 3.17. Latitudinal-depth contours of dissolved oxygen concentration in the upper 300 m on AMT-16 and -17.

The latitudinal contours of AOU concentrations are plotted in Figure 3.18. In surface waters, AOU concentrations were not significantly different from zero due to an exchange of water mass with the atmosphere. However, in water masses isolated from the atmosphere, a concentration gradient was clearly present in the whole section. In the EQA, AOU concentrations rapidly increased from zero to >150 µmol kg^{-1}, showing a strong concentration gradient that was characterised by equatorial upwelling. In the SAG, the vertical gradient was less pronounced, with a concentration of ~50 µmol kg^{-1} found at 300 m. The profiles of AOU concentrations did not show clearly seasonal variability.

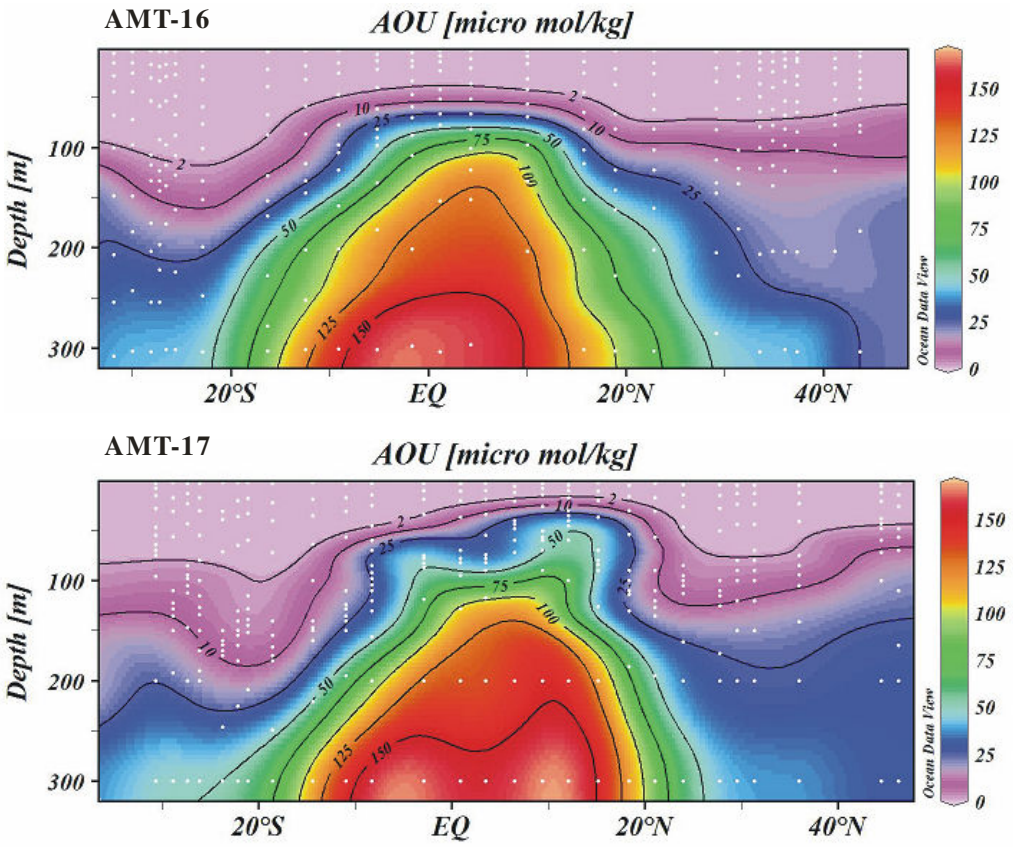

Figure 3.18. Latitudinal-depth contours of AOU concentration in the upper 300 m on AMT-16 and -17.

3.7. Distribution of nanoeukaryotic and picoeukaryotic phytoplankton, *Prochlorococcus* and *Synechococcus* spp. and heterotrophic bacterioplankton

The nanoeukaryotic and picoeukaryotic phytoplankton were the most abundant in the subsurface chlorophyll maximum, with nanoeukaryotic phytoplankton cell numbers ranging from 260 to 500 cells cm^{-3} and picoeukaryotic phytoplankton cell numbers ranging from 1,500 to 6,000 cells cm^{-3} on AMT-16 (Fig. 3.19) (nano- and picoeukaryotic phytoplankton cell numbers are not available). Peak abundance was recorded within the EQA, reaching 500 cells cm^{-3} for nanoeukaryotes at ~55 m and 6,000 cells cm^{-3} for picoeukaryotes at ~75 m. At ~40°N and ~35°S, nanoeukaryotic phytoplankton abundance exceeded 1,000 cells cm^{-3} and picoeukaryotic phytoplankton abundance exceeded 5,000 cells cm^{-3}. This may be caused by a sampling in the

relatively high productivity areas of the northern temperate waters during boreal spring and the west coast of South Africa.

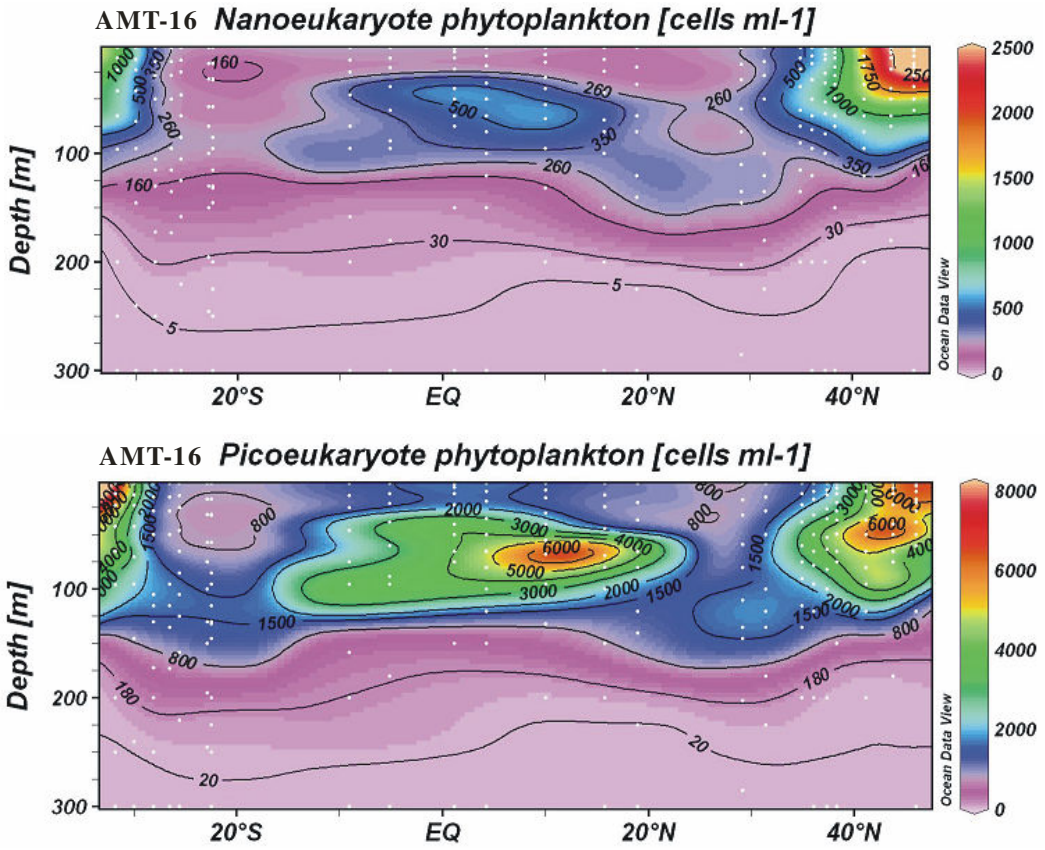

Figure 3.19. Latitudinal-depth contours of nanoeukaryotic and picoeukaryotic phytoplankton abundance in the upper 300 m for AMT-16.

The latitudinal-depth contours of *Prochlorococcus* spp. abundance are plotted in Figure 3.20, showing relatively high abundance in surface waters and relatively low values at depth. The highest populations of *Prochlorococcus* spp. were found in the equatorial region, peaking at >250,000 cells cm^{-3} on both AMT cruises, as sell as in the central southern subtropical gyre (~20°S) and at the northeast flank of the northern subtropical gyre (>40°N) on AMT-17. In surface waters of the subtropical gyres, *Prochlorococcus* abundance ranged from 100,000 cells cm^{-3} to 225,000 cells cm^{-3}. At

300 m, the populations decreased to generally <100 cells cm^{-3} across the section, apart from in the central southern subtropical region where the abundance was ~5,000 cells cm^{-3}. The profiles of *Prochlorococcus* spp. abundance showed clear seasonal variations in the SASG, but not in the EQA and the SASG.

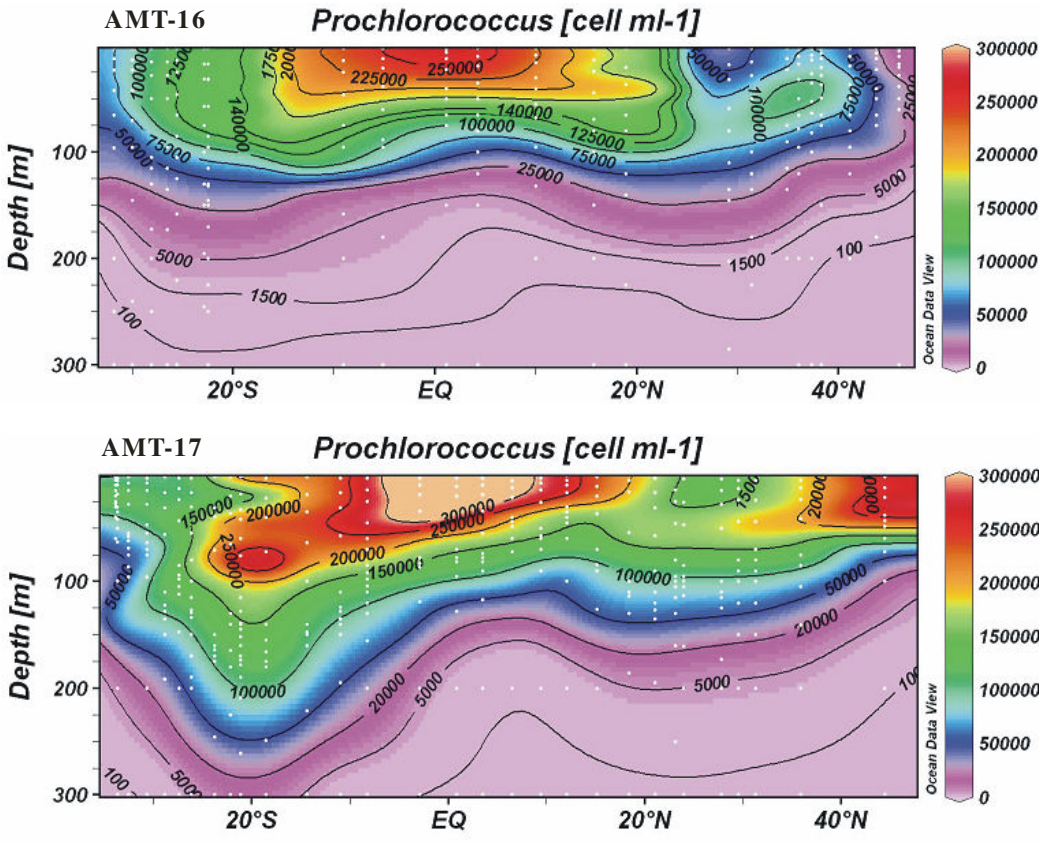

Figure 3.20. Latitudinal-depth contours of *Prochlorococcus* spp. abundance in the upper 300 m for AMT-16 and -17.

The latitudinal-depth contours of *Synechococcus* spp. populations are plotted in Figure 3.21, showing highest abundance (>4,000 cells cm^{-3}) in surface waters of the equatorial region, and at the flanks of the northern and southern subtropical gyres. In surface waters of the central subtropical gyres, *Synechococcus* populations were generally <2,000 cells cm^{-3}. At 300 m, *Synechococcus* abundance decreased to <50 cells cm^{-3}

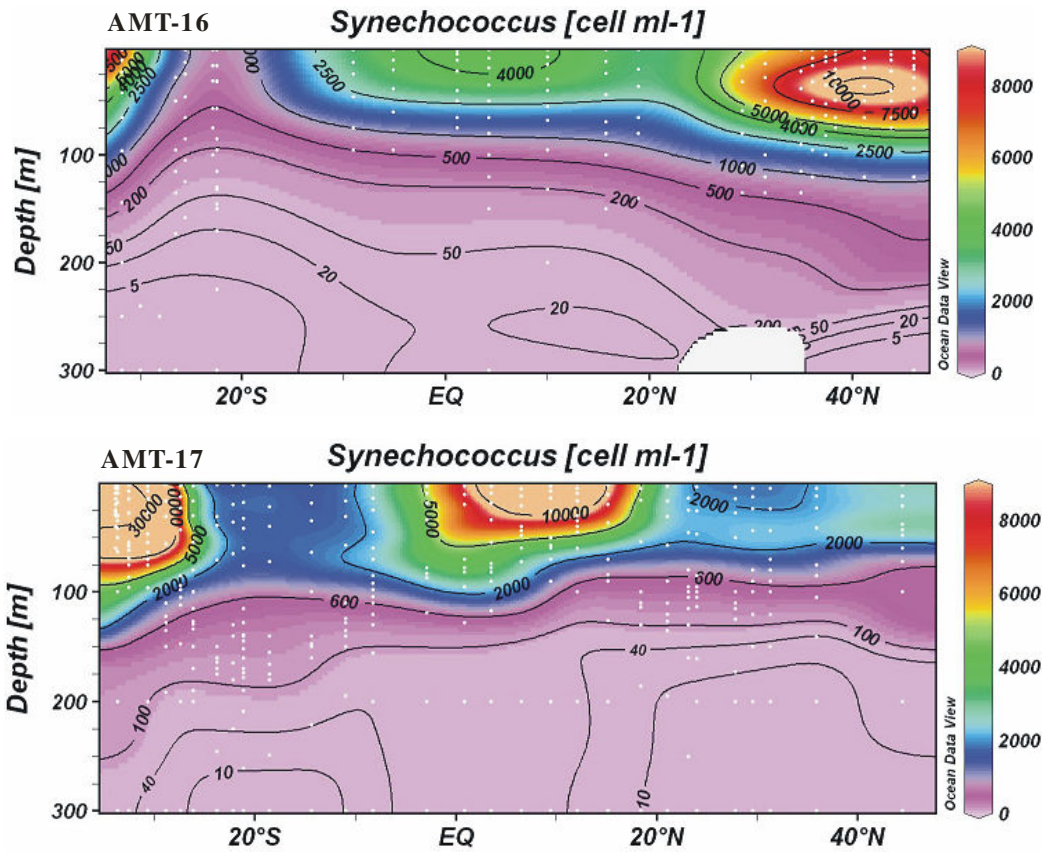

Figure 3.21. Latitudinal-depth contours of *Synechococcus* spp. abundance in the upper 300 m for AMT-16 and -17.

throughout the section. Comparing two AMT cruises, there were relatively higher populations of *Synechococcus* observed in the EQA on AMT-17 relative to AMT-16; at ~40^{o}N, enhancement of *Synechococcus* abundance was found in boreal spring relative to boreal autumn; at ~30^{o}S, an elevation of *Synechococcus* populations was found in austral spring relative to austral autumn. The differences in *Synechococcus* abundance observed between AMT-16 and -17 cruises suggested that seasonal variations seemed to be more pronounced in temperate waters. However, the intercruise differences in the equatorial region need a further assessment.

The profiles of heterotrophic bacterioplankton populations are shown in Figure 3.22.

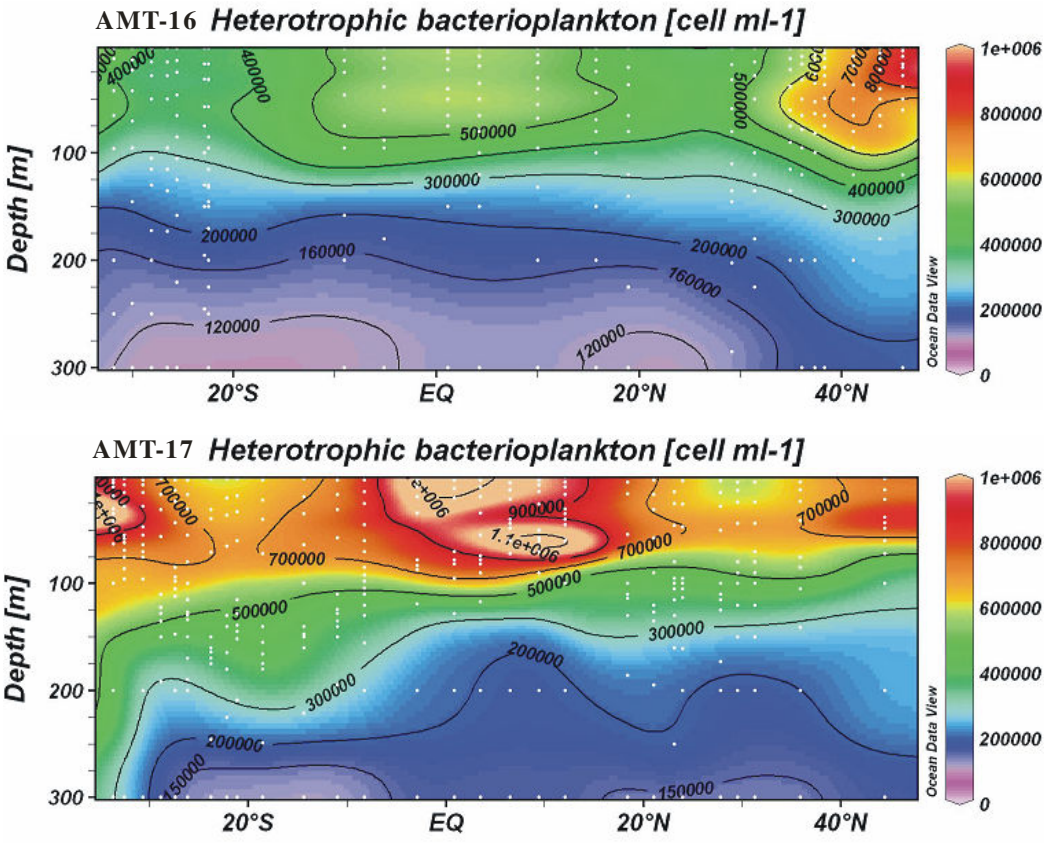

Figure 3.22. Latitudinal-depth contours of heterotrophic bacterioplankton abundance in the upper 300 m for AMT-16 and -17.

Relatively high abundance was found in surface waters of the equatorial region, peaking at >500,000 cells cm^{-3} on AMT-16, and >600,000 cells cm^{-3} on AMT-17. The highest populations (>800,000 cells cm^{-3}) were observed at the flanks of the NASG and SASG, although relatively low abundance (>400,000 cells cm^{-3}) was found at the flank of the SASG on AMT-16. This high abundance observed in surface water of the temperate regions was likely a consequence of the elevated concentrations of dissolved organic nutrients and suspended particles serving as food substrate in support of microbial community. Compared with the equatorial and the temperate regions, the populations were relatively low in the central gyres, with <500,000 cells cm^{-3} observed on AMT-16 and <700,000 cells cm^{-3} observed on AMT-17, respectively. Enhanced

abundance of heterotrophic bacterioplankton observed in surface waters rapidly decreased with increasing water depth. From surface waters to a depth of 300 m, concentrations decreased by 70-85%. The latitudinal-depth contours of heterotrophic bacterioplankton abundance showed relatively more pronounced seasonal variability in the SASG compared to the NASG. The intercruise differences in the EQA require further investigation.

4. Discussion

4.1. Comparison of DOC, DON and DOP concentrations with literature values

A summary of concentrations of DOC, DON and DOP for the surface and deep-ocean is presented in Table 4.1. Data on the concentrations from selected open ocean basins are summarised, and a range of values of DOC, DON and DOP is presented in Table 4.2. My results show a good agreement with literature findings. Table 4.2, a summary of Table 4.1, suggests that in surface (0-50 m) waters of the open oceans the highest DOM concentrations are generally present in equatorial and continental shelf regions due to enhanced primary production sourced by upwelled nutrients, and the lowest concentrations are present in Antarctic waters as well as the Southern Ocean where low-DOM, deep-ocean water mixes to the surface. Furthermore, in the deep (>1000 m) waters the highest concentrations are present in Atlantic deep water and Antarctic bottom water, with the lowest values generally present in Pacific deep water, possibly as a consequence of slow abiotic transformation of refractory DOM during water mass movement following the great “oceanic conveyor belt” (Hansell 2002).

Location	Sampling date	Depth (m)	DOC			DON			DOP		
			Method	Concentration (μM)	Reference	Method	Concentration (μM)	Reference	Method	Concentration (μM)	Reference
Atlantic											
Northern subtropical gyre (BATS site)	1988 - 1993	0 - 50	HTC	62 - 85	Ducklow *et al.* 1995						
		200	HTC	53 - 63	Ducklow *et al.* 1995						
	1994 - 1998	0 - 100	HTC	60 - 70*	Hansell and Carlson 2001	UV	4.0 - 5.5*	Hansell and Carlson 2001			
		1000 - 4500	HTC	43.0 - 44.2*	Hansell and Carlson 2001	UV	2.7 - 3.5*	Hansell and Carlson 2001			
Northern subtropical gyre	Apr - May 2000	0 - 100				UV	4.0 - 6.5	Mahaffey *et al.* 2004	UV	0.05 - 0.40	Mahaffey *et al.* 2004
	May - Jun 2005	0 - 50	HTC	65 - 80	this study						
		300	HTC	53 - 56	this study						
		1000 - 5000	HTC	42 - 44	this study						
Northern subtropical gyre	Oct - Nov 2005	0 - 50	HTC	65 - 78	this study	HTC	4.5 - 6.5	this study	UV	0.20 - 0.28	this study
		300	HTC	45 - 55	this study	HTC	2.8 - 4.3	this study	UV	0.05 - 0.06	this study
		1000 - 5000	HTC	43 - 44	this study	HTC	1.9 - 2.5	this study	UV	0.019 - 0.024	this study
Northwestern Sargasso Sea (BATS site and Hydrostation S)	Spring 1992	0 - 50	HTC	65 - 85*	Carlson *et al.* 1994						
	Summer 1992 and 1993	0 - 50	HTC	65 - 80*	Carlson *et al.* 1994						
	Autumn 1991 and 1992	0 - 50	HTC	68 - 71*	Carlson *et al.* 1994						
	Winter 1992 and 1993	0 - 50	HTC	62 - 66*	Carlson *et al.* 1994						
Southern subtropical gyre	Apr - May 2000	0 - 100				UV	3.0 - 5.5	Mahaffey *et al.* 2004	UV	~ 0.10	Mahaffey *et al.* 2004
	May - Jun 2005	0 - 50	HTC	70 - 82	this study						
		300	HTC	53 - 55	this study						
		1000 - 5000	HTC	43.0 - 46.4	this study						
	Oct - Nov 2005	0 - 50	HTC	65 - 81	this study	HTC	4.8 - 6.5	this study	UV	0.12 - 0.28	this study
		300	HTC	48 - 45	this study	HTC	2.6 - 3.6	this study	UV	0.04 - 0.05	this study
		1000 - 5000	HTC	43.1 - 44.4	this study	HTC	2.0 - 2.4	this study	UV	0.020 - 0.025	this study
Equatorial Atlantic	Aug 1991 and Nov 1992	surface	HTC	66 - 97	Thomas *et al.* 1995						

(Continues)

(Continued)

Location	Sampling date	Depth (m)	DOC Method	DOC Concentration (µM)	DOC Reference	DON Method	DON Concentration (µM)	DON Reference	DOP Method	DOP Concentration (µM)	DOP Reference
Atlantic											
Equatorial Atlantic	Oct - Nov 1995	0 - 100				PO	7.0 - 11.0	Vidal *et al.* 1999	PO	0.1 - 0.3	Vidal *et al.* 1999
	Apr - May 2000	0 - 100				UV	5.0 - 6.5	Mahaffey *et al.* 2004	UV	0.10 - 0.25	Mahaffey *et al.* 2004
	May - Jun 2005	0 - 50	HTC	70 - 82	this study						
		300	HTC	53 - 55	this study						
		1000 - 5000	HTC	43 - 45	this study						
	Oct - Nov 2005	0 - 50	HTC	60 - 78	this study	HTC	4.3 - 6.0	this study	UV	0.12 - 0.28	this study
		300	HTC	50 - 55	this study	HTC	3.5 - 4.0	this study	UV	0.04 - 0.08	this study
Northeastern Atlantic	Jun - Jul 1996	0 - 50	HTC	50 - 65	Däfner and Koeve 2001	HTC	~ 6.0	Kahler and Koeve 2001			
		1000 - 2500	HTC	~ 44	Däfner and Koeve 2001	HTC	< 5.0	Kahler and Koeve 2001			
	Oct 1987 and July 1990	Surface	HTC and PO	61 - 62	Aminot and Kerouel 2004	PO	4.2 - 4.5	Aminot and Kerouel 2004	UV	0.07 - 0.14	Aminot and Kerouel 2004
		1500 - 2000	HTC and PO	44 - 46	Aminot and Kerouel 2004	PO	2.6 - 2.8	Aminot and Kerouel 2004	UV	0.02 - 0.03	Aminot and Kerouel 2004
Pacific											
Northern subtropical gyre	May 1980 - May 1981	0 - 100				UV	~ 3.6	Smith *et al.* 1986	UV	~ 0.20	Smith *et al.* 1986
		900				UV	1.5	Smith *et al.* 1986	UV	< 0.02	Smith *et al.* 1986
	Nov 1997	0 - 50	HTC	63 - 75*	Abell *et al.* 2000	UV	5.2 - 6.6*	Abell *et al.* 2000	UV	0.14 - 0.25*	Abell *et al.* 2000
		300	HTC	40 - 45*	Abell *et al.* 2000	UV	2.5 - 3.5*	Abell *et al.* 2000	UV	< 0.06*	Abell *et al.* 2000
Northern subtropical gyre (Sta. ALOHA)	Oct 1988 - Dec 1997	0 - 100				UV	4.0 - 8.0*	Karl *et al.* 2001	UV	0.10 - 0.35*	Karl *et al.* 2001
		300				UV	3.0 - 5.0*	Karl *et al.* 2001	UV	0.05 - 0.20*	Karl *et al.* 2001
		1000				UV	1.5 - 2.5*	Karl *et al.* 2001	UV	0.01 - 0.04*	Karl *et al.* 2001

(Continues)

(Continued)

Location	Sampling date	Depth (m)	DOC Method	DOC Concentration (µM)	DOC Reference	DON Method	DON Concentration (µM)	DON Reference	DOP Method	DOP Concentration (µM)	DOP Reference
Pacific											
Equatorial Pacific	Feb - Apr 1992	surface	HTC and PO	60 - 79*	Sharp *et al.* 1995						
		1000 - 4000	HTC and PO	35 - 40*	Sharp *et al.* 1995						
	Feb - Mar and Aug - Sep 1992	0 - 50	HTC	60 - 80*	Peltzer and Hayward 1996						
		1000 - 4500	HTC	38 - 40*	Peltzer and Hayward 1996						
	Sep - Nov 1992	0 - 40				PO	7.0 - 9.4*	Libby and Wheeler 1997			
		200				PO	< 5.0*	Libby and Wheeler 1997			
North Pacific		surface							PO	0.10 - 0.22	Yoshimura *et al.* 2007
	Jun 1995	0 - 100	UV	63 - 72	Loh and Bauer 2000	PO	3.9 - 4.5	Loh and Bauer 2000	HTA	0.225 - 0.229	Loh and Bauer 2000
		1000 - 4000	UV	37 - 40	Loh and Bauer 2000	PO	1.7 - 2.7	Loh and Bauer 2000	HTA	0.073 - 0.105	Loh and Bauer 2000
East Pacific		0 - 30	HTC	~ 80*	Hansell and Waterhouse 1997	UV	5.0 - 7.5	Hansell and Waterhouse 1997			
Continental shelf											
Georges Bank	Apr 1993	surface	HTC	72 - 85	Chen *et al.* 1996						
		1000 - 1500	HTC	50 - 55	Chen *et al.* 1996						
	Mar and Aug 1996	surface	HTC	~ 125	Hopkinson *et al.* 1997	UV	~ 10.2	Hopkinson *et al.* 1997	UV	~ 0.3	Hopkinson *et al.* 1997
		~ 1600	HTC	~ 46.7	Hopkinson *et al.* 1997	UV	~ 2.76	Hopkinson *et al.* 1997	UV	~ 0.03	Hopkinson *et al.* 1997
Mid-Atlantic Bight	Apr 1994, Mar 1996 and Aug 1996	0 - 20	HTC	60 - 165	Vlahos *et al.* 2002						
		200	HTC	42 - 56	Vlahos *et al.* 2002						

(Continues)

(Continued)

Location	Sampling date	Depth (m)	DOC Method	DOC Concentration (µM)	DOC Reference	DON Method	DON Concentration (µM)	DON Reference	DOP Method	DOP Concentration (µM)	DOP Reference
Continental shelf											
Southern California Bight	Apr, Jul and Aug 1990	0 - 50	HTC	85 - 98	Hansell *et al.* 1993	HTC	1 - 10	Hansell *et al.* 1993			
		600 - 800	HTC	62 - 74	Hansell *et al.* 1993	HTC	1 - 7	Hansell *et al.* 1993			
Southern Ocean											
56°S - 65°S, 140°W	Sep - Nov 1995	0 - 50	PO plus UV	50 - 62	Däfner *et al.* 1999						
		1000 - 4500	PO plus UV	42 - 48	Däfner *et al.* 1999						
	Jan 1995	surface	HTC	45 - 55	Ogawa *et al.* 1999	HTC	4.0 - 9.0	Ogawa *et al.* 1999			
		1000 - 3500	HTC	40 - 46	Ogawa *et al.* 1999	HTC	2.0 - 4.0	Ogawa *et al.* 1999			
47°S - 60°S, 6'W	Oct - Nov 1993	0-100	HTC	38 - 55	Däfner *et al.* 1997	HTC	5.0 - 9.0	Däfner *et al.* 1997			
		300 - 4000	HTC	34 - 38	Däfner *et al.* 1997						
34°50'N, 123°0'W	Dec 1995 - Jan 1996	0 - 100	HTC	50 - 53	Loh and Bauer, 2000	PO	4.0 - 4.4	Loh and Bauer 2000	HTA	0.148 - 0.225	Loh and Bauer 2000
		1000 - 4000	HTC	39 - 46	Loh and Bauer, 2000	PO	3.0 - 4.4	Loh and Bauer 2000	HTA	0.074 - 0.169	Loh and Bauer 2000
Antarctica											
Ross Sea polynya	1994 - 1997	0 - 50	HTC	41 - 65	Carlson *et al.* 2000						
		0 - 150	HTC		Carlson *et al.* 2000	HTC	2.1 - 6.3	Carlson *et al.* 2000			
		> 150	HTC		Carlson *et al.* 2000	HTC	2.1 - 2.7	Carlson *et al.* 2000			
		300 - 800	HTC	41.0 - 42.6	Carlson *et al.* 2000						
Drake Passage	Dec 1997 - Jan 1998	0 - 50				UV	3.0 - 7.0*	Sanders and Jickells 2000	UV	0.08 - 0.16*	Sanders and Jickells 2000
		1000 - 3500				UV	2.0 - 3.0*	Sanders and Jickells 2000	UV	0.05* - ND	Sanders and Jickells 2000

(Continues)

(Continued)

[a] high temperature combustion

[b] ultra-violet oxidation

[c] Persulphate oxidation

[d] Non-detectable

[e] High temperature ashing

* Sampling without filtration

Table 4.1. Selected DOC, DON and DOP concentrations from different oceanographic environments.

Location	Range of DOC Concentration (μM)	Range of DON Concentration (μM)	Range of DOP Concentration (μM)
0 - 50 m			
Northern Atlantic subtropical gyre	62-85	4.5-6.5	0.20-0.28
Southern Atlantic subtropical gyre	65-82	4.8-6.5	0.12-0.28
Equatorial Atlantic	60-97	4.3-6.0	0.12-0.28
Northeastern Atlantic	50-65	4.2-6.0	0.07-0.14
Northern Pacific subtropical gyre	63-75	5.2-6.6	0.14-0.25
Equatorial Pacific		7.0-9.4	
Continental shelf	60-165	1.0-10.2	~0.3
Southern Ocean	45-62	4.0-9.0	
Ross Sea	41-65	3.0-7.0	0.08-0.16
Greater than 1000 m			
Northern Atlantic subtropical gyre	42-45	1.9-3.5	0.019-0.024
Southern Atlantic subtropical gyre	43.0-46.4	2.0-2.4	0.020-0.025
Equatorial Atlantic	43-45		
Northeastern Atlantic	44-46	2.6-2.8	0.02-0.03
Northern Pacific subtropical gyre		1.5-2.5	0.01-0.04
Equatorial Pacific	35-40		
Continental shelf	46-55	2.7	0.03
Southern Ocean	39-48	2.0-4.4	0.074-0.169
Ross Sea		2.0-3.0	< 0.05

Table 4.2. Summarised DOC, DON and DOP concentration ranges of Table 4.1.

4.2. Implications from the vertical profiles of DOC, DON and DOP

DOC measurements on samples collected from below 1000 m (Fig. 4.1) showed an average concentration of 44 μM (43.0-46.4 μM). If the refractory pool of DOM is best presented by the deep ocean DOM stocks (>1000 m) (Williams and Druffels 1987; Bauer et al., 1992), 44 μM DOC can be classed as the refractory pool. In other words, 50-80% of the DOC accumulated in the upper 50 m was not biologically utilisable. Other studies have reported that refractory DOC accounted for 62%, 62-73% and 73-88% of the bulk DOC pool in the equatorial Pacific Ocean (Carlson and Ducklow 1995), in the Sargasso Sea at the BATS site (Hansell and Carlson 2001a) and in the Southern Ocean (Ogawa *et al.* 1999), respectively. The profiles of DOC (Fig 3.4) suggest that the bulk DOC concentrations decreased by 18-43% from the values in

surface (0-30 m) waters to 300 m depth, and that the semilabile DOC concentrations decreased by 46-97% (Tab. 4.3) within this depth range. In the EQA province, the semilabile DOC decreased by 69-74% on AMT-16 compared to 84-95% on AMT-17; in the SAG province, the semilabile DOC decreased by 57-74% on AMT-16 compared to 46-97% on AMT-17. The intercruise difference is more pronounced in the equatorial region, which may be caused by a different strength of the equatorial upwelling during these two AMT cruises. A stronger upwelling during AMT-17 was evidenced by the presence of the water mass with a temperature of <12.5°C at 150 m compared to 250 m during AMT-16. As a result, subsurface (250-300 m) waters in the equatorial region were occupied by the water mass with a DOC concentration of <48 µM on AMT-17 compared to those with a DOC concentration of <56 µM on AMT-16, leading to the pronounced intercruise differences in DOC distributions in the upper 300 m in the EAQ province.

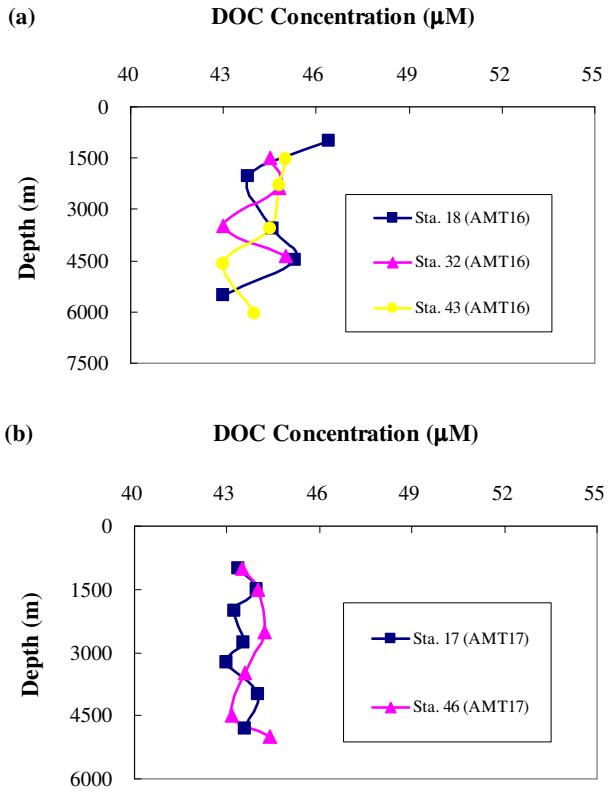

Figure 4.1. Depth profiles of DOC concentrations on samples collected from below 1000 m on (a) AMT-16 and (b) AMT-17.

DOC pool	Percentage (%)	DOC pool	Percentage (%)
Bulk DOC			
AMT-16		AMT-17	
SASG	23-27 (27)	SASG	18-36 (25)
EQA	31-35 (33)	EQA	37-43 (39)
NASG	22-35 (29)	NASG	26-42 (31)
Semilabile (labile) DOC			
AMT-16		AMT-17	
SASG	62-74 (65)	SASG	46-87 (70)
EQA	69-74 (71)	EQA	84-94 (91)
NASG	57-74 (69)	NASG	54-97 (75)

Table 4.3. Reduction with depth of bulk and semilabile (labile) DOC concentrations from the surface (0-50 m) to 300 m. Concentrations in parentheses are mean values.

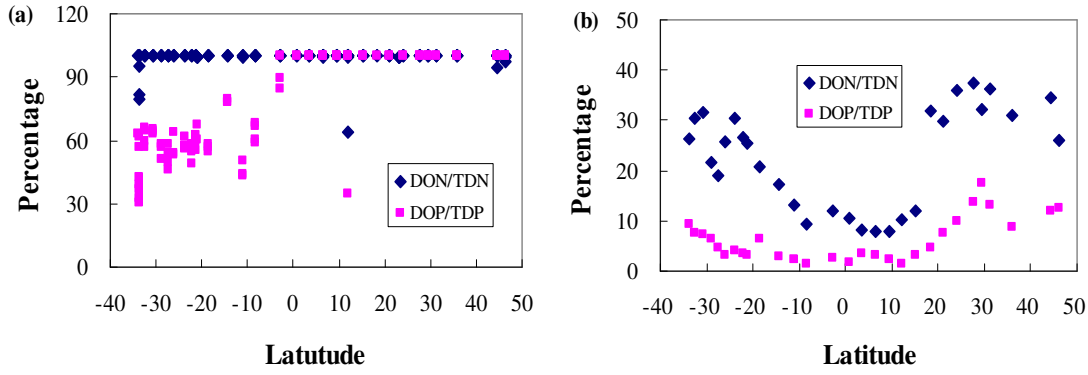

Figure 4.2 DON and DOP concentrations as percentage of TDN and TDP (a) in surface (0-50 m) waters and (b) at 300 m depth on AMT-17.

In the upper 50 m, DON and DOP dominated TDN and TDP pools and accounted for an average of 99% and 80% of the total dissolved pools, respectively (Fig. 4.2a). The dissolved organic nutrient contribution to the total dissolved nutrient concentration decreased rapidly with increasing water depth. At 300 m, DON accounted for ~22% of the TDN pool and DOP accounted for ~6% of the TDP pool (Fig. 4.2b). Within this depth range, the bulk DON concentrations decreased by 14-46%, and the bulk DOP concentrations decreased by 68-82% (Tab. 4.4). Measurements on samples collected from below 1000 m indicated a mean of 2.3 µM (1.9-2.5 µM) DON and 0.020 µM

(0.019-0.024 μM) DOP which can be classed as biologically refractory pools (Fig. 4.3), implying that in the upper 50 m 47-65% of the DON and 87-93% of the DOP were semilabile. Compared with DON, a major part of DOP in surface waters was in a semilabile form. This semilabile DOP was mineralised more efficiently (or overturned more rapidly) than the semilabile DON, leading to a reduction of 90-93% for the semilabile DOP pool compared to 48-65% for the semilabile DON pool within the upper 300 m (Tab. 4.4). Other studies have reported that the semilabile DON accounted for 33-42%, 38-81%, 31-62% and 33-71% of the surface DON pool in the Northeastern Atlantic (Aminot and Kerouel 2004), the northern subtropical Pacific (Karl *et al.* 2001a), the North Pacific Ocean (Loh and Bauer 2000), and Drake Passage (Sanders and Jickells 2000), respectively, and that the semilabile DOP accounted for 57-80%, 60-97%, 53-68% and 38-69% of the surface DOP pool in the Northeastern Atlantic (Aminot and Kerouel 2004), the northern subtropical Pacific (Karl *et al.* 2001), the North Pacific Ocean (Loh and Bauer 2000), and Drake Passage (Sanders and Jickells 2000), respectively. My results are in agreement with literature findings.

DON pool	Percentage (%)	DOP pool	Percentage (%)
Bulk pool			
SASG	20-35 (26)	SASG	68-82 (76)
EQA	27-46 (34)	EQA	75-80 (77)
NASG	14-31 (23)	NASG	73-76 (74)
Semilabile (labile) pool			
SASG	37-57 (43)	SASG	75-88 (81)
EQA	49-78 (61)	EQA	83-87 (85)
NASG	26-62 (41)	NASG	80-84 (83)

Table 4.4. Reduction with depth of bulk and semilabile (labile) DON and DOP concentrations from the surface (0-50 m) to 300 m. Concentrations in parentheses are mean values.

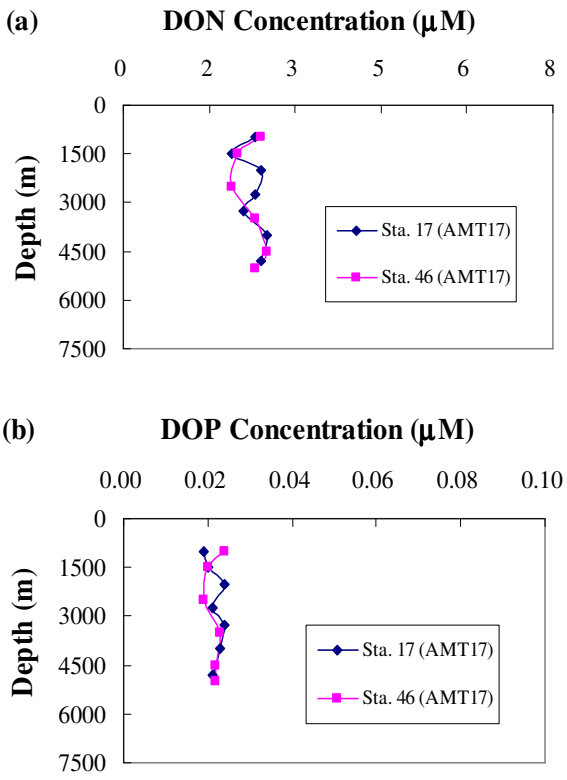

Figure 4.3. Depth profiles of (a) DON and (b) DOP concentrations on samples collected from below 1000 m on AMT-17.

4.3. Biological controls on the distributions of DOC, DON and DOP in surface waters

Carlson *et al.* (1994) emphasised that concentrations of DOM in the surface oceans were controlled by both physical and biological processes. In this section, I focus on biological indicators to discern the importance of biological processes on DON and DOP distributions in euphotic waters with a density <26 σ_t. This depth interval was chosen in order to aid comparison with the depth range chosen by Mahaffey *et al.* (2004) and Roussenov *et al.* (2006), who provided evidence that physical processes (*i.e.* Ekman transport) were important in the distributions of DON and DOP in the Atlantic Ocean. There were extremely limited studies to make even rudimentary assessments of the factors controlling the storage of DOM (Hansell and Waterhouse 1997), although the importance of biology to the turnover of DOM is self-evident (Hansell 2002). The paucity of this study was due to the fact that the roles of biological and chemical processes in directly controlling the storage of DOC were very difficult to quantify (Hansell and Waterhouse 1997). The measured biological and chemical variables were

the net production due to the decoupling of biological production and consumption processes (Carlson 2002). These bulk measurements did not provide insight into the separated production and consumption processes, not to mention their roles in regulating DOC accumulation.

To facilitate an evaluation of the potential biological controls, correlations of DOC, DON and DOP were compared with chlorophyll-a, rates of primary production, DIN, DIP, *Prochlorococcus*, *Synechococcus* and heterotrophic bacterioplankton using Model-II regressions. This approach was chosen over Model-I regression, as Model-II regression minimised residuals perpendicular to the line of best fit rather than minimising residuals in the y-direction (Sanders and Jickells 2000). As discussed in Chapter 3, there existed certain spatial variations in these biological and chemical variables. Hence, the correlation analyses for the entire Atlantic Ocean may not reflect the regional relationships between these variables. For this reason, I compared DOC, DON and DOP with these biological and chemical variables for the SASG, EQA and NASG, respectively, for both AMT cruises (if applicable).

4.3.1. Relations with chlorophyll-a and rates of carbon fixation

There were no statistically significant correlations between the relationships of DOC/DON/DOP, chlorophyll-a and the rates of carbon fixation (Fig. 4.4), suggesting that phytoplankton biomass and primary production were not the important controls of the cumulative DOC, DON and DOP in surface waters of the Atlantic Ocean. Hansell and Waterhouse (1997) reported a poor correlation between DOC and rates of primary production, based on a transect in the Pacific Ocean between ~70^{o}S and ~25^{o}N. The authors suggested that physical processes or other factors may primarily support the DOC accumulation in the Pacific Ocean. The weakened correlations between DOM and chlorophyll-a and rates of carbon fixation reflected the consequence of the interaction between the physical processes and biological responses of the planktonic ecosystem.

Clearly, in open oceans accumulation of phytoplankton biomass and enhancement of productivity can take place where increased vertical mixing allowed for the existence of relatively higher levels of nutrients in surface waters, thereby illuminating the layers or the depth of the nutricline shoaled in the euphotic zone (Marañón *et al.* 2000). As a result, there was normally a relatively higher growth rate of phytoplankton and

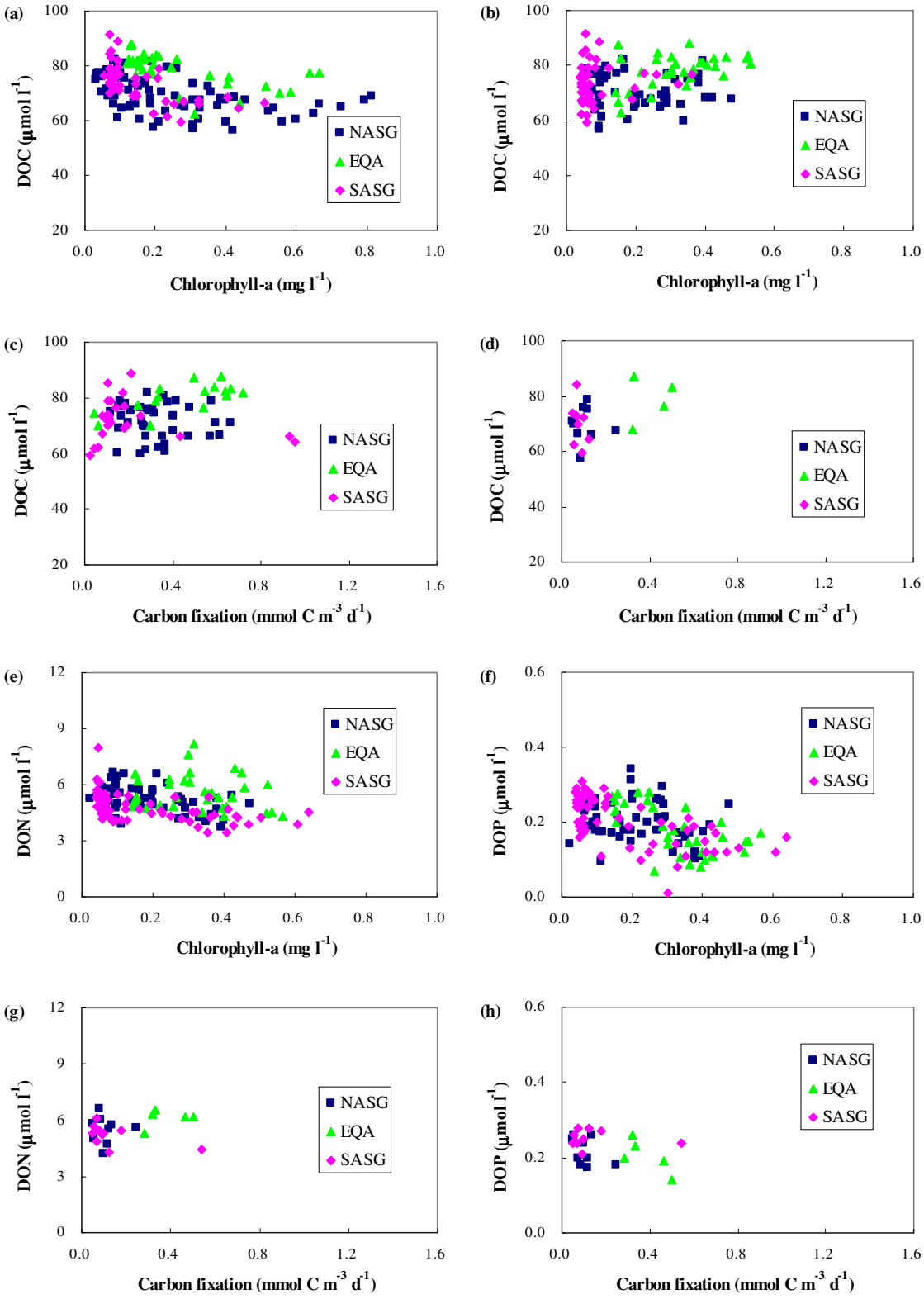

Figure. 4.4. Correlations of (a) DOC and chlorophyll-a for AMT-16, (b) DOC and chlorophyll-a for AMT-17, (c) DOC and rate of carbon fixation for AMT-16, (d) DOC and rate of carbon fixation for AMT-17, (e) DON and chlorophyll-a for AMT-17, (f) DOP and chlorophyll-a for AMT-17, (g) DON and rate of carbon fixation for AMT-17, and (h) DOP and rate of carbon fixation for AMT-17.

production that was associated with a relatively deepening of MLD (Marañón *et al.* 2000). However, the changes observed in the rates of primary production did not covary with the changes observed in phytoplankton biomass (Fig. 4.5). The relative constancy of phytoplankton biomass in spite of the changes in productivity implied an important role for grazing as a control of phytoplankton stocks. Studies have shown that a difference in the trophic structure (*i.e.* zooplankton assemblages) can lead to a significant variation in the rate of phytoplankton growth (Marañón 2005). Reported growth rates of phytoplankton ranged from average values of ~0.2 d^{-1} (Goericke and Welshmeyer 1998; Marañón *et al.* 2000) to average values near (Malone *et al.*1993; Quevedo and Anadon 2001) or well above 1 d^{-1} (Laws *et al.* 1987) in the Atlantic Ocean. Zooplankton grazing can remove 1-77% of the phytoplankton production, depending on the ecosystem (Sherr and Sherr 1988). Unfortunately, the composition of zooplankton community in the Atlantic Ocean was unclear, leading to the null hypothesis that zooplankton grazing may play an important control in controlling phytoplankton standing stock, thus causing decoupled correlations between DOM and chlorophyll-a and the rates of primary production.

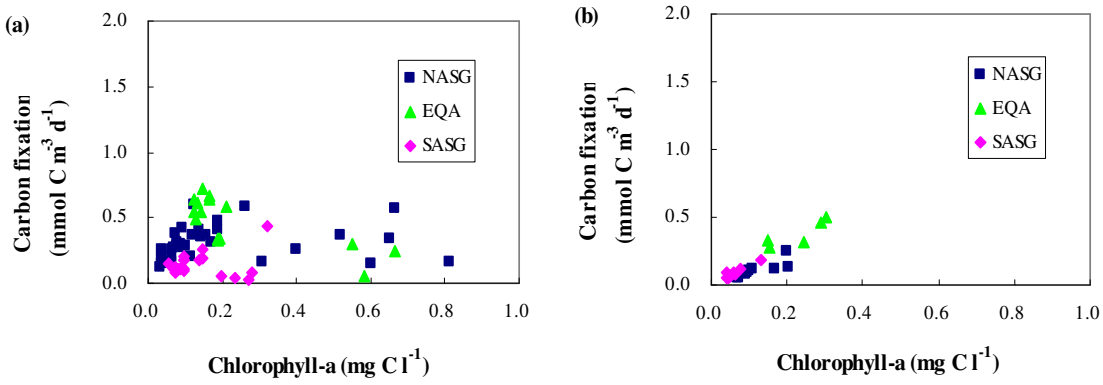

Figure 4.5. Correlations of (a) chlorophyll-a and rate of carbon fixation for AMT-16 and (b) chlorophyll-a and rate of carbon fixation for AMT-17. Rates of carbon fixation were determined only at 55% light depth during AMT-17.

4.3.2. Relations with dissolved inorganic nutrients

DOM is a byproduct of photosynthetic production (Ducklow and Carlson 1992), and N and P are the key elements that limit biological productivity (Redfield *et al.* 1963).

Therefore, the importance of availability of DIN and DIP to DOM production is self-evident (Smith *et al.* 1986). Assessments of DIN and DIP in controlling the storage of DOM are essential for understanding the global budgets and cycling of C, N and P.

Correlation analyses of dissolved inorganic and dissolved organic nutrients suggested that DIN and DIP were not highly coupled with DOC, DON and DOP (Fig. 4.6). Thomas *et al*. (1971) reported that DON concentrations in the North Pacific were greatest where inorganic nitrogen concentrations were lowest. Butler *et al.* (1979) found strong relationships between DIN and DON in the English Channel, where most of the nitrate drawdown was explained by the DON increase. Orrett and Karl (1987) reported a pronounced increase in $DO^{32}P$ that followed by a decrease in $DI^{32}P$ during seawater incubations undertaken in the North Pacific Ocean. The data published by Libby and Wheeler (1997) suggested a coupled relationship of DON and DIN in the equatorial Pacific Ocean. Sanders and Jickells (2000) found that DON and DOP were decoupled with DIN and DIP in Drake Passage. Zee and Chou (2005) reported covariations of DIN-to-DON and DIP-to-DOP relationships in Southern Bight of the North Sea.

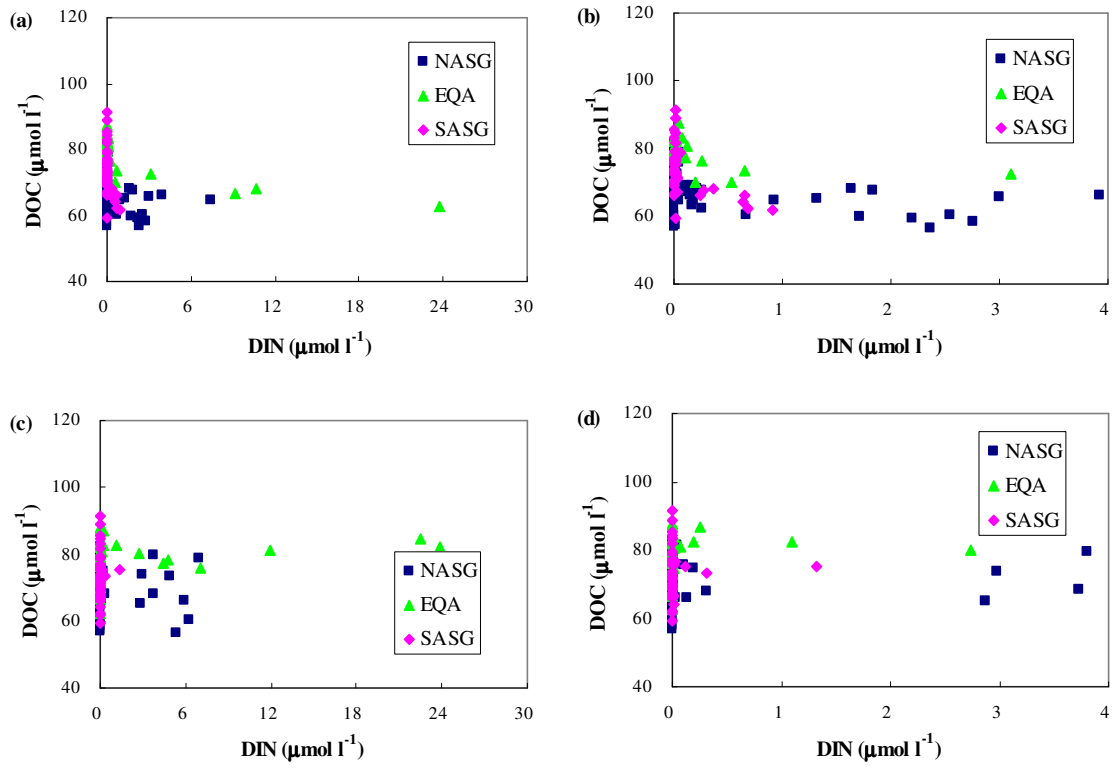

(*Continues*)

(*Continued*)

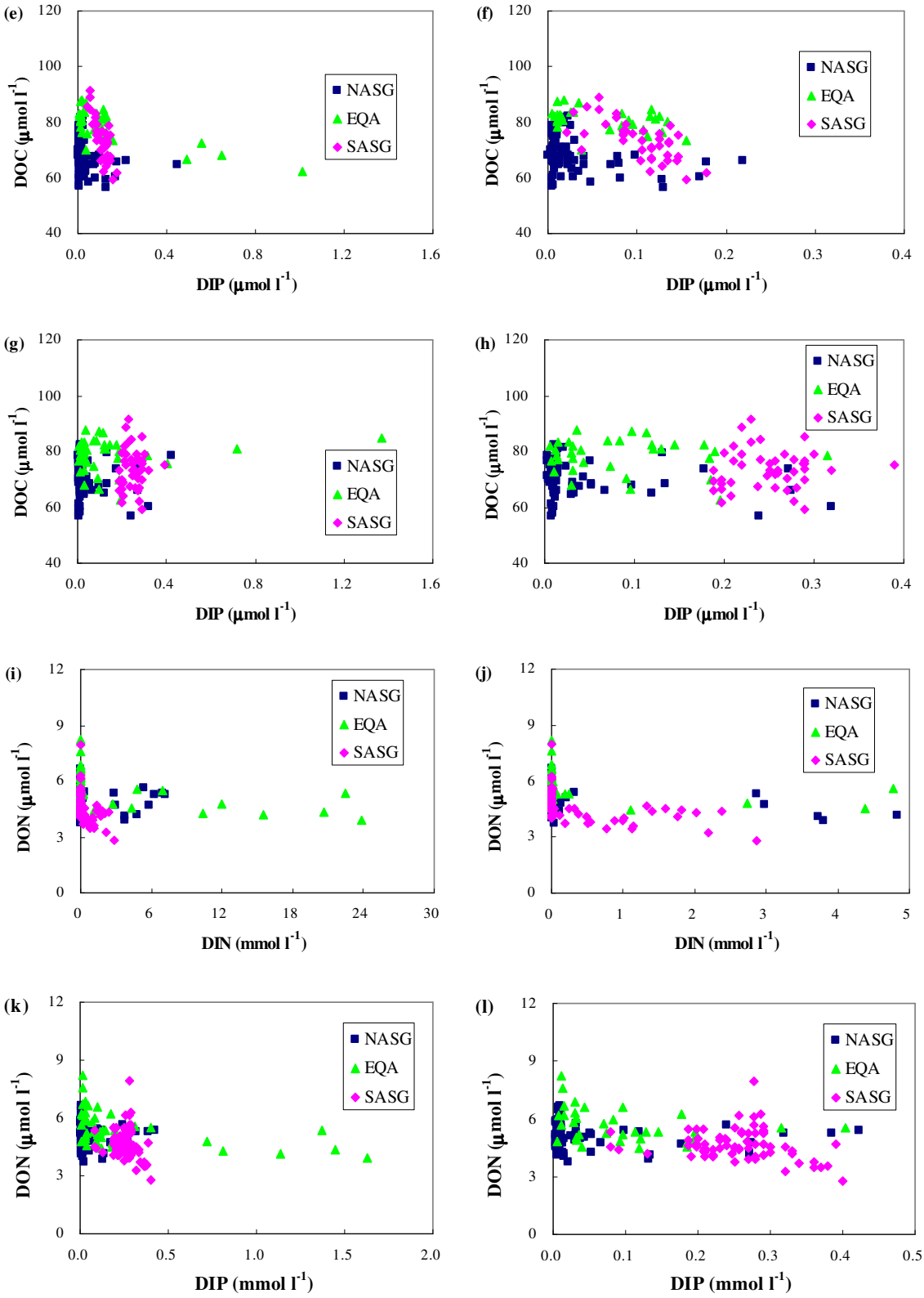

(*Continues*)

(*Continued*)

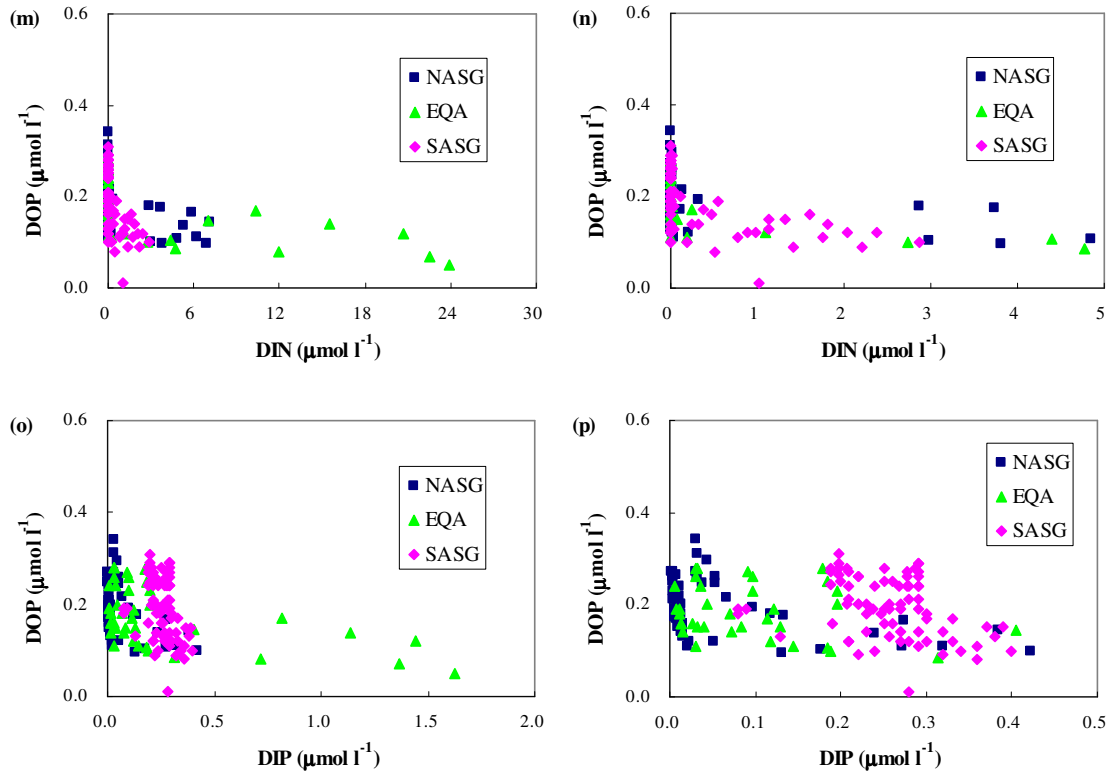

Figure 4.6. Correlations of (a) DOC and DIN for AMT-16, (b) DOC and DIN (<4 µM) for AMT-16, (c) DOC and DIN for AMT-17. (d) DOC and DIN (<4 µM) for AMT-17, (e) DOC and DIP for AMT-16, (f) DOC and DIP (<0.4 µM) for AMT-16, (g) DOC and DIP for AMT-17, (h) DOC and DIP <0.4 µM) for AMT-17, (i) DON and DIN for AMT-17, (j) DON and DIN (<5 µM) for AMT-17, (k) DON and DIP for AMT-17, (l) DON and DIP (<0.5 µM) for AMT-17, (m) DOP and DIN for AMT-17, (n) DOP and DIN (<5 µM) for AMT-17, (o) DOP and DIP for AMT-17, and (p) DOP and DIP (<0.5 µM) for AMT-17

The weak correlations found in the Atlantic Ocean did not suggest an efficient transfer of N and P between the dissolved inorganic and dissolved organic pools. One possibility explaining the poor relationships is that N and P were retained in the organic pool due to a relatively insufficient functioning of the microbial loop, which was evidenced by the weak correlations between heterotrophic bacteria and DOC/DON/DOP and DIN/DIP (Fig. 4.7). DOM produced in the Atlantic Ocean was probably more refractory compared to that produced in the Pacific Ocean. The relatively longer biological turnover time of DON and DOP allowed the satisfaction of N and P retained in the dissolved organic pool in surface waters, leading to poorly coupled relationships of dissolved organic and inorganic nutrients.

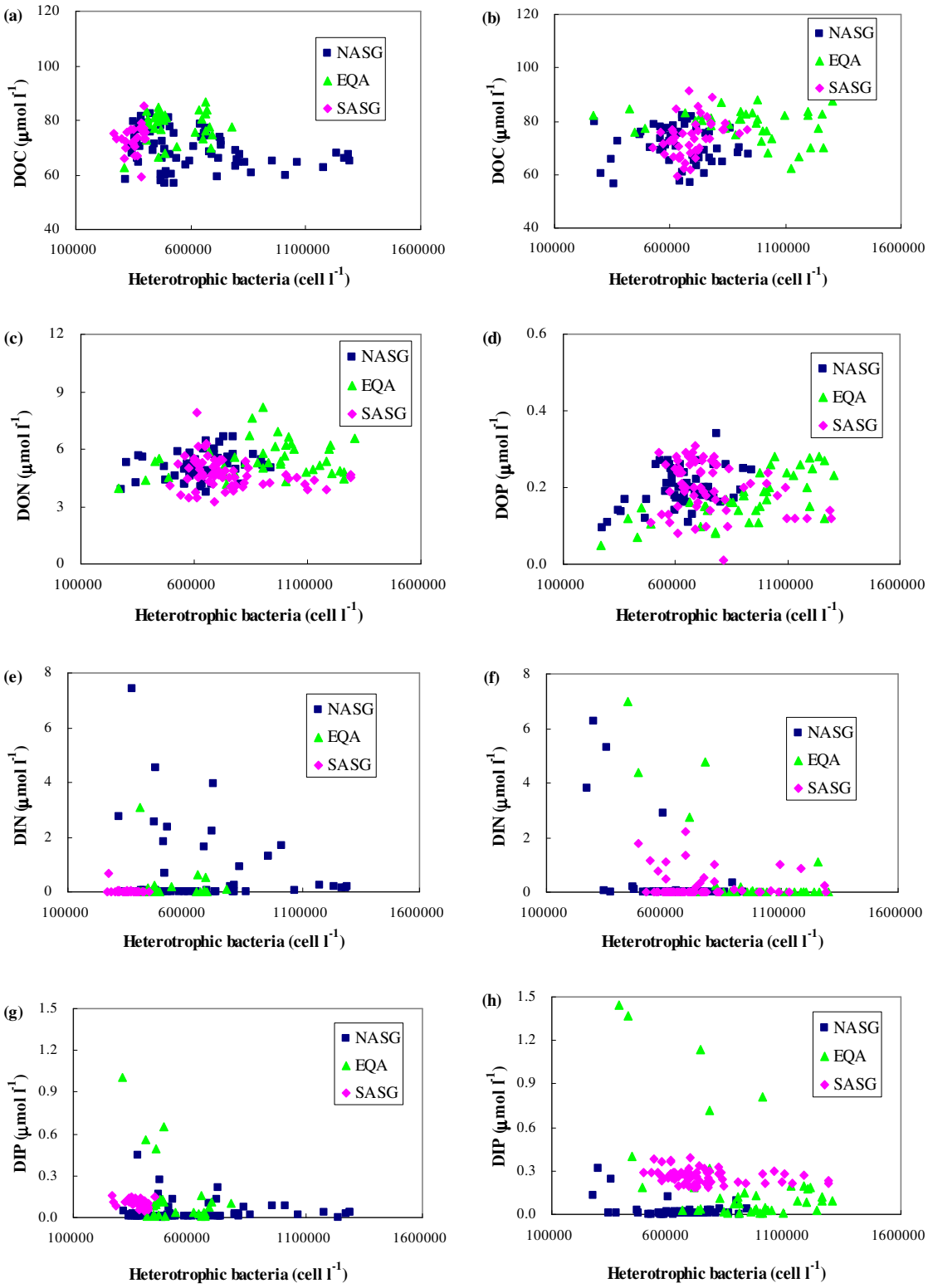

Figure 4.7. Correlations of (a) DOC and heterotrophic bacteria on AMT-16, (a) DOC and heterotrophic bacteria on AMT-17, (c) DON and heterotrophic bacteria on AMT-17, (d) DOP and heterotrophic bacteria on AMT-17, (e) DIN and heterotrophic bacteria on AMT-16, (f) DIN and heterotrophic bacteria on AMT-17, (g) DIP and heterotrophic bacteria on AMT-16, and (h) DIP and heterotrophic bacteria on AMT-17.

Another possibility of the weakened correlations between the dissolved organic and inorganic nutrients is due to the vertical migrators. Studies in the Pacific Ocean found that *Rhizosolenia* mats migrated vertically between surface waters and deep nitrate pool, bringing an equivalent of 50% of new nitrogen requirements into the surface waters (Villareal *et al.* 1993). Since the success of vertical migrators is likely to be dependent on the proximity of the nitracline to the euphotic zone (Hansell and Waterhouse 1997), which was the case in the Atlantic Ocean shown in Fig. 3.5 and 3.6, it seems reasonable to believe the existence of an important vertical migration in the Atlantic Ocean. If the vertical migration was significant in bringing new nitrate and phosphate into the surface waters, strong correlations between dissolved organic (including DOC) and inorganic nutrients should not be anticipated. However, this hypothesis cannot be tested in this study.

In addition, literatures have suggested that the surface waters of the tropical and northern subtropical Atlantic in particular were nitrogen and phosphorus limited (*e.g.* Tyrrell 1999; Karl *et al.* 2001b; Mills *et al.* 2004). The southern Atlantic subtropical gyre waters were nitrogen and iron limited (Achterberg unpublished data). The limitation of N, P and Fe may play a role in regulating the distributions of DON and DOP. Unfortunately, so far the impact of this limitation on the cumulative DOM still remains unclear (Hansell and Waterhouse 1997).

4.3.3. Relations with *Prochlorococcus* and *Synechococcus* spp.

Size fractioned chlorophyll-a measurements have shown that picophytoplankton (<2 μm in diameter) formed a dominant fraction of 80-90% of the biomass of autotrophs in the tropical and subtropical Atlantic, with the remaining of 10-20% contributed by nanophytoplankton (>2 μm in diameter) (Poulton *et al.* 2006). The reason picophytoplankton outcompeted larger phytoplankton in nutrient-depleted surface waters is their relatively higher surface area to volume ratios, which allowed more efficient nutrient uptake (*e.g.* Karl *et al.* 2001a; Mackey *et al.* 2007). To facilitate the investigation of the significance of *Prochlorococcus* and *Synechococcus spp.* in DOM distributions, concentrations of DOC, DON and DOP were compared with abundance of *Prochlorococcus* and *Synechococcus spp.* (Fig. 4.8).

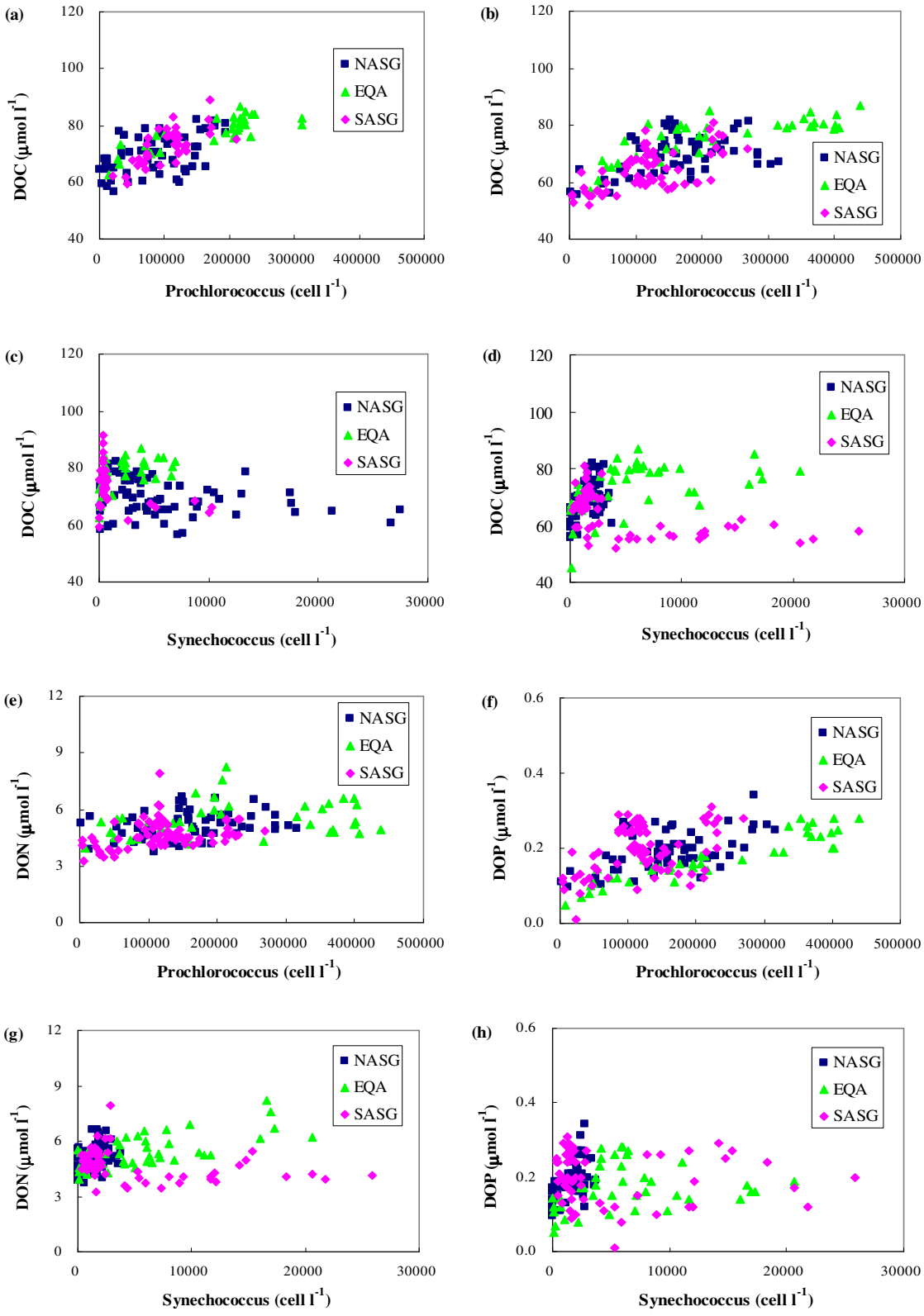

Figure 4.8. Correlations of (a) DOC and *Prochlorococcus* on AMT-16, (b) DOC and *Prochlorococcus* on AMT-17, (c) DOC and *Synechococcus* on AMT-16, (d) DOC and *Synechococcus* on AMT-17, (e) DON and *Prochlorococcus* on AMT-17, (f) DOP and *Prochlorococcus* on AMT-17, (g) DON and *Synechococcus* on AMT-17, (h) DOP and *Synechococcus* on AMT-17.

Correlation analyses showed that *Prochlorococcus* was statistically related with DOC, DON and DOP (Tab. 4.5). However, such strong correlations did not hold for the relationships with *Synechococcus*. The findings suggested that *Prochlorococcus spp.* but not *Synechococcus spp.* was an important control of the distributions of DOC, DON and DOP. The difference in the correlations of DOM-to-*Prochlorococcus* and DOM-to-*Synechococcus* relationships can be explained by the different mechanisms in meeting their energy demand. Zubkov *et al.* (2003) provided evidence that ~33% of the total bacterioplankton turnover of amino acids, determined with a representative [^{35}S] methionine precursor and flow sorting, was assigned to *Prochlorococcus* spp., and <3% was assigned to *Synechococcus* spp. By tapping into both dissolve inorganic and labile dissolved organic forms of nutrients (*i.e.* mixotrophy) in a nutrient poor environment, *Prochlorococcus* outcompeted other autotrophic algae and other bacteria (Zubkov *et al.* 2004). As discussed in the results section, 20-45%, 47-65% and 87-93% of the DOC, DON and DOP, respectively, observed in the upper 50 m were biologically labile (or semilabile). Therefore, strong correlations between *Prochlorococcus* and DOC, DON and DOP were anticipated.

Parameters	df[a]	r[b]	Critical value	Significance level (%)
AMT-16				
DOC versus *Prochlorococcus*				
NASG	62	0.41	0.319	99
EQA	31	0.83	0.442	99
SASG	41	0.68	0.389	99
AMT-17				
DOC versus *Prochlorococcus*				
NASG	56	0.44	0.336	99
EQA	39	0.76	0.398	99
SASG	75	0.55	0.292	99
DON versus *Synechococcus*				
NASG	56	0.45	0.336	99
EQA	39	0.45	0.398	99
SASG	75	0.55	0.292	99
DOP versus *Synechococcus*				
NASG	56	0.53	0.336	99
EQA	39	0.91	0.398	99
SASG	75	0.41	0.292	99

(*Continues*)

(*Continued*)

[a] Degree of freedom

[b] Standardised coefficient

Table 4.5. Statistics of Model-II regression between DOC, DON, DOP, *Prochlorococcus* and *Synechococcus* in the euphotic zone on AMT-16 and -17.

4.4. Stoichiometry of DOC, DON and DOP

As early as 1963, Redfield and his colleagues (Redfield *et al.* 1963) summarised the early research on C, N and P stoichiometry of dissolved and particulate organic matter pools in the oceans and combined these data sets into an important unifying concept that has served as the basis for many subsequent field and modeling studies in oceanic biogeochemistry. The so-called Redfield ratio of 106C:16N:1P has achieved nearly canonical status in aquatic sciences (Karl *et al.* 2001b).

Considerable knowledge has been gained based on the investigation of the C:N:P stoichiometry of particle formation, settling and mineralisation (Martin *et al.* 1987), little is known about the C:N:P stoichiometry of the dissolved organic pool (Hopkinson *et al.* 1997). Instead, the Redfield stoichiometry is achieved only during maximum cell growth rate in nutrient-sufficient cultures (Goldman *et al.* 1979; Laws and Bannister, 1980). When either energy (including light) or nutrient limitations is imposed on prokaryotic and eukaryotic microbial populations, there are offsets in the C:N:P ratios (Karl *et al.* 2001b). Evaluation of the concentrations of DOC, DON and DOP with great coverage of large geographic regions such as AMT programme provides valuable insight into the C:N:P stoichiometry of dissolved organic pool, and the spatial distribution of the stoichiometry.

4.4.1. The C:N:P stoichiometry of the bulk DOM pool

The latitudinal-depth contours of C:N, C:P and N:P ratios of the bulk DOM pool are shown in Figure 4.9. The stoichiometry of DOC:DON deviated from the classical Redfield ratio of 6.6, ranging from 11 to 18 in the upper 300 m. There were no evident vertical gradients of the C:N ratios present in the section. In the upper 100 m, the relatively high ratios (C:N>14) were found in the northern subtropical gyre, the

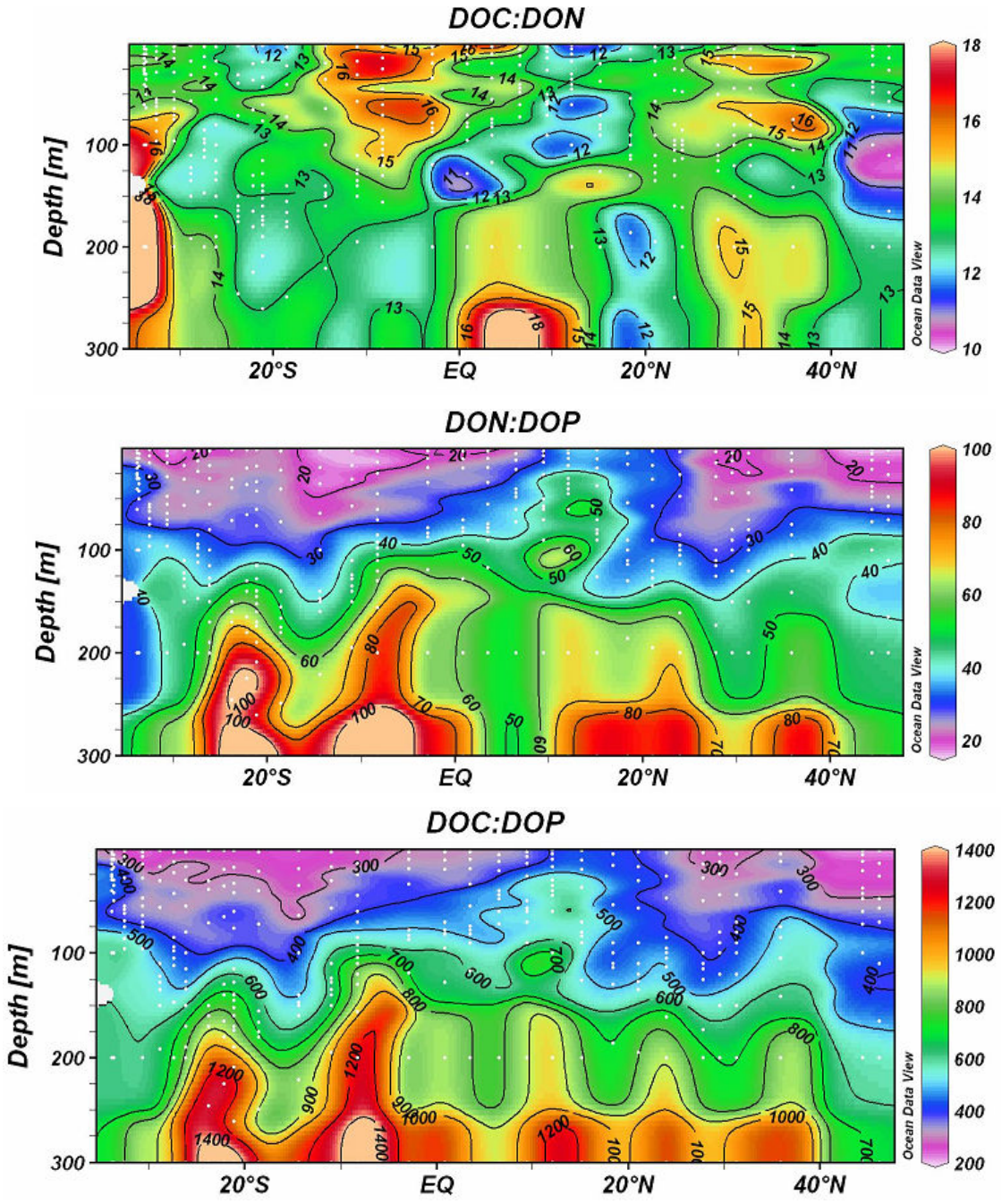

Figure 4.9. The C:N, N:P and C:P stoichiometry of the bulk DOM pool in the upper 300 m for AMT-17.

southern equatorial region, and the northern part of the southern subtropical gyre. High C:N (>14) ratios were also observed in the subsurface waters of the northern subtropical gyre, northern equatorial region, and the southeast boundary of the southern subtropical gyre. The lowest C:N (<11) ratios were found on the northeast edge of the northern subtropical gyre and the central equatorial region at a depth of ~120 m. The profiles of

the C:N ratios reflected that the bulk DOM pool in the upper 300 m was C-rich relative to N compared to the Redfield ratio. The lack of the vertical gradient of the C:N ratios did not suggest pronounced preferential remineralisation between C and N.

The N:P and C:P stoichiometry also deviated from the Redfield ratio (N:P = 16; C:P = 106), ranging from 20-100 and 300-1400, respectively, suggesting that the cumulative DOM in the upper 300 m was rich in C and N relative to P compared to the Redfield ratio. The lowest ratios (N:P<30; C:P<400) were found in the surface waters across the section. At 300 m, the ratios of N:P and C:P ranged from 50-100 and 800-1400, respectively. The pronounced vertical gradients of the ratios of the bulk DON:DOP and DOC:DOP suggested preferential remineralisation of P relative to C and N.

4.4.2. The C:N:P stoichiometry of the semilabile (and labile) DOM pool

The spatial variability of the C:N:P stoichiometry of the semilabile (and labile) DOM are shown in Figure 4.10. The C:N ratios in the upper 300 m generally agreed with the Redfield stoichiometry of 6.6, apart from those found in the surface (100 m) waters of the equatorial region, the northern part of the SASG, and the central NASG, where the C:N ratios reached >10. The high C:N ratios were also found in the subsurface waters of the EQA and the southeast boundary of the SASG. Of these water masses, the cumulative semilabile (and labile) DOM was enriched in C relative to N compared to the Redfield ratio. The latitudinal-depth contour of the C:N ratios did not suggest preferential remineralisation between semilabile (and labile) DOC and DON in the upper 300 m.

The N:P and C:P ratios in the upper 30 m were generally agreed with the Redfield stoichiometry of N:P = 16 and C:P = 106, apart from the relatively high ratios (N:P>20; C:P>150) found in the northern equatorial and the northern subtropical regions. However, the N:P and C:P ratios were generally greater than the Redfield ratio at below 100 m, with N:P = 20-30 and C:P = 100-150 found at 100 m and N:P = 25-100 and C:P = 150-500 found at 300 m. The vertical gradients were less pronounced in the equatorial region where the N:P and C:P ratios may reflect the C:N:P stoichiometry of the upwelled waters from below. The vertical increases of the N:P and C:P ratios suggested preferential remineralisation of the semilabile (and labile) DOP relative to semilabile (and labile) DOC and DON. This preferential remineralisation was likely more

significant in the SASG than in the NASG, leading to the elevated N:P and C:P ratios observed in the subsurface waters of the SASG.

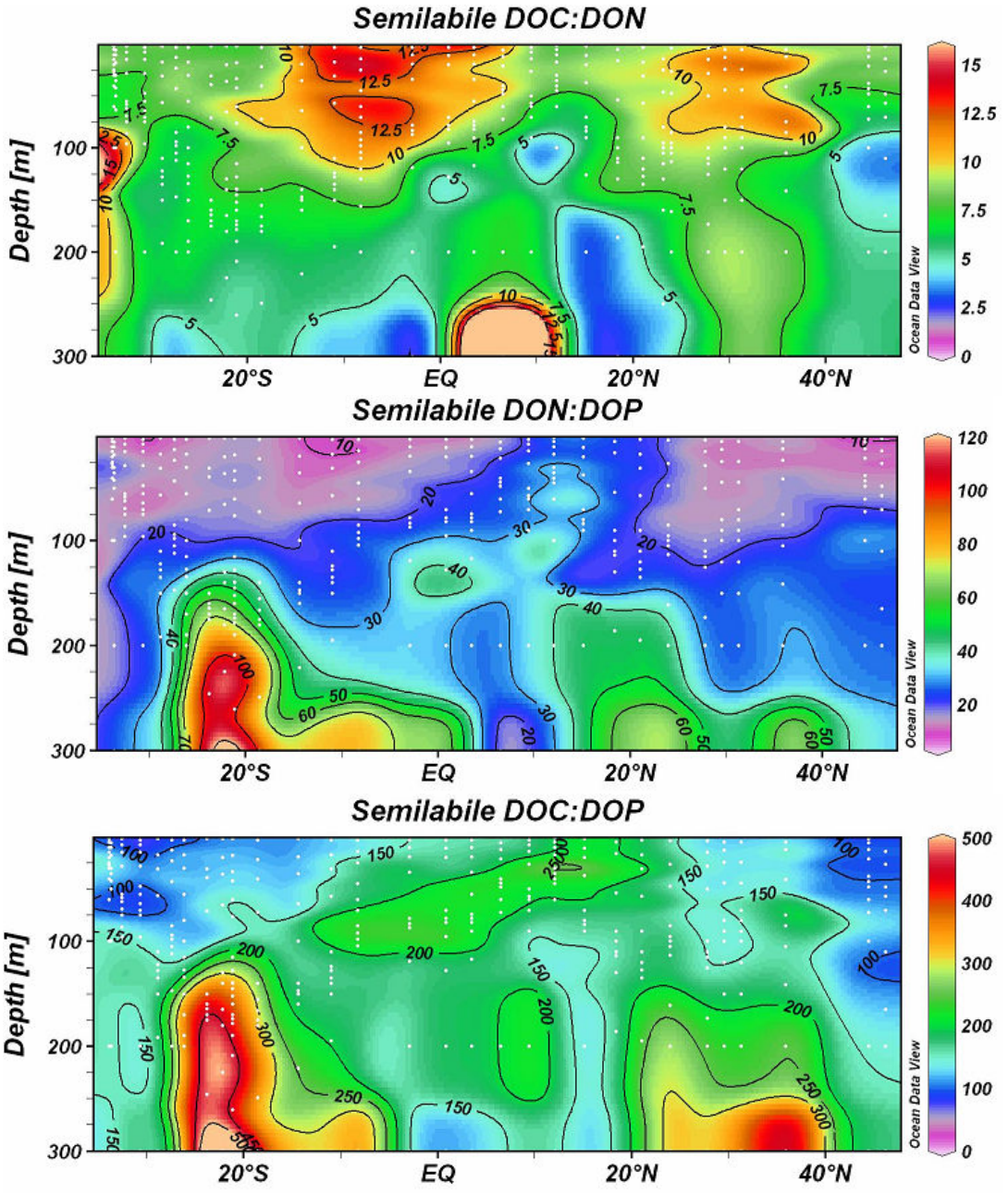

Figure 4.10. The C:N, N:P and C:P stoichiometry of the semilabile (and labile) DOM pool in the upper 300 m for AMT-17.

4.4.3. The C:N:P stoichiometry of the refractory DOM pool

The C:N, N:P and C:P stoichiometries of the refractory DOM pool, based on the measurements of the samples collected from below 1000 m, were 17-24, 79-132 and

1791-2442, respectively, suggesting that the refractory DOM was significantly rich in C relative to N and P, and N relative to P, compared to the Redfield ratio.

4.4.4. The C:N:P stoichiometry of DOM deviated from the Redfield trajectories

The C:N:P stoichiometry of the bulk and semilabile (and labile) pools in the surface mixed layer, and of the refractory pool from this study was compared with literature findings reviewed by Hopkinson and Vallino (2005) (Tab. 4.6). The relatively large standard deviations of the elemental ratios of this study were due to wide coverage of the tropical and subtropical Atlantic. Table 4.6 suggested that the C:N:P stoichiometry of DOM pool in the open oceans was greater than the classical Redfield ratio. Karl *et al.* (2001b) reported that under conditions of limiting N and P, such as oligotrophic waters, certain photoautotrophic organisms can store C as lipid or carbohydrate, thereby increasing their C:N and C:P ratios. When the total bioavailable (labile DON and DOP plus bioavailable DIN and DIP) N:P ratio is greater than 16:1 by atoms, for example, possibly in the northern subtropical Atlantic due to nitrogen fixation as an extra N source, selected groups of microorganisms can produce biomass with C:P and N:P ratios significantly greater than the hypothesised Redfield ratios of 106:1 and 16:1,

DOM stoichiometry	Georges Bank	Middle Atlantic Bight	Hawaiian Ocean Time Series	This study
Bulk pool (surface mixed layer)				
C:N	12 (0.8)	14 (0.6)	15 (0.5)	14 (2)
N:P	35 (1.4)	26 (0.9)	19 (0.4)	25 (8)
C:P	444 (17)	374 (11)	281 (5)	336 (92)
Semilabile (and labile) pool (surface mixed layer)				
C:N	9.8 (1.4)	10 (0.9)	8.7 (0.6)	10 (3)
N:P	25 (2.5)	20.2 (1.1)	17.8 (0.5)	20 (7)
C:P	245 (29)	193 (17)	154 (10)	144 (54)
Refractory pool (below 1000 m)				
C:N	15 (2.1)	21 (2.5)	34 (2.2)	20 (3)
N:P	139 (14)	110 (16)	163 (16)	104 (22)
C:P	2035 (162)	2370 (196)	4768 (196)	2155 (275)

Table 4.6. Comparison of the C:N:P stoichiometry of bulk DOM pools in surface (mixed layer), semilable (and labile) DOM pool in surface (mixed layer), and refractory DOM pool from below 1000 m. Numbers in parentheses are standard deviations. Values were taken from Hopkinson and Vallion (2005). Method: UV photooxidation.

respectively (Karl *et al.* 2001b). If the argument in Raven (1994) that C:P ratio in small cyanobacteria should be higher than in average eukaryotic phytoplankton cells could be applied to the Atlantic Ocean where *Prochlorococcus* and *Synechococcus spp.* accounted for 80-90% of the biomass of autotrophs (Poulton *et al.* 2006), a higher DOC:DOP ratio relative to the Redfield ratio should, therefore, be anticipated.

Interestingly, the C:P ratios of the semilabile (and labile) DOM found in surface waters of Georges Bank and the Middle Atlantic Bight were higher than those found in the Atlantic Ocean. This finding was unanticipated. In coastal upwelling regions, nutrients (*e.g.* nitrate and phosphate) are introduced into the euphotic zone via the upwelling current, satisfying N and P requirements for primary producers. On the contrast, the surface waters of the Atlantic Ocean are subject to N and P limitation. There, in theory, should not be a lower C:P ratio found on Georges Bank and in the Middle Atlantic Bight. One possible explanation of the relatively higher C:P ratios is the molecular composition of the DOP compounds produced in those regions. There may exist enhanced production of polymeric phosphate ester (C-O-P bonded compounds) and other organically bound phosphorus compounds that were resistant to UV photooxidation method (Ormaza-Gonzalez and Statham 1996).

The C:N:P stoichiometries of the refractory DOM pool deviated substantially from the Redfield trajectories, and were much higher than those of the semilabile (and labile) or the bulk DOM pools in surface waters. Decreased C:N:P stoichiometry was also reported by Hopkinson and Vallino (2005), based on samples collected throughout the water column on Georges Bank, in the Middle Atlantic Bight and at the Sta. ALOHA, suggesting preferential remineralisation of P relative to C and N, and N relative to C. Other relevant studies have shown that DON and DOP were preferentially remineralised relative to DOC (Williams *et al* 1980; Martin *et al.* 1987; Hopkinson *et al.* 1997; Clark *et al.* 1998; Loh and Bauer 2000; Hopkinson *et al.* 2002). Evidence that the C:N and C:P ratios in sinking particles increased with depth in subtropical oceanic ecosystems has been provided by Knauer *et al.* (1979), Martin *et al.* (1987) and Karl *et al.* (1996), suggesting preferential remineralisation of PON and POP relative to POC. A consistently greater remineralisation length scale for organic-C relative to organic-N and -P produces a long-term, steady flux of C from the surface to the deep ocean (Christian *et al.* 1997). CO_2 fixed in the upper ocean during planktonic photosynthesis is

continuously "pumped" into the ocean interior, and stored in the deep ocean up to thousands of years. The upper ocean DIC deficit is then balanced by a transfer of CO_2 from the atmosphere to the upper ocean. Hence, the biological carbon pump functions as a sink for atmospheric CO_2.

The C:N, N:P and C:P ratios of the refractory DOM pool were relatively higher at Sta, ALOHA during Hawaiian Ocean Time Series study than those in the Atlantic Ocean and continental shelf waters. The elevated C:N:P stoichiometry found at Sta. ALOHA may be due to the relatively lower concentrations of the refractory DON (<2.0 μM at 1000 m) and DOP (<0.01 μM at 1000 m) (see data in Karl *et al.* 2001b).

4.5. Importance of DOC degradation in the thermocline

In this section, the fraction of oxygen consumption in the Atlantic ocean that is related to DOC degradation is investigated. Clearly, this exercise should be undertaken using samples from water masses isolated from the atmosphere, since invasion of oxygen into surface water masses in contact with the atmosphere would skew this approach. Therefore, the samples collected in the upper thermocline (*i.e.* from below the euphotic zone to 300 m within the 26-27 σ_t isopycnal layer) were considered for this purpose.

4.5.1. Spatial variability of AOU derived from DOC

DOC exported to depth during diffusive mixing is mineralised, contributing to oxygen consumption in the subsurface waters (Hansell and Carlson 2001b). The contribution of DOC to AOU along isopycnal surfaces can be determined after converting AOU to carbon equivalents using the Redfield ratio (Doval and Hansell 2000). However, the previously used Redfield formula for the average composition of the organic content of marine phytoplankton, $(CH_2O)_{106}(NH_3)_{16}(H_3PO_4)$, was found to be in disagreement with observations with respect to the oxygen and hydrogen content (Anderson 1995). Based on considerations of metabolite composition and various observations, a new formula, $C_{106}H_{175}0_{42}N_{l6}P$, was proposed by Anderson (1995), which was a better approximation to mean algal elemental composition in the oceans (*e.g.* Doval and Hansell 2000; Hansell and Carlson 2001a). The "corrected" Redfield ratio suggested that the degradation of 0.72 mole of organic carbon would require the consumption of 1 mole of O_2 (*i.e.* $\Delta C:\Delta O_2 = -0.72$). This C/O ratio (-0.72) is known as respiratory quotient (RQ), and has been widely used to convert AOU to carbon equivalents (Doval and Hansell

2000).

Regression of DOC on AOU concentrations in the 26-27 σ_t isopycnal layer is plotted in Figure 4.11, showing a statistically significant correlation (slope = -0.14, n = 147, r^2 = 0.36, p<0.001), with the regression slope ranging from -0.10 to -0.18. Given a RQ of -0.72 (Anderson 1995), the DOC/AOU ratios of the data set suggested that 15% (-0.10 divided by -0.72) to 25% (-0.18 divided by -0.72) of the AOU can be derived from DOC degradation over the entire Atlantic Ocean from the euphotic zone to 300 m depth. The remaining of 75%-85% was contributable to POC decomposition.

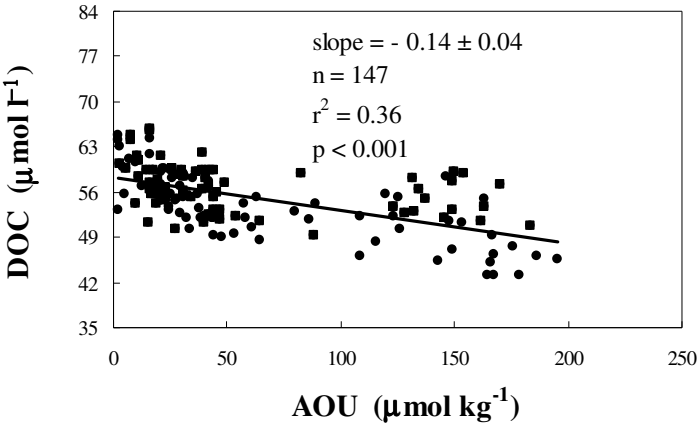

Figure 4.11. Regression of DOC (µM, y-axis) on AOU (µmol kg^{-1}, x-axis) on the 26-27 σ_t isopycnal layer (*i.e.* from below the euphotic zone to 300 m). Circles indicate values from AMT-16, while squares indicate values from AMT-17.

4.5.2. Regional variability of AOU derived from DOC

The bulk estimate of DOC contribution to AOU may conceal the potential regional variability. For this reason, the ratio of DOC to AOU in the 26-27 σ_t isopycnal layer was determined at individual stations, in order to explore the fraction of oxygen utilisation associated with the respiration of DOC mixed out of the upper ocean in diapycnal mixing on a regional basis. A Model-II regression of AOU against DOC was performed in this density region for each station. At four stations, no significant relationship was observed between DOC and AOU at the 95% confidence level and these four stations were therefore excluded from the regression analyses.

Figure 4.12 plots the DOC/AOU ratios as a function of latitude. In the upper 300 m a total of 15-55% of AOU was suggested to be associated with the degradation of DOC. On average the fraction of AOU attributable to DOC respiration was up to 2 times higher in the central gyres (15-55%) than in the equatorial region (15-25%).

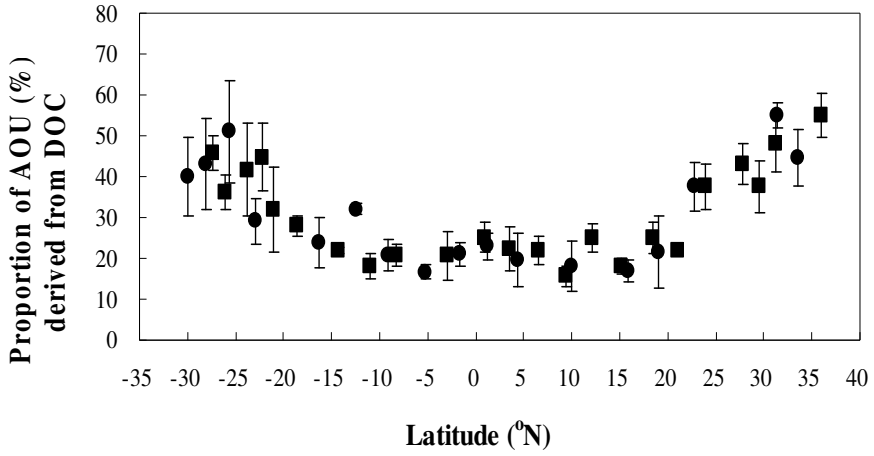

Figure 4.12. Plot of percentage of AOU derived from DOC degradation against latitude. Circles indicate values obtained on AMT-16 cruise, while squares indicate values obtained on AMT-17 cruise.

Several data sets have reported some degree of covariance between DOC and AOU (Tab. 4.7.). Assuming a RQ of -0.72, literature values suggested that 10-80% the AOU can be explained by DOC degradation in open ocean regions. Both Figure 4.12 and Table 4.7 show relatively smaller contributions of DOC to AOU in the nutrient-enriched equatorial and coastal regions. In the next section, the likely causes are investigated.

Study regions	Depth (m)	DOC/AOU molar ratio	AOU derived from DOC (%)	Reference
North Atlantic Ocean	full depth	- 0.29	40	Druffel *et al.* 1992
North Atlantic Ocean	full depth	- 0.25	35	Kepkay and Wells 1992
Equatorial Atlantic Ocean	< 700	- 0.09 and - 0.14	13 and 19	Thomas *et al.* 1995
North Pacific Ocean	< 500	- 0.59	82	Druffel *et al.* 1992
South Pacific Ocean	23–27 σ_θ	- 0.26	36*	Doval and Hansell 2000
Equatorial Pacific Ocean	90-400	- 0.074	10	Peltzer and Hayward 1996

(*Continues*)

(*Continued*)

Study regions	Depth (m)	DOC/AOU molar ratio	AOU derived from DOC (%)	Reference
Western North Pacific Ocean	< 500	- 0.23	32	Ogura 1970
NW Indian Ocean	full depth	- 0.062	9	Kumar *et al.* 1990
Southern California Bight	full depth	- 0.068	9	Hansell *et al.* 1993
Gulf of Mexico	< 250	- 0.152	21	Guo *et al.* 1994

* Unfiltered samples

Table 4.7. Selected literature values for DOC/AOU molar ratios and percentage of AOU derived from DOC degradation (assuming a RQ of - 0.72).

4.5.3. Causes of the regional variability of AOU

The most likely explanation for the variation of AOU relative to DOC degradation in relation to determining oxygen utilisation is regional variability in the export of POC, which was anticipated to be highest in the high nutrient regions of the equatorial and coastal regions and at the poleward margins of the subtropical gyres. Relative to the SAG, chlorophyll-a concentrations were ~2 times higher in the EQA, leading to enhancements in productivity, POC stocks and particle export in these regions (Thomalla *et al.* 2006; Poulton *et al.* 2006).

A statistically significant relationship was observed between the proportion of AOU derived from DOC respiration and column integrated production ($n = 14$, $r = -0.56$, $p<0.05$; Fig 4.13 a). The relationship between POC stocks and the fraction of AOU attributable to DOC degradation was also statistically significant ($n = 50$, $r = 0.80$, $p<0.001$; Fig 4.13 b). However, there was no significant correlation between the proportion of AOU derived from DOC respiration and integrated chlorophyll-a ($n = 33$, $r = -0.12$, $p>0.05$; Fig 4.13 c).

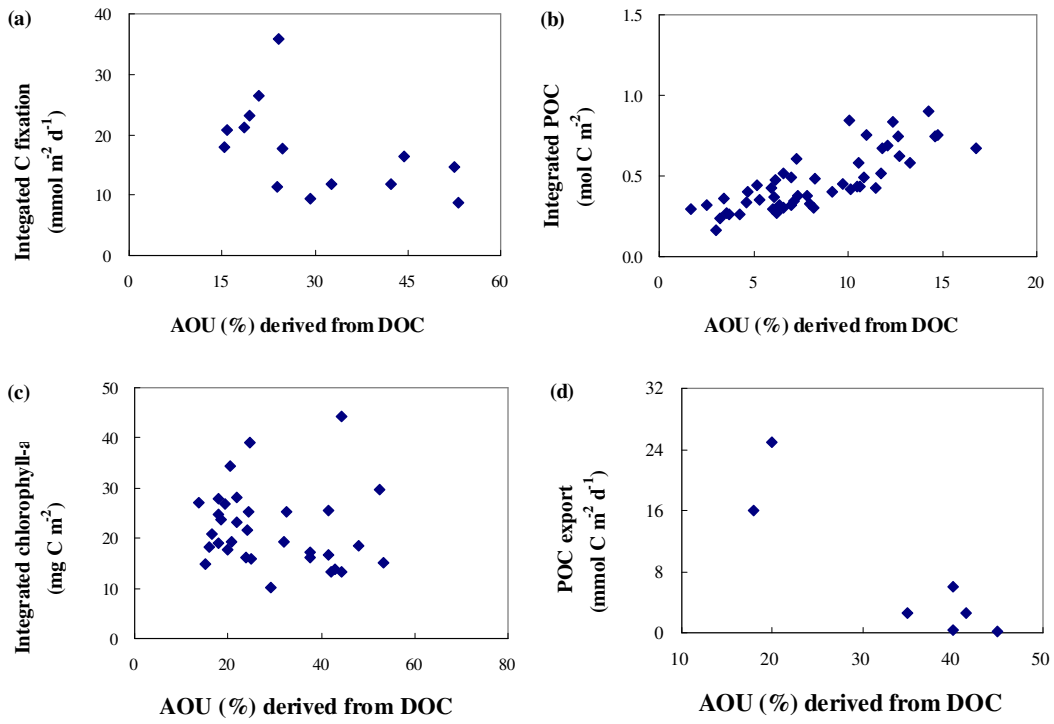

Figure 4.13. Regression of (a) proportion of AOU derived from DOC degradation versus integrated carbon fixation, (b) proportion of AOU derived from DOC degradation versus integrated POC stock, (c) proportion of AOU derived from DOC degradation versus integrated chlorophyll-a, and (d) proportion of AOU derived from DOC degradation versus POC export efficiency.

The export of POC, estimated using ^{234}Th disequilibrium, was ~4-5 times higher in equatorial waters than in the subtropical gyres (Thomalla *et al.* 2006). Comparison of Thomalla *et al.* (2006) estimates of export efficiency with the proportion of AOU attributable to DOC degradation generated a significant relationship ($n = 7$, $r = -0.83$, $p<0.05$; Fig 4.13 d). Given the findings of the correlation analyses presented above, it seems to be reasonable to conclude that the regional variation of AOU relative to DOC degradation with respect to oxygen utilisation was resulted from the different magnitude of the export of particles. DOC formed an important contribution to AOU in oligotrophic regions, while POC was the primary control of observed AOU values in upwelling regions.

4.6. Importance of DON and DOP degradation in the thermocline

Some freshly-produced fractions of DON and DOP, with turnover times of months to years (*i.e.,* the semilabile fraction; Carlson 2002), are capable of escaping rapid

microbial degradation in surface waters and will become entrained into deep waters via diffusive mixing (Copin-Montégut and Avril 1993). Extracellular hydrolysis takes place to allow the semilabile dissolved organic nutrients to be used by heterotrophic bacterioplankton (Münster and De Hann 1998), regenerating inorganic nutrients. In this section, the importance of degradation of dissolved organic nutrients to inorganic nutrients via diffusion processes is investigated.

4.6.1. Heterotrophic respiration of dissolved organic nutrients

There are very limited studies showing the relationships between heterotrophic bacteria populations and concentrations of dissolved organic nutrients. A few culture experiments have suggested that uptake of dissolved free amino acids can support 4-41% of the bacterial N demand in the open oceans and up to 100% in the coastal regions (Kirchman 2000), and that glucose uptake can represent 27-35% of the net bacterial production in the equatorial Pacific (Rich *et al.* 1996) and up to 100% in the Arctic (Rich *et al.* 1997). Direct uptake of glycerophosphoric acid, Adenosine 5'-triphosphate (Ruby *et al.* 1985; Wanner 1993) and nucleotide monophosphates (Karl and Björkman 2002) by certain marine heterotrophic bacteria was also observed.

The concentrations of DON and DOP were compared with heterotrophic bacterioplankton abundance for samples collected from below the euphotic zone and 300 m depth (*i.e.* the ~26-~27 σt isopycnal surface) using Model-II regression analyses. Strong correlations were achieved between dissolved organic nutrients and

	df[a]	r[b]	Critical value	Confidence level (%)
DON vs. AOU	100	-0.41	0.254	99
DON vs. total heterotrophic bacteria	126	0.21	0.169	95
DOP vs. AOU	100	-0.53	0.254	99
DOP vs. total heterotrophic bacteria	126	0.72	0.228	99

[a] Degree of freedom

[b] Standardised coefficient

Table 4.8. Model-II regression between DON, DOP, AOU and total heterotrophic bacteria for samples collected between the euphotic zone and 300 m depth (*i.e.* within the 26 and 27 σt isopycnal layer) on AMT-17.

heterotrophic bacterioplankton as well as AOU (Tab. 4.8). The findings suggested that heterotrophic bacteria respiration was an important mechanism regulating the distributions of dissolved organic nutrients in subsurface waters.

4.6.2. Contributions of DON and DOP to regenerated DIN and DIP

Depth profiles of DON and DOP concentrations (Fig. 3.11 and 3.12) suggested downward fluxes of dissolved organic nutrients from surface waters, and depth profiles of DIN and DIP concentrations (Fig. 3.6 and 3.8) suggested upward fluxes of dissolved inorganic nutrients into the euphotic zone. Fluxes of the upward and downward dissolved nutrients into and from surface waters are demonstrated conceptually in Figure 4.14.

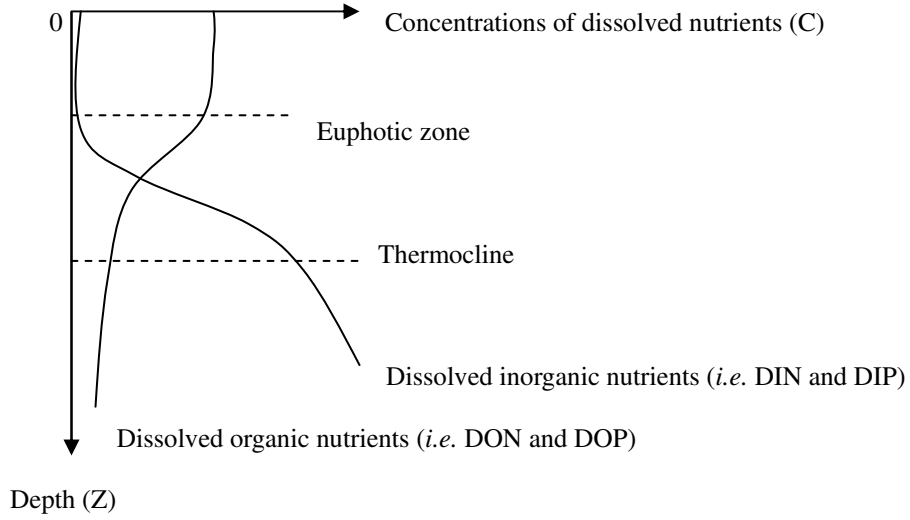

Figure 4.14. Conceptual cartoon of fluxes of dissolved organic nutrients from surface waters and dissolved inorganic nutrients into surface waters.

The key question here is what magnitude of the upward inorganic nutrients (*i.e.* DIN and DIP) that were derived from the downward dissolved organic nutrients (*i.e.* DON and DOP) is. In order to estimate the nutrient fluxes, a simple equation was raised by Smith *et al.* (1986) and Vidal *et al.* (1999), *i.e.* Flux = K_z (dC/dZ), where K_z is diapycnal mixing coefficient and dC/dZ is the gradient in the measured nutrient concentration across the thermocline. The determination dC/dZ is unproblematic, however, the diapycnal mixing coefficient (k_z) is not straightforward to estimate (*e.g.* Smith *et al.* 1986; Large *et al.* 1994). Taking this thought, Smith *et al.* (1986) alternatively

calculated the relative flux of dissolved nutrients rather than absolute fluxes, simply by taking the regression slope of dissolved organic and inorganic nutrients in the thermocline, *i.e.*

$$F_{DON} / F_{DIN} = dC_{DON} / dC_{DIN}$$
$$F_{DOP} / F_{DIP} = dC_{DOP} / dC_{DIP}.$$

The authors argued that determination of the flux ratio did not require an independent knowledge of the diapycnal mixing coefficient (k_z), and that the flux ratio reflected the percentage of dissolved organic nutrients mixed out of the euphotic zone relative to inorganic nutrients supplied into the euphotic zone (Smith *et al.* 1986).

To facilitate the calculation of the relative flux of dissolved nutrients, correlation analyses of DIN-to-DON and DIP-to-DOP relationships were performed using a Model-II regression approach for samples collected from the water column from the euphotic zone to 300 m depth. The statistically significant correlations between these two forms of dissolved nutrients (Fig. 4.15) suggested that during diffusive mixing, degradation of the downward dissolved organic nutrients formed an important contributor to the upward regenerated inorganic nutrients.

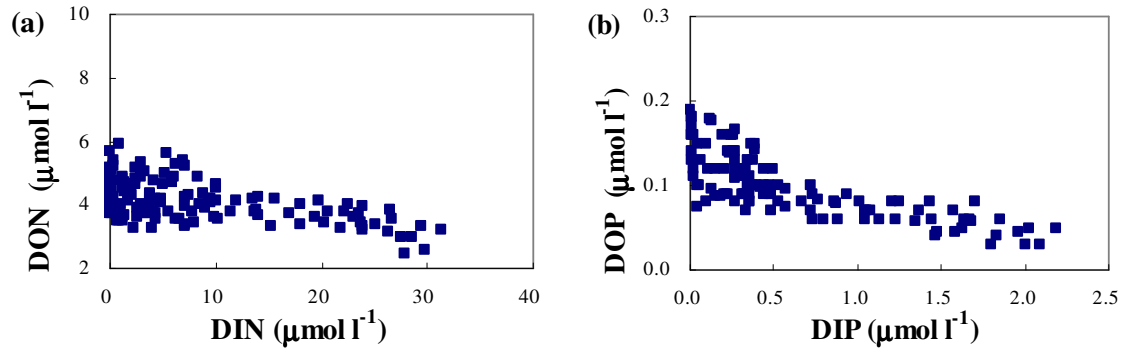

Figure 4.15 Model-II regression between (a) DON and DIN (slope: -0.0418; degree of freedom: 144; standardised coefficient: -0.56; critical value of the 99% confidence level: 0.21), and (b) DOP and DIP (slope: -0.0492; degree of freedom: 116; standardised coefficient: -0.76; critical value of the 99% confidence level: 0.24) for samples collected from the euphotic zone to 300 m depth on AMT-17.

Correlation analyses generated the regression slopes of -0.04 and -0.05 for the DIN-to-DON and DIP-to-DOP relationships, respectively. The findings suggested that the downward fluxes of DON and DOP contributed to a total of 4% and 5% of the upward fluxes of DIN and DIP, respectively, from the euphotic zone to 300 m. The remaining of 95% of the upward dissolved inorganic nutrients must fall out of the euphotic zone as particles in order to prevent nutrient accumulation (Smith *et al.* 1986) and to maintain nutrient integrity of the pelagic ecosystem.

4.6.3. Various contributions of dissolved organic to inorganic nutrients

In comparison with literature findings, Jackson and Williams (1985) reported that 10% and 6% of the upward DIN and DIP were derived from the downward DON and DOP, respectively, at various sites in the Pacific Ocean (<1000 m). Smith *et al.* (1986) found that the downward DON and DOP accounted for 6% and 4% of the upward dissolved DIN and DIP, respectively, in the northern Pacific subtropical gyre (>900 m). Hopkinson *et al.* (1997) reported that 19% and 15% of the upward DIN and DIP was attributable to the downward DON and DOP, respectively, on the continental shelf in the vicinity of Georges Bank (<1500 m).

Contributions of dissolved organic nutrients to regenerated inorganic nutrients seemed to be relatively more important on Georges Bank than in open oceans. In the thermocline, the downward dissolved organic nutrients contributed to as much as 20% of the regenerated inorganic nutrients in the Georges Bank region, compared to 5% in the open oceans. Georges Bank is a highly productive region. Elevated DOC concentrations were reported (Hopkinson *et al.* 1997), surface water concentrations of DON and DOP, however, were similar to reports from the oligotrophic ocean (Jackson and Williams 1985; Maita and Yanada 1990). Literatures have suggested that phytoplankton exudation was an important autochthonous source of DON and DOP that were characteristic of a very short turnover time in continental shelf waters (*e.g.* Hopkinson *et al.* 2002). If phytoplankton exudation was an important source of DOM in the Georges Bank region, there may exist a relatively large portion of recycled DON and DOP production (Hopkinson *et al.* 1997), which could thus be available for export from surface waters. The short water residence time (Hopkinson *et al.* 1997) may favour a great potential for the export of this recycled DOM from surface waters into depth, resulting in a relatively high percentage of regenerated inorganic nutrients that was

derived from dissolved organic nutrients in the Georges Bank region.

On the contrary, the findings of this study did not suggest that phytoplankton exudation was an important source of the cumulative DOM in the euphotic zone (discussed in Section 4.3.1). If this led to a relatively longer turnover time of DON and DOP in the open ocean compared to the Georges Bank region, there may be a much less portion of recycled production of DON and DOP in surface waters that can be exported into depth. Thus, there was a relatively low percentage of regenerated inorganic nutrients that was attributable to dissolved organic nutrients in the open ocean. Biological availability of dissolved organic nutrients produced in surface waters was hypothesised to be the important factor that led to the difference in percentage of remineralised inorganic nutrients in the thermocline that was derived from downward dissolved organic nutrients between the open ocean and continental shelf region.

5. Conclusions

Global warming has become a dominant issue in environmental science. The increased use of fossil fuels in the postindustrial period has resulted in enhanced emissions of greenhouse gases, including CO_2. However, the oceans form an important sink of atmospheric CO_2, through the biological carbon pump (Ducklow *et al.* 2001). Atmospheric CO_2 is fixed by primary producers in the surface ocean, and the resulting organic matter is exported to deeper waters (Ducklow *et al.* 2001), transferring atmospheric C to the deep ocean for medium (1000's of years) to long (millions of years) time periods (Carlson 2002). The export of sinking biogenic materials drives respiration in the ocean interior and helps to maintain the strong vertical gradients of inorganic carbon and inorganic nutrients in the ocean. DOM forms one of the largest exchangeable C, N and P reservoirs on earth (Carlson 2002) must play an important role in the global cycling of C, N and P. Therefore, there is a clear need to improve our understanding of the biogeochemistry of DOC, DON and DOP.

Based on the high-temperature catalytic combustion technique for determinations of DOC and TDN, and UV oxidation method for determinations of TDP of samples collected on AMT cruise 16 and 17, highest concentrations of DOM (70-80 μM DOC, 4.8-6.5 μM DON and 0.20-0.30 μM DOP) were found in the upper 30 m, and decreased rapidly with increasing water depth. At 300 m, DOC was less than 55 μM, DON was less than 4.0 μM, and DOP was less than 0.07 μM. Lowest DOM concentrations were found at 1000 m, with average concentrations of 44 μM DOC, 2.3 μM DON and 0.02 μM DOP. In the upper 300 m, the semilabile (and labile) DOC, DON and DOP decreased by 46-97%, 48-65% and 90-95%, respectively, from their surface values. No evident seasonal variations in DOC concentrations were found in the equatorial and northern subtropical regions between AMT-16 and -17 cruises. However, relatively higher concentrations of DOC were present in the southern subtropical region in austral autumn than in austral spring. Since the concentrations of

DON and DOP on AMT-16 were excluded in this study, further research of the seasonal variability of DON and DOP concentrations could be undertaken.

Concentrations of DOC, DON and DOP were compared with biological variables in the euphotic zone. Correlation analyses showed that concentrations of DOC, DON and DOP were not statistically related to concentrations of chlorophyll-a, DIN and DIP and to rates of carbon fixation. The findings suggested that the distributions of the cumulative DOC, DON and DOP in the upper ocean were not significantly controlled by phytoplankton biomass, rates of primary production or dissolved inorganic nutrients. Zooplankton grazing may be significant in regulating phytoplankton standing stocks and indirectly controlling rates of productivity, leading to the decoupled correlations between the DOM-to-chlorophyll-a and DOM-to-rates of carbon fixation relationships. There may exist a relatively insufficient functioning of microbial degradation of DOM, resulting in N and P that were retained in the organic pool and causing the poor correlations of DOM and inorganic nutrients. Alternatively, vertical migration of zooplankton may be significant in bringing new nutrients into surface waters in the Atlantic Ocean, weakening the correlations between DOM and inorganic nutrients. Effective uptake of labile (and semilabile) dissolved organic nutrients (including DOC) by *Prochlorococcus* may be important in controlling the distributions of DOC, DON and DOP. However, the poor correlations between DOM and *Synechococcus* probably reflected the inability of this type of cyanobacteria to assimilate labile (and semilabile) dissolved organic nutrients (including DOC). Correlation analyses between DOM and biological variables reflected that chemical composition of DOM, zooplankton community and trophic structures may be important in controlling the distributions of DOC, DON and DOP in surface waters of the Atlantic Ocean. In comparison with literature finds, Hansell and Waterhouse (1997) reported that in the tropical and subtropical Pacific Ocean, DOC distribution was controlled by both biological and physical processes, and DON distribution was controlled primarily by biological

processes. Based on a modelling study, Mahaffey *et al.* (2004) found that physical processes can be important in controlling the distributions of DON and DOP in the Atlantic Ocean. Further work is required to continue the study of the possible factors and/or processes that control the distributions of DOC, DON and DOP.

Prior to the U.S. Joint Global Ocean Flux Study years, the biological carbon pump exclusively referred to particle sinking processes, and the role of DOM as a component of export received little attention beyond speculative modelling (Hansell and Carlson 2001b). Indeed, DOM export in the ocean takes place as a result of accumulation in the surface ocean, redistribution with the wind-driven circulation, winter overturning, and eventual transport to depth with thermohaline circulation (Hansell and Carlson 2001b). Microbial degradation of the exported DOC takes place, causing oxygen utilisation. AOU is a measure of remineralisation of sinking biogenic particles and downward dissolved organic material, and reflects the total oxidation of biogenic carbon along specific density layers (Hansell and Carlson 2001b). Evaluating the contribution of DOM to oxygen consumption can be best undertaken by normalising the gradients in DOC concentrations to the gradients in AOU. This study suggested that in the upper thermocline (<300 m, *i.e.* the 26-27 σ_t isopycnal surface) of the Atlantic Ocean, 25% of the AOU can be attributed to DOC degradation, with the remaining of 75% derived from POC decomposition. Regional studies of DOC and AOU suggested that 15-55% of the AOU was contributable to DOC degradation in the subtropical gyres, and 15-25% in the equatorial region. The regional variability of AOU attributable to DOC was caused by the different magnitude in the export of POC, with a relatively higher fraction of AOU being contributable to particle sinking in the equatorial region.

Some freshly-produced fractions of DON and DOP with turnover times of months to years were capable of escaping rapid microbial degradation in surface waters and became transported into deep waters via diffusive mixing. Subsequent microbial

degradation of these downward dissolved organic nutrients regenerated inorganic nutrients in the thermocline. Flux calculations of dissolved organic and inorganic nutrients suggested that the downward fluxes of DON and DOP accounted for 4% and 5% of the upward fluxes of DIN and DIP, respectively, in the upper thermocline (*i.e.* above 300 m), suggesting that the downward flux of dissolved organic nutrients contributed to ~5% of the upward flux of inorganic nutrients into the euphotic zone. The remaining of ~95% of the upward inorganic nutrients must fall out of the euphotic zone as particles in order to prevent nutrient accumulation and to maintain nutrient integrity of the pelagic ecosystem. The relatively small portion of the upward DIN and DIP derived from the downward DON and DOP reflected the importance of particulate organic nitrogen and phosphorus with respect to regenerated inorganic nutrients in the Atlantic Ocean.

For the bulk DOM pool the elemental stoichiometry was C:N = 12-16, N:P = 20-25, and C:P = 300-350 in the upper 30 m, C:N = 12-18, N:P = 50-100, and C:P = 700-1400 at 300 m, and C:N = 17-24, N:P = 79-132; C:P = 1791-2442 at 1000 m. Compared to the Redfield ratio, the cumulative DOM in the water column was enriched in C relative to N and P, and N relative to P. The increased C:N, N:P and C:P ratios with depth suggested preferential remineralisation of P relative to C and N, and N relative to C. A greater remineralisation length scale for DOC relative to DON and DOP produced a long-term, steady flux of C from the surface to the deep ocean. CO_2 fixed in the upper ocean during planktonic photosynthesis was continuously “pumped” into the ocean interior, and stored in the deep ocean up to thousands of years. The C:N, N:P and C:P stoichiometry of the semilabile (and labile) DOM pool generally agreed with the Redfield ratio (C:N = 6; N:P = 16; C:P = 106) in the upper 30 m. At 100 m C:N ratio was 5-12, C:P ratio was 20-30, and C:P ratio was 100-150. At 300 m, C:N ratio was 5-12, N:P ratio was 25-100, and C:P ratio was 150-500. The findings suggested that in the upper 300 m, there was no preferential remineralisation between

the semilabile (and labile) DOC and DON, however, the semilabile (and labile) DOP seemed to be preferentially remineralised relative to the semilabile (and labile) DOC and DON.

There are still many other unknowns with respect to marine DOM. Central questions include: what are the rates, biogeographical locations and controls on elemental cycling? what are the biological and physicochemical sources and sinks? what is the composition of the pools and what does this tell us about elemental cycling? (Hansell and Carlson 2002). Quantitative constraints on organic matter cycling are particularly difficult to assess in the physically and biologically active upper surface ocean (Quay 1997), where DOM versus POM exports are difficult to distinguish and DOM photodegradation can accompany photosynthesis (Hedges 2002). Given the susceptibility of DOM to photolysis (Kieber *et al.* 1989; Vodacek *et al.* 1997) and subsequently biodegradation (Benner and Biddanda 1998), as well as the rapid increases in UV irradiation of the deeply mixed hub for thermohaline circulation in the Southern Ocean (Solomon 1999), an assumption that the oceanic DOM pool is at steady state seems questionable (Hedges 2002). Furthermore, some molecules dissolved in seawater can strongly complex trace metal ions. Does this characteristic significantly affect its bioavailability and toxicity (Buffle 1988; Kozelka and Bruland 1998; Hedges 2002)? Finally, do we understand DOM in elemental cycling well enough to accurately represent the processes in numerical models (Hansell and Carlson 2002)? The amount of carbon residing in the pool of DOC in the ocean is equivalent to the amount in the pool of atmospheric CO_2. Thus a small change in the size of the DOC pool could have a major effect on the air-sea exchange of carbon. A fuller understanding of the role of DOC in the ocean carbon cycle and how it might respond to environmental perturbation is essential to our ability to predict the effects of changing climate on the global ocean.

To improve our understanding of the global cycling of C, N and P, future research in marine biogeochemistry of DOC, DON and DOP could include

1. Improvement of analytical methodology of TDN and TDP, including instrument accuracy, precision, sensitivity and recovery efficiency,
2. Improvement of understanding of labile (and semilabile) DOM (such as urea and amino acids) with respect to chemical composition, biological availability and turnover time,
3. Improvement of the geographic coverage of Arctic and Antarctic waters, and
4. Improvement of bacteria remediation of DOM production and removal.

6. References

Abell, J., S. Emerson, and P. Renaud. (2000). Distributions of TOP, TON and TOC in the North Pacific subtropical gyres: Implications for nutrient supply in the surface ocean and remineralisation in the upper thermocline. *J. Mar. Res.* **58**: 203-222.

Aiken, J., N. Rees, S. Hooker, P. Holligan, A. Bale, D. Robins, G. Moore, R. Harris, and D. Pilgrim. (2000). The Atlantic Meridional Transect: Overview and synthesis of data. *Progress Oceanogr.* **45**: 257-312.

Aminot, A. and R. Kerouel. (2004). Dissolved organic carbon, nitrogen and phosphorus in the N-E Atlantic and the N-W Mediterranean with particular reference to non-refractory fractions and degradation. *Deep-Sea Res. I* **51**: 1975-1999.

Amon, R.M.W. and R. Benner. (1994). Rapid cycling of high-molecular-weight dissolved organic matter in the ocean. *Nature* **369**: 549-552.

Amon, R.M.W. and R. Benner. (1996). Bacteial utilisation of different size classes of dissolved organic matter. *Limnol. Oceanogr.* **41**: 41-51.

Anderson, L.A. (1995). On the hydrogen and oxygen content of marine phytoplankton. *Deep-Sea Res. I* **42**: 1675-1680.

Anderson, T.R. and P.J. Williams. (1999). A one-dimensional model of dissolved organic carbon cycling in the water column incorporating combined biological-photochemical decomposition. *Global Biogeochem. Cycles* **13**: 337-349.

Alvarez-Salgado, X. A. and A.E.J. Miller. (1998). Simultaneous determination of dissolved organic carbon and total dissolved nitrogen in seawater by high temperature

catalytic oxidation: Conditions for precise shipboard measurements. *Mar. Chem.* **62**, 325-333.

Azam, F., T. Fenchel, J.G. Field, J.S. Gray, L.A. Meyer-Reil, and F. Thingstad. (1983). The ecological role of water-column microbes in the sea. *Mar. Ecol. Prog. Ser.* **10**: 257-263.

Azam, F, and B.C. Cho. (1987). Bacterial utilisation of organic matter in the sea. *In* "Symposium of the society for general microbiology. 4.1. Ecology of microbial communities." University Press, Cambridge, England.

Azam, F, and J.A. Fuhrman. (1984). Measurement of bacterioplankton growth in the sea and its regulation by environmental conditions. *In* "Heterotrophic activity in the sea" (J. Hobbie and P.J. le B Williams, Eds). pp. 179-196. Plenum Press, New York.

Azam, F. and R.E. Hodson. (1977). Size distribution and activity of marine microheterotrophs. *Limnol. Oceanogr.* **22**: 492-501.

Baines, S.B. and M.L. Pace. (1991). The production of dissolved organic matter by phytoplankton and its importance to bacteria: Patterns across marine and freshwater systems. *Limnol. Oceanogr.* **36**: 1078-1090.

Bauer, J.E., P.M. Williams and E.R.M. Druffel. (1992). ^{14}C activity of dissolved organic carbon fractions in the north-central Pacific and Sargasso Sea. *Nature* **357**: 667-670.

Bauer, J.E. and E.R.M. Druffel. (1998). Ocean margins as a significant source of organic matter to the deep ocean. *Nature* **392**: 482-485.

Becquevort S, P, Menon and C. Lancelot (2000). Differences of the protozoan biomass and grazing during spring and summer in the Indian sector of the Southern Ocean. *Polar Biol.* **23**: 309-320.

Behrenfeld, M.L.J. and P.G. Falkowski. (1997). Photosynthetic rates derived from satellite-based chlorophyll concentration. *Limnol. Oceanogr.* **42**: 1-20.

Benner, R. (2002). Chemical composition and reactivity. *In* "Biogeochemistry of marine dissolved organic matter" (D.A. Hansell and C.A. Carlson, Eds). pp. 59-90. Academic Press, San Diego.

Benner, R. and M. Strom. (1993). Determination of he sources of high blank values associated with DOC measurements by high temperature catalytic oxidation. *Mar. Chem.* **41**: 153-160.

Benner, R.H., J.D. Pakulski, M. MaCarthy, J.I. Hedges, and P.G. Hatcher. (1992). Bulk chemical characteristics of dissolved organic matter in the ocean. *Science*. **255**: 1561-1564.

Benson, B.B. and D. Krause. (1984). The concentration and isotopic fractionation of oxygen dissolved in freshwater and seawater in equilibrium with the atmosphere. *Limnol. Oceanogr.* **29**: 620-632.

Berman, T., C. Béchemin, and S.Y. Maestrini. (1999). Releases of ammonium and urea from dissolved organic nitrogen in aquatic ecosystems. *Aquat. Microb. Ecol.* **16**: 295-302.

Berman T. and D. Bronk. (2003). Dissolved organic nitrogen: A dynamic participant in

aquatic ecosystems. *Aquat. Microb. Ecol.* **31**: 279-305.

Björkman, K., A.L. Thomason-Bulldis, and D.M. Karl. (2000). Phosphorus dynamics in the North Pacific subtropical gyre. *Aquat. Microb. Ecol.* **22**: 185-198.

Blank, M., M. Leinen, and J.M. Prospeo.r (1985). Major Asian Aeolian inputs indicated by the mineralogy of aerosols and sediments in the western North Pacific. *Nature* **314**: 84-86.

Boyer, E.W., C.L. Goodale., N.A. Jaworski, and R.W. Howarth. (2002). Anthropogenic nitrogen sources and relationships to riverine nitrogen expert in the northeastern USA. *Biogeochemistry* **57-58**: 137-169.

Bratbak, G., J.K. Egge, and M. Heldal. (1992). Viral mortality of the marine alga *Emiliana huxleyi* (Haptophyceae) and termination of algal bloom. *Mar. Ecol. Prog. Ser.* **83**: 273-280.

Brewer, P.G.. and Riley, J.P. (1965). The automatic determination of nitrate in seawater. *Deep-Sea Res.* **12**: 765-772.

Bronk, D.A. (2002). Dynamics of DON. *In* "Biogeochemistry of marine dissolved organic matter" (D.A. Hansell and C.A. Carlson, Eds). pp. 153-247. Academic Press, San Diego.

Bronk, D.A., P.M. Glibert, T.C. Malone, S. Banahan, and E. Sahlsten. (1998). Inorganic and organic nitrogen cycling in Chesapeake Bay: Autotrophic versus heterotrophic processes and relationships to carbon flux. *Aquat. Microb. Ecol*. **15**: 177-189.

Bronk, D.A., J. H. See, P. Bradley, and L. Killberg. (2006). DON as a source of bioavailable nitrogen for phytoplankton. *Biogeosciences Discuss.* **3**: 1247-1277.

Bulter, E.I., S. Knox and M.I. Liddicoat. (1979). The relationship between inorganic and organic nutrients in sea water. *J. Mar. Biol. Assoc. UK,* **59**: 239-250.

Burdige, D.J. (2002). Sediment pore waters. *In* ‘‘Biogeochemistry of marine dissolved organic matter’’ (D.A. Hansell and C.A. Carlson, Eds.), pp.611-663. Academic Press, San Diego.

Burdige, D.J., M.J. Alpering, J. Homstead, and C.S. Martens. (1992). The role of benthic fluxes of DOC in oceanic and sedimentary carbon cycling. *Geophys. Res. Lett.* **19**: 1851-1854.

Burdige, D.J. and J. Homstead. (1994). Fluxes of DOC from Chesapeake Bay sediments. *Geochim. Cosmochim. Acta.* **58**: 3407-3424.

Burdige, D.J. and S. Zheng. (1998). The biogeochemical cycling of dissolved organic nitrogen in estuarine sediments. *Limnol. Oceanogr.* **43**: 1796-1813.

Carlson, C.A. (2002). Production and removal processes. *In* “Biogeochemistry of marine dissolved organic matter” (D.A. Hansell and C.A. Carlson, Eds). pp. 91-151. Academic Press, San Diego.

Carlson, C.A. and H.W. Ducklow. (1995). Dissolved organic carbon in the upper ocean of the central equatorial Pacific Ocean, 1992: Daily and finescale vertical variations. *Deep-Sea Res. II* **42**: 639-656.

Carlson, C.A. and H.W. Ducklow. (1996). Growth of bacterioplankton and consumption of dissolved organic carbon in the Sargass Sea. *Aquat. Microb. Ecol.* **10**: 69-85.

Carlson, C.A., H.W. Ducklow, and A.F. Michaels. (1994). Annual flux of dissolved organic carbon from the euphotic zone in the northwestern Sargasso Sea. *Nature* **371**: 405-408.

Carlson, C.A., N.R. Bates, H.W. Ducklow, and D.A. Hansell. (1999). Estimations of bacterial respiration and growth efficiency in the Ross Sea, Antarctica. *Aquat. Microb. Ecol.* **19**: 229-244.

Carlson, C.A., D.A. Hansell, E.T. Peltzer, and W.O. Smith. (2000). Stocks and dynamics of dissolved and particulate organic matter in the southern Ross Sea, Antarctica. *Deep-Sea Res. II* **47**: 3201-3225.

Carlsson, P. and E. Granéli. (1993). Availability of humic bound nitrogen for coastal phytoplankton. *Estuarine Coastal Shelf Sci.* **36**: 433-447.

Carlsson, P., A.Z. Segatto, and E. Granéli. (1993). Nitrogen bound to humic matter of terrestrial origin - A nitrogen pool for coastal phytoplankton? *Mar. Ecol. Prog. Ser.* **97**: 105-116.

Cauwet, G. (2002). DOM in the coastal zone. *In* "Biogeochemistry of marine dissolved organic matter" (D.A. Hansell and C.A. Carlson, Eds). pp. 579-609. Academic Press, San Diego.

Cherrier, J., J.E. Bauer, and E.R.M. Druffel. (1996). Utilisation and turnover of labile

dissolved organic matter by bacterial heterotrophs in eastern North Pacific surface waters. *Mar. Ecol. Prog. Ser.* **139**: 267-279.

Chester, R. (1990). Marine geochemistry. Chapman and Hall, London.

Cho, B.C. and F. Azam. (1988). Major role of bacteria in biogeochemical fluxes in the ocean's interior. *Nature* **332**: 441-443.

Clark, L., E. Ingall, and R. Benner. (1998). Marine phosphorus is selectively remineralized. *Nature* **393**: 426.

Christian, J.R. (1995). "Biochemical mechanisms of bacterial utilisation of dissolved and particulate organic matter in the upper ocean." PhD. Dissertation, University of Hawaii.

Christian, J.R. and D.M. Karl. (1995). Bacterial ectoenzymes in marine waters: Activity ratios and temperature responses in three oceanographic provinces. *Limnol. Oceanogr.* **40**: 1042-1049.

Christian, J.R., M.R., Lewis, and D.M. Karl. (1997). Vertical fluxes of carbon, nitrogen and phosphorus in the North Pacific Subtropical Gyre near Hawaii. *J. Geophys. Res.* **102**: 15667-15677.

Collier, J.L., B. Brahamsha, and B. Palenik (1999). The marine cyanobacterium Synechococcus sp. WH7805 requires urease (urea amidohydrolase EC 3.5.1.5) to utilise urea as a nitrogen source: Molecular-genetic and biochemical analysis of the enzyme. *Microbiology* **145**, 447-459.

Collos, Y., G. Dohler, and I. Biermann. (1992). Production of dissolved organic nitrogen during uptake of nitrate by Synedra planctonica: Implications for estimating new production in the oceans. *J. Plankton Res.* **14**: 1025-1029.

Conover, R.J. and K.R. Gustavson. (1999). Sources of uear in arctic seas: Zooplankton metabolism. *Mar. Ecol. Prog. Ser.* **179**, 41-54.

Copin-Montégut, G. and B. Avril. (1993). Vertical distribution and temporal variation of dissolved organic carbon in the North-Western Mediterranean Sea. *Deep-Sea Res. I,* **40**: 1963-1972.

Dafner, E.V. and P.J. Wangersky. (2002b). A brief overview of modern directions in marine DOC studies. Part I. Methodological aspects. *J. Environ. Monit.* **4**: 48-54.

Dafner, E. V. and P. J. Wangersky. (2002b). A brief overview of modern directions in marine DOC studies. Part II: Recent progress in marine DOC studies. *J. Environ. Monit.* **4**: 55-69.

Daly, K.L. and W.O. Smith. (1993). Physical-biological interactions influencing marine plankton production. *A Rev. Ecol. Syst.* **24**:555-585.

del Giorgio, P. and J.J. Cole. (2000). Bacterial energetics and growth efficiency. *In* "Microbial ecology of the oceans" (D.L. Kirchman, Ed), pp. 289-325. Wiley-Liss, New York.

Diaz, F. and P. Raimbault. (2000). Nitrogen regeneration and dissolved organic nitrogen release during spring in a NW Mediterranean coastal zone (Gulf of Lions): Implications for the estimation of new production. *Mar. Ecol. Prog. Ser.* **197**, 51-65.

Doval, M.D. and D.A. Hansell. (2000). Organic carbon and apparent oxygen utilisation in the western South Pacific and the central Indian Oceans. *Mar.Chem.* **68**: 249-264.

Druffel, E. R. M., P.M. Williams, J.E. Bauer, and J.R. Ertel. (1992). Cycling of dissolved and particulate organic matter in the open ocean. *J. Geophys. Res.* **97**:15639-15659.

Druffel, E.R.M., J.E. Bauer, P.M. Williams, S. Griffin, and D. Wolgast. (1996). Seasonal variability of particulate organic radiocarbon in the northeast Pacific Ocean. *J. Geophys. Res.* **101**: 543-552.

Druffel, E.R.M., S. Griffins, J.E. Bauer, D.M. Wolgast, and X.C. Wang. (1998). Distribution of particulate organic carbon and radiocarbon in the water column from the upper slope to the abyssal NE Pacific Ocean. *Deep-Sea Res. II* **45**: 667-687.

Ducklow, H.W. and C.A. Carlson. (1992). Oceanic bacterial production. *In* "Advances in microbial ecology" (K.C. Marshall, Ed.), Vol. 12, pp.113-181. Plenum Press, New York.

Ducklow, H.W., D.K. Steinberg, and K.O. Buesseler. (2001). Upper ocean carbon export and the biological pump. *Oceanography* **14**: 50-58.

Ducklow, H.W., D.A. Purdie, P.J. Williams, and J.M. Davies. (1986). Bacterioplankton: A sink for carbon in a coastal plankton community. *Science* **232**: 865.

Durand, M.D., R.J. Olson, and S.W. Chisholm. (2001). Phytoplankton population dynamics at the Bermuda Atlantic Time-Series station in the Sargasso Sea. *Deep-Sea Res. II* **48**: 1983-2003.

Emerson, S., P.D. Quay, C. Stump, D. Wilbur, and R. Schudlich. (1995). Chemical tracers of productivity and respiration in the subtropical Pacific Ocean. *J. Geophys. Res.* **100**: 15873-15887.

Fileman, E.S. and R.J.G. Leakey. (2005). Microzooplankton dynamics during the development of the spring bloom in the north-east Atlantic. *J. Mar. Biol. Ass. U.K.* **85**: 741-753.

Föllmi, K.B. (1996). The phosphorus cycle, phosphogenesis and marine phosphate-rich deposits. *Earth Sci. Rev*. **40**: 55-124.

Fuhrman, J.A. (1999). Bacterioplankton roles in cycling of organic matter: The microbial food web. *In* "Primary productivity and biogeochemical cycles in the sea" (P.G. Falkowski and A.D. Woodhead, Eds.), pp. 361-383. Plenum Press, New York.

Fuhrman, J.A. (1999). Marine viruses and their biogeochemical and ecological effects. *Nature*, **399**: 541-548.

Fuhrman, J.A. and R.L. Ferguson. (1986). Nanomolar concentrations and rapid turnover of dissolved free amino acids in seawater: Agreement between chemical and microbiological measurements. *Mar. Ecol. Prog. Ser.* **33**: 237-242.

Garcia-Fernandez, J.M., N.T. Marsac, and J. Diez. (2004). Streamlined Regulation and Gene Loss as Adaptive Mechanisms in *Prochlorococcus* for optimaised nitrogen utilisation in oligotrophic environments. *Microbiol Mol. Biol. Rev.* **68**: 630-638.

García, H.E. and L.I. Gordon. (1992). Oxygen solubility in seawater: Better fitting equations. *Limnol. Oceanogr.* **37**: 1307-1312.

Garside, C. (1982). A chemiluminescent technique for the determination of nanomolar concentrations of nitrate and nitrite in seawater. *Mar. Chem.* **11**: 159-167.

Gobler, C.J., D.A. Hutchins, N.S. Fisher, E.M. Cosper, and S.A. Sañudo-Wilhelmy. (1997). Release and bioavailability of C, N, P, Se, and Fe following viral lysis of a marine chrysophyte. *Limnol. Oceanogr.* **42**: 1492-1504.

Goericke, R., and N.A. Welschmeyer. (1998). Response of Sargasso Sea phytoplankton biomass, growth rates and primary production to seasonally varying physical forcing. *J. Plankton Res.* **20:** 2223–2249.

Goldman, J.D., D.A. Hansell, and M. Dennet. (1992). Chemical characterisation of three large oceanic diatoms: potential impact on water column chemistry. *Mar. Ecol. Prog. Ser.* **88**: 257-270.

Hansell, D.A. (2002). DOC in the global ocean carbon cycle. *In* "Biogeochemistry of marine dissolved organic matter" (D.A. Hansell and C.A. Carlson, Eds). pp. 685-715. Academic Press, San Diego.

Hansell, D.A. and C.A. Carlson. (1998). Deep-ocean gradients in the concentration of dissolved organic carbon. *Nature* **395**: 263-266.

Hansell, D.A. and C.A. Carlson. (2001a). Biogeochemistry of total organic carbon and nitrogen in the Sargasso Sea: Control by convective overturn. *Deep-Sea Res. II* **48**: 1649-1667.

Hansell, D.A. and C.A. Carlson. (2001b). Marine dissolved organic matter and the carbon cycle. *Oceanography,* **14**, 41-49.

Hansell, D.A. and C.A. Carlson. (2002). Preface. *In* "Biogeochemistry of marine dissolved organic matter" (D.A. Hansell and C.A. Carlson, Eds). xxi-xxii. Academic Press, San Diego.

Hasegawa, T., I. Koike and H. Mukai. (2000). Release of dissolved organic nitrogen by size-fractionated natural planktonic assemblages in coastal waters. *Mar. Ecol. Prog. Ser.* **198**: 43-49.

Hedges, J.I. (1992). Global biogeochemical cycle: Progress and problems. *Mar Chem.* **39**: 67-93.

Hedges, J.I. (2002). Why dissolved organic matter. *In* "Biogeochemistry of marine dissolved organic matter" (D.A. Hansell and C.A. Carlson, Eds). pp. 1-33. Academic Press, San Diego.

Heywood, J. L., M.V. Zubkov, G.A Tarran, B.M. Fuchs, and P.M. Holligan. (2006). Proharyoplankton standing stocks in oligotrophic gyre and equatorial provinces of the Atlantic Ocean: Evaluation of inter-annual variability. *Deep-Sea Res. II* **53**: 1530-1547.

Holm-Hansen, O., J.D.H. Strickland, and P.M. Williams. (1966). A detailed analysis of biological important substances in a profile off southern California. *Limnol. Oceanogr.* **11**: 548-561.

Hopkinson, C.S., B. Fry. and A.L. Nolin. (1997). Stoichiometry of dissolved organic matter dynamics on the continental shelf of the northeastern U.S.A. *Continent. Shelf Res.* **17**: 473-489.

Hopkinson, C.S., J.J. Vallino, and A. Nolin. (2002). Decomposition of dissolved organic matter from the continental margin. *Deep-Sea Res. II* **49**: 4461-4478.

Hopkinson, C.S. and J.J. Vallino. (2005). Efficient export of carbon to deep ocean through dissolved organic matter. *Nature* **433**: 142-145.

Hoppe, H.G. (1991). Microbial extracellular enzyme activity: A new key parameter in aquatic ecology. *In* "Microbial enzymes in aquatic environments" (R.J. Chrost, Ed.), pp.60-83. Springer-Verlag, New York.

Hudson, J.J. and W.D. Taylor. (1996). Measuring regeneration of dissolved phosphorus in planktonic communities. *Limnol. Oceanogr.* **41**: 1560-1565.

Imai, I., Y. Ishida. and Y. Hata. (1993). Killing of marine phytoplankton by a gliding bacterium *Cytophaga* sp., isolated from the coastal sea of Japan. *Mar. Biol*. **116**, 527-532.

Isla, J.A., M. Llope, and R. Anadón. (2004). Size-fractionated mesozooplankton biomass, metabolism and grazing along a 50°N to 30°S transect of the Atlantic Ocean. *J. Plankton Res.* **26**: 1301-1313.

Jackson, G. A. and P.M. Williams. (1985). Importance of dissolved organic nitrogen and phosphorus to biological nutrient cycling. *Deep-Sea Res.* **32**: 223-235.

Jørgensen, N.O.G., L.J. Tranvik and G.M. Berg. (1999). Occurrence and bacterial cycling of dissolved nitrogen in the Gulf of Riga, the Baltic Sea. *Mar. Ecol. Prog. Ser.* **191**: 1-18.

Jumars, P.A., D.L. Penry, J.A. Baross, M.J. Perry and B.W. Frost. (1989). Closing the microbial loop: Dissolved carbon pathway to heterotrophic bacteria from incomplete ingestion, digestion and absorption in animals. *Deep-Sea Rea*. **36**: 483-495.

Kähler, P., P.K. Björnsen, K. Lochte, and A. Anita. (1997). Dissolved organic matter and its utilization by bacteria during spring in the Southern Ocean. *Deep-Sea Res. II* **44**: 341-353.

Karl, D. M., G. Tien, J. Dore, and C.D. Winn (1993). Total dissolved nitrogen and phosphorous concentrations at US-JGOFS Station ALOHA: Redfield reconciliation. *Mar. Chem.* **41**: 203-208.

Karl, D.M., J.R. Christian, J.E. Dore, D.V. Hebel, R.M. Letelier, L.M. Tupas, and C.D. Winn. (1996). Seasonal and interannual variability in primary production and particle flux at Station ALOHA. *Deep-Sea Res. II* **43**: 539-568.

Karl, D.M., R.R. Bidigare, and R.M. Letelier. (2001a). Long-term changes in plankton community structure and productivity in the North Pacific Subtropical Gyre: The domain shift hypothesis. *Deep-Sea Res. II* **48**: 1449-1470.

Karl, D.M., K.M.B Jörkman, J.E. Dore, L. Fujieki, D.V. Hebel, T. Houlihan, R.M. Letelier, and L.M. Tupas. (2001b). Ecological nitrogen-to-phosphorus stiochiometry at station ALOHA. *Deep-Sea Res. II* **48**: 1529-1566.

Karl, D.M. and K.M. Björkman. (2002). Dynamics of DOP. *In* "Biogeochemistry of marine dissolved organic matter" (D.A. Hansell and C.A. Carlson, Eds). pp. 249-366. Academic Press, San Diego.

Karner, M. and G.J. Herndl. (1992). Extracellular enzymatic activity and secondary production in free-living and marine-snow-associated bacteria. *Mar. Biol.* **113**: 341-347.

Keil, R.G. and D.L. Kirchman. (1991). Contribution of dissolved free amino acids and ammonium to the nitrogen requirements of heterotrophic bacterioplankton. *Mar. Ecol. Prog. Ser.* **73**: 1-10.

Keil, R.G. and D.L. Kirchman. (1994). Abiotic transformation of labile protein to refractory protein in sea water. *Mar. Chem.* **45**: 187-196.

Keil, R.G. and D.L.Kirchman. (1999). Utilisation of dissolved protein and amino acids in the northern Sargasso Sea. *Aquat. Microb. Ecol.* **18**: 293-300.

Kirchman, D.L. (2000). Uptake and regeneration of inorganic nutrients by marine heterotrophic bacteria. *In* "Microbial ecology of the oceans" (D.L. Kirchman, Ed.). pp. 261-288. Wiley-Liss, New York.

Kirchman, D. L., C. Lancelot, M. Fashman, L. Legendre, G. Radach, and M. Scott. (1993). Dissolved organic matter in biogeochemical models of the ocean. *In* "Towards a model of ocean biogeochemical processes". (G.T. Evans and M.J.R. Fasham, Eds.), pp.209-225. Springer-Verlag Berlin.

Kirkwood, D. (1989). Simultaneous determination of selected nutrients in sea water. International Council for the Exploration of the Sea Council Meeting papers 1989/C:29.

Knauer, G.A., J.H. Martin, and K.W. Bruland. (1979). Fluxes of particulate carbon, nitrogen and phosphorus in the upper water column of the northeast Pacific. *Deep-Sea Res.* **26**: 97-108.

Koike, I. and L. Tupas. (1993). Total dissolved nitrogen in the Northern North Pacific assessed by a high-temperature combustion method. *Mar. Chem.* **41**: 209-214.

Krom, M.D., E.M.S. Woodward, B. Herut, N. Kress, P. Carbo, R.F.C. Mantoura, G. Spyres, T.F. Thingstad, P. Wassmann, C. Wexels-Riser, V. Kitidis, C.S. Law, G. Zodiatis, and T. Zohary. (2005). Nutrient cycling in the south east Levantine basin of the Eastern Mediterranean: Results from a phosphate starved system. *Deep-Sea Res. II* **52**: 2879-2896.

Large, W.G., J.C. McWilliams, and S.C. Doney. (1994). Oceanic vertical mixing: A review and a model with nonlocal boundary layer parameterisation. *Rev. Geophys*. **32**: 363-403.

Laws, E.A., G.R. DiTullio, and D.G. Redalje. (1987). High phytoplankton growth and production rates in the North Pacific subtropical gyre. *Limnol. Oceanogr.* **32:** 905-918.

Laws, E.A., and T.T. Bannister. (1980). Nutrient- and light-limited growth of *Thalassiosira* y*uviatilis* in continuous culture, with implications for phytoplankton growth in the ocean. *Limnol. Oceanogr.* **25**: 457-473.

Lee, C. and S.M. Henrichs. (1993). How the nature of dissolved organic matter might affect the analysis of dissolved organic carbon. *Mar. Chem.* **41**: 105-120.

Libes, S.M. (1992). An introduction to marine biogeochemistry. John Wiley & Sons, Inc. Canada.

Libby, P.S. and P.A. Wheeler. (1997). Particulate and dissolved organic nitrogen in the central and eastern equatorial Pacific. *Deep-Sea Res. I* **44**: 345-361.

Loh, A.N. and J.E. Bauer. (2000). Distribution, partitioning and fluxes of dissolved and particulate organic C, N and P in the eastern North Pacific and Southern Oceans. *Deep-Sea Res. I* **47**: 2287-2316.

Mackey, R.M., R.G. Labiosa, M. Calhoun, J.H. Street, A.F. Post, and A. Paytan. (2007). Phosphorus availability, phytoplankton community dynamics, and taxon-specific phosphorus status in the Gulf of Aqaba, Red Sea. *Limnol. Oceanogr.* **52**, 873-885.

Mahaffey, C., R.G. Williams, and G.A. Wolff. (2004). Physical supply of nitrogen to phytoplankton in the Atlantic Ocean. *Global Biogeochem. Cycles*, **18** (GB1034): doi:10.1029/2003GB002129.

Maita, Y. and M. Yanada. (1990). Vertical distribution of total dissolved nitrogen and dissolved organic nitrogen in seawater. *Geochem. J.* **24**: 245-254.

Malone, T.C., S.E. Pike, and D.J. Conley. (1993). Transient variations in phytoplankton productivity at the JGOFS Bermuda time series station. *Deep-Sea Res. I* **40:** 903–924.

Marañón, E., P.M. Holligan, M. Varela, B. Mouriño, and A.J., Bale. (2000). Basinscale variability of phytoplankton biomass, production and growth in the Atlantic Ocean. *Deep-Sea Res. I* 47, 825-857.

Marañón, E., P. Cermeño, and V. Pérez. (2005). Continuity in the photosynthetic production of dissolved organic carbon from euphotic to oligotrophic waters. *Mar. Ecol. Prog. Ser.* **299**: 7-17.

Martin, J., G. Knauer, D. Karl, and W. Broenkow. (1987). VERTEX: Carbon cycling in

the northeast Pacific. *Deep-Sea Res.* **34**: 267-285.

McCarthy, M.D., J.I.Hedges, and R. Benner. (1998). Major bacterial contribution to marine dissolved organic nitrogen. *Science* **281**: 231-234.

Michaels, A.F., A.H. Knap, R.L. Dow, K. Gundersen, R.J. Johnson, J. Sorensen, A. Close, G.A. Knauer, S.E. Lohrenz, V.A. Asper, M. Tuel, and R. Bidigare. (1994). Seasonal patterns of ocean biogeochemistry at the United-States JGOFS Bermuda Atlantic Time-Series Study site. *Deep-Sea Rea. I* **41**: 1013-1038.

Miller, C.A. and D.J. Glibert. (1980). Nitrogen exretion by the calanoid copepod Acartia tonsa: Results from mesocosm experiments. *J. Plankton Res.* **20**, 1767-1780.

Mills, M.M., C. Ridame, M. Davey, J.L. Roche, and R.J. Geider. (2004). Iron and phosphorus co-limit nitrogen fixation in the eastern tropical North Atlantic. *Nature* **429**: 292-294.

Moore, C.M., M.M. Mills, R. Langlois, A. Milne, E.P. Achterberg, J.L. Roche, and R.J. Geider. Relative influence of nitrogen and phosphorus availability on phytoplankton physiology and productivity in the oligotrophic subtropical North Atlantic Ocean. Submitted to *Limnol. Oceanogr.*

Moore, L.R., A.F. Post, G. Rocap, and S.W. Chisholm. (2002). Utilization of different nitrogen sources by the marine cyanobacteria, Prochlorococcus and Synechococcus. *Limnol. Oceanogr.* **47**: 989-996.

Mopper, K., X.L. Zhou, R.J. Kieber, D.J. Kieber, R.J. Sikorski, and R.D. Jones. (1991). Photochemical degradation of dissolved organic carbon and its impact on the oceanic

carbon cycle. *Nature* **353**: 60-62.

Moran, M.A. and R.G. Zepp. (1997). Role of photoreactions in the formation of biologically labile compounds from dissolved organic matter. *Limnol. Oceanogr.* **42**: 1307-1316.

Münster, U. and H. De Hann. (1998). The role of microbial extracelluar enzymes in the transformation of dissolved organic matter in humic waters. *In* "Aquatic humic substances" (D.O. Hessen and L.J. Tranvik, Eds.), pp. 199-257. Springer-Verlag, Berlin.

Nagata, T. and D.L. Kirchman. (1996). Bacterial degradation of protein absorbed to model submicron particles in seawater. *Mar. Ecol. Prog. Ser.* **132**: 241-248.

Ogawa, H., R. Fukuda, and I. Koike. (1999). Vertical distributions of dissolved organic carbon and nitrogen in the Southern Ocean. *Deep-Sea Res. I.* **46**: 1809-1826.

Ogura, N. (1972). Rate and extent of decomposition of dissolved organic matter in surface seawater. *Mar. Biol.* **13**: 89-93.

Ormaza-Gonzalez, F.I. and P.J. Statham. (1996). A comparison of methods for the determination of dissolved and particulate phosphorus in natural waters. *Water Res.* **30**: 2739-2747.

Orrett, K. and D.M. Karl. (1987). Dissolved organic phosphorus production in surface seawaters. *Limnol. Oceanogr.* **32**: 383-395.

Palenik, B. and F.M.M. Morel. (1990a). Amino acid utilisation by marine

phytoplankton: A novel mechanism. *Limnol. Oceanogr.* **35**: 260-269.

Palenik, B. and F.M.M. Morel. (1990b). Comparison of cell-surface L-amino acid oxidases form several marine phytoplankton. *Mar. Ecol. Prog. Ser.* **59**: 195-201.

Pan, X., R. Sanders, A.D. Tappin, P.J. Worsfold, and E.P. Achterberg. (2005). Simultaneous determination of dissolved organic carbon and total dissolved nitrogen on a coupled high temperature combustion total organic carbon-nitrogen chemiluminescence detection (HTC TOC-NCD) system. *J. Autom. Method Manag.* **2005**: 240-246.

Pan, X., R. Sanders, A.J. Poulton, C. Robinson, and E.P. Achterberg. Dissolved organic carbon and apparent oxygen utilisation in the Atlantic Ocean. Submitted to *GBC*.

Peltzer, E.T. and N.A. Hayward. (1996). Spatial and temporal variability of total organic carbon along 140oW in the equatorial Pacific Ocean in 1992. *Deep-Sea Res. II* **43**: 1155-1180.

Pinet, P.R. (2003). Invitation to oceanography. 3rd Edition. Jones and Bartlett Publishers, Inc. U.S.

Pomeroy, L.R. (1974). The ocean's food web, a changing paradigm. *Bioscience*, **24**: 499-504.

Pomeroy, L.R., J.E. Sheldon, W.M. Sheldon, and F. Peters. (1995). Limits to growth and respiration of bacterioplankton in the Gulf of Mexico. *Mar. Ecol. Prog. Ser.* **117**: 259-268.

Poulton, A.J., P.M. Holligan, A. Hickman, Y.N. Kim, T.R. Adey, M.C. Stinchcombe, C. Holten, S. Root, and E.M.S. Woodward. (2006). Phytoplankton carbon fixation, chlorophyll biomass and diagnostic pigments in the Atlantic Ocean. *Deep-Sea Res. II.* **53**: 1593-1610.

Prasil, O., M.Y. Gorbunov, F. Bruyant, S. Bonnet, C. Guieu, P. Raimbault, H. Claustre, and P.G. Falkowski. (2006). Iron and Nitrogen Limitation of Primary Production in South Pacific oceanic gyre. *Eos Trans. AGU.* **87**: Ocean Sci. Meet. Suppl., Abstract.

Proctor, L.M. and J. A. Fuhrman. (1990). Viral mortality of marine bacteria and cyanobacteria. *Nature* **343**: 60-62.

Proctor, L.M. and J. A. Fuhrman. (1992). Mortality of marine bacteria in response to enrichments of the virus size fraction from seawater. *Mar. Ecol. Prog. Ser.* **87**, 283-293.

Puddu, A., A. Zoppini, and M. Pettine. (2000). Dissolved organic matter and microbial food web interactions in the marine environment: the case of the Adriatic Sea. *Int. J. Environ. Pollut.* **13**: 473-494.

Quay, P. (1997). Was a carbon balance measured in the equatorial Pacific during JGOFS? *Deep-Sea Res.* **44**: 1765-1781.

Quevedo, M., and R. Anadón. (2001). Protist control of phytoplankton growth in the subtropical north-east Atlantic. *Mar. Ecol. Prog. Ser.* **221:** 29-38.

Raimbault, P., G., Slawyk, B. Boudjellal, C. Coatanoan, P. Conan, B. Coste, N. Garcia, T. Moutin, and M. Pujo-Pay. (1999). Carbon and nitrogen uptake and export in the

equatorial Pacific at 105°W: Evidence of an efficient regenerated production cycle. *J. Geophys. Res*. **104**: 3341-3356.

Raven, J.A. (1994). Why are there no picoplankton O_2 evolvers with volumes less than 10^{-19} m^3? *J. Plankton Res.* **16**: 565-580.

Redfield, A.C. (1958). The biological control of chemical factors in the environment. *Amer. Scient.* **46**: 205-221.

Redfield, A. C., B.H. Ketchum, and F.A. Richards. (1963). The influence of organisms on the composition of seawater. *In* "The Sea" (M.N. Hill, Ed.), Vol.2, pp. 26-77. Interscience, New York.

Rees, A.P., E.M.S. Woodward, and I. Joint, I. (2006). Concentrations and uptake of nitrate and ammonium in the Atlantic Ocean between 60°N and 50°S. *Deep-Sea Res. I* **53**: 1649-1665.

Rich, J. H., H.W. Ducklow, and D.L. Kirchman. (1996). Concentrations and uptake of neutral monosaccharides along 140°W in the equatorial Pacific: Contribution of glucose to heterotrophic bacterial activity and the DOM flux. *Limnol. Oceanogr.* **4**: 595-604.

Rich, J., M. Gosselin, E. Sherr, B. Sherr, and D.L. Kirchman. (1997). High bacterial production, uptake and concentrations of dissolved organic matter in the Central Arctic Ocean. *Deep-Sea Res. II*, **44**: 1645-1663.

Ridal, J.J. and R.M. Moore. (1992). Dissolved organic phosphorus concentrations in the northeast subarctic Pacific Ocean. *Limnol. Oceanogr.* **37**, 1067-1075.

Robinson, C., A.J. Poulton, P.M. Holligan, A.R. Baker, G. Forster, N. Gist, T.D. Jickells, G. Malin, R. Upstill-Goddard, R.G. Williams, E.M.S. Woodward, and M.V. Zubkov. (2006). The Atlantic Meridional (AMT) programme: A contextual view 1995-2005. *Deep-Sea Res. II* **53**: 1485-1515.

Rønn, R., M. Gavito, J. Larsen, I. Jakobsen, H. Frederiksen, and S. Christensen, (2002). Response of free-living soil protozoa and microorganisms to elevated atmospheric CO_2 and presence of mycorrhiza, *Soil Biol. Biochem.* **34**: 923-932.

Roussenov, V., R.G., Williams, C. Mahaffey, and G.A. Wolff. (2006). Does the transport of dissolved organic nutrients affect export production in the Atlantic Ocean? *Global Biogeochem. Cycles* **20** (GB3002): doi:10.1029/2005GB002510.

Ruby, E.G., J.B. McCabe, and J.I. Barke. (1985). Uptake of intact nucleoside monophosphates by *Bdellovibrio bacteriovorus* 109J. *J. Bacteriol.,* **163**: 1087-1094.

Sanders, R. and T. Jickells. (2000). Total organic nutrients in Drake Passage. *Deep-Sea Res. I* **47**: 997-1014.

Sarmiento, J.L. and U. Siegenthaler. (1992). New production and the global carbon cycle. In Primary productivity and biogeochemical cycles in the sea (Ed. P.G. Falkowski and A.D. Woodhead). pp. 317-332. New York. Plenum Press

Seitzinger, S.P., and C. Kroeze. (1998), Global distribution of nitrous oxide production and N inputs in freshwater and coastal marine ecosystems. *Global Biogeochem. Cycles* **12**: 93-113.

Sherr, E., and B. Sherr. (1988). Role of microbes in pelagic food webs: a revised

concept. *Limnol. Oceanogr.* **33**: 1225-1227.

Sharp, J. H., R. Benner, L. Bennett, C.A. Carlson, S.E. Fitzwater, E.T. Peltzer, and L.M. Tupas. (1995). Analysese of dissolved organic carbon in seawater: The JGOFS Equatorial Pacific methods comparison. *Mar. Chem.* **48**: 91-108.

Siegenthaler, U. and J.L. Sarmiento. (1993). Atmospheric carbon dioxide and the ocean. *Nature* **365**: 119-125.

Skoog, A. and R. Benner. (1997). Aldoses in various size fractions of marine organic matter: Implications for carbon cycling. *Limnol. Oceanogr.* **42**: 1803-1813.

Skoog, A., B. Biddanda, and R. Benner. (1999). Bacterial utilisation of dissolved glucose in the upper water column of the Gulf of Mexico. *Limnol. Oceanogr.* **44**: 1625-1633.

Slawyk, G. and P. Raimbault. (1995). Simple procedure for simultaneous recovery of. dissolved inorganic and organic nitrogen in ^{15}N-tracer experiments and improving the isotopic mass balance. *Mar. Ecol. Prog. Ser.* **124**: 289-299.

Slawyk, G., P. Raimbault, and N. Garcia. (1998). Measuring gross uptake of ^{15}N-labeled nitrogen by marine phytoplankton without particulate matter collection. Evidence of low 15N losses to the dissolved organic nitrogen pool. *Limnol. Oceanogr.* **43**: 1734-1739.

Smith, D., M. Simon, A.L. Alldredges, and F. Azam. (1992). Intense hydrolytic enzyme activity on marine aggregates and implications for rapid particle dissolution. *Nature* **359**: 139-142.

Smith, D., M. G.F. Steward, R.A. Long, and F. Azam. (1995). Bacterial mediation of carbon fluxes during a diatom bloom in a mesocosm. *Deep-Sea Res. II* **42**: 75-98.

Smith, S. V., W.J. Kimmerer, and T.W. Walsh (1986). Vertical flux biogeochemical turnover regulate nitrient limitation of net organic production in the North Pacific gyre. *Limnol. Oceanogr.* **31**: 161-167.

Soloviev, A., and R. Lukas. (2006). The near-surface layer of the ocean: Structure, dynamics and applications. Springer-Verlag Berlin

Søndergarrd, M., P.J. Williams, G. Cauwet, B. Riemann, C. Robinson, S. Terzic, E.M.S., Woodward, and J. Worm. (2000). Net accumulation and flux of dissolved organic carbon and dissolved organic nitrogen in marine plankton communities. *Limnol. Oceanogr.* **45**: 1097-1111.

Sprintall, J. and M. Tomczak. (1992). Evidence of the barrier layer in the surface layer of the tropics. *J. Geophys. Res.* **97**: 7305-7316.

Spyres, G., M. Nimmo, P.J. Worsfold, E.A. Achterberg, and A.E.J. Miller. (2000). Determination of DOC in seawater using HTCO techniques. *Tr. Analyt. Chem.* **19**: 498-506.

Steinberg, D.K., C.A. Carlson, N.R. Bates, S.A. Goldthwait, J.P. Madin, and A.F. Michaels. (2000). Zooplankton vertical migration and the active transport of dissolved organic and inorganic carbon in the Sargasso Sea. *Deep-Sea Res. I* **47**: 137-158.

Steinberg, D.K., C.A. Carlson, N.R. Bates, R.J. Johnson, A.F. Michaels, and A.H. Knap.

(2001). Overview of the US JGOFS Bermuda Atlantic Time-series Study (BATS): A decade-scale look at ocean biology and biogeochemistry. *Deep-Sea Res. II* **48**, 1405-1447.

Steward, G.F., D.C. Smith, and F. Azam. (1996). Abundances and production of bacteria and viruses in the Chukchi Sea. *Mar. Ecol. Prog. Ser.* **131**: 287-300.

Strom, S.L., R. Benner, and S. Ziegler, and M.J. Dagg. (1997). Planktonic grazers are a potentially important source of marine dissolved organic carbon. *Limnol. Oceanogr.* **42**, 1364-1374

Suttle, C.A., A.M. Chan, and M.T. Cottrell. (1990). Infection of phytoplankton by viruses and reduction of primary productivity. *Nature* **347**: 467-469.

Suttle, C.A. (1992). Inhibition of photosynthesis in phytoplankton by the submicron size fraction concentrated from seawater. *Mar. Ecol. Prog. Ser.* **87**, 105-112.

Suttle, C.A. (1994). The significance of viruses to mortality in aquatic microbial communities. *Microb. Ecol.* **28**, 237-243.

Tanoue, E., S. Nishiyama, M. Kamo, and A. Tsugita. (1995). Bacterial membrane: Possible source of a major dissolved protein in seawater. *Geochim. Cosmochim. Acta* **59**: 2643-2648.

Takahashi, T., R.T. Wanninkhof, R.A. Feely, R.F. Weiss, D.W. Chipman, N.R. Bates, J. Olafsson, C.L. Sabine, and C.S. Sutherland. (1999). Net sea-air CO_2 flux over the global ocean: An improved estimate based on air-sea pCO_2 differences. *In* "Proceeding of the 2nd symposium on CO_2 in the oceans" (Y. Nojiri, Ed.), pp. 9-15. Tsukuba, Japan.

Tarran, G.A., J.L., Heywood, and M.V. Zubkov (2006). Latitudinal changes in the standing stocks of nano- and picophytoplankton in the Atlantic Ocean. *Deep-Sea Res. II* **53**: 1516-1529.

Teira, E., B. Mouriño, E. Marañón, V. Perez, M.J. Pazo, P. Serret, D. de Armas, J. Escanez, E.M.S. Woodward, and E. Fernández, (2005). Variability of chlorophyll and primary production in the eastern North Atlantic Subtropical Gyre: Potential factors affecting phytoplankton activity. *Deep-Sea Res*. I **52**: 569-588.

Thibault, D., S. Roy, C.S. Wong, and J.K. Bishop. (1999). The downward flux of biogenic material in the NE subarctic Pacific - Importance of algal sinking and mesozooplankton herbivory. *Deep-Sea Res. II* **46**: 2669-2697.

Thingstad, T.F. (2005). Simulating the response to phosphate additions in the oligotrophic eastern Mediterranean using an idealised four-member microbial food web model. *Deep-Sea Res. II* **52**: 3074-3089.

Thingstad, T.F., U.L. Zweifel, and F. Rassoulzadegan. (1998). P-limitation of both phytoplankton and heterotrophic bacteria in NW Mediterranean summer surface waters. *Limnol. Oceanogr.* **43**: 88-94.

Thomalla, S., R., Turnewitsch, M. Lucas, and A. Poulton. (2006). Particulate organic carbon export from the North and South Atlantic gyres: The 234Th/238U disequilibrium approach. *Deep-Sea Res. II* **53**: 1629-1648.

Thomas, W. H., E.H. Renger, and A.N. Dodson. (1971) Near-surface organic nitrogen in the eastern tropical Pacific Ocean. *Deep-Sea Res.* **18**: 65-71.

Toggweiler, J.R. (1989). Deep-sea carbon, a burning issue. *Nature* **334**: 468.

Toggweiler, J.R. (1999). Oceanography: An ultimate limiting nutrient. *Nature* **400**: 511-512.

Tyrrell, T. (1999). The relative influences of nitrogen and phosphorus on oceanic primary production. *Nature* **400**: 525-531.

Urban-Rich, J. (1999). Release of dissolved organic carbon from copepod fecal pellets in the Greenland Sea. *J. Exp. Mar. Ecol.* **232**, 107-124.

Vernet, M., P.A. Matrai and I. Andreassen. (1998). Synthesis of particulate and extracellular carbon by phytoplankton at the marginal ice zone in the Barents Sea. *J. Geophys. Res.* **103**: 1023-1037.

Vidal, M., C.M. Duarte, and S. Agusti. (1999). Dissolved organic nitrogen and phosphorus pools and fluxes in the central Atlantic Ocean. *Limnol. Oceanogr.* **44**: 106-115.

Villareal, T.A., M.A. Altabet, and K. Culver-Rymsza. (1993). Nitrogen transport by vertically migrating diatom mats in the north Pacific Ocean. *Nature* **363**: 709-712.

Vodacek A., M. D. DeGrandpre, E. T. Peltzer, R. K. Nelson, and N. V. Blough. (1997). Seasonal variation of CDOM and DOC in the Middle Atlantic Bight: Terrestrial inputs and photooxidation. *Limnol. Oceanogr.* **42**: 674-686.

Walsh, T.W. (1989). Total dissolved nitrogen in seawater: A new high-temperature combustion method and a comparison with photo-oxidation. *Mar. Chem.* **26**: 295-311.

Wanner, B.L. (1993). Gene regulation by phosphate in entire bacteria. *J. Cell. Biochem,* **51**: 47-54.

Ward, B.B. and D.A. Bronk. (2001). Net nitrogen uptake and don release in surface waters: Importance of trophic interactions implied from size fractionation experiments. *Mar. Ecol. Prog. Ser.* **219**: 11-24.

Watt, W.D. and F.R. Hyes. (1963). Tracer study of the phosphorus cycle in sea water. *Limnol. Oceanogr.* **8**: 276-285.

Willey, J.D., R.J. Kieber, M.S. Eyman, and G.B. Avery. (2000). Rainwater DOC: Concentration and global flux. *Global Biogeochem. Cycles* **14**: 139-148.

Williams, P.J. le B. (1970). Heterotrophic utilisation of dissolved organic compound in the sea. I. Size distribution of population and relationsjip between respiration and incorporation of growth substrates. *J. Mar. Biol. Assoc. UK* **50**: 859-870.

William, P.J. le B. (1981a). Incorporation of microheterotrophic processes into the classical paradigm of the planktonic food web. *Kiel. Meeresforsch* **5**: 1-28.

William, P.J. le B. (1981). Microbial contribution to overall marine plankton metabolism: Direct measurements of respiration. *Oceanologica Act* **4**, 359-364.

Williams, P.J. le B. (2000). Heterotrophic bacteria and the dynamics of dissolved organic material. *In* ‘‘Microbial ecology of the oceans’’ (D.L. Kirchman, Ed.). pp.153-200. Wiley-Liss, New York.

Williams, P.M., A.F. Carlucci, and R. Olson. (1980). A deep profile of some

biologically important properties in the central North Pacific gyre. *Oceanol. Acta* **3**: 471-476.

Williams, P.M and N.W. Jenkinson, (1982). A transportable microprocessor-controlled precise Winkler titration suitable for field station and shipboard use. *Limnol. Oceanogr.* **27**: 576-584.

Williams, P.M. and E.R.M. Druffel. (1987). Radiocarbon in dissolved organic matter in the central North Pacific Ocean. *Nature* **330**: 246-248.

Williams, P.M. and E.R.M. Druffel. (1988). Dissolved organic matter in the ocean: Comments on a controversy. *Oceanography* **1**: 14-17.

Williams, R. G., A.J. McLaren, and M.J. Follow. (2000). Estimating the convective supply of nitrate and implied variability in export production over the North Atlantic. *Global Biogeochem. Cycles* **14**: 1299-1313.

Wong, C.S., Z. Yu, N.A.D. Waser, F.A. Whitney, and W.K. Johnson. (2002). Seasonal changes in the distribution of dissolved organic nitrogen in coastal and open-ocean waters in the North East Pacific: Sources and sinks. *Deep-Sea Res II* **49**: 5759-5773.

Woodward, E.M.S. (2002). Nanomolar detection for phosphate and nitrate using liquid waveguide technology. EOS Transactions. *American Geophysical Union*, Supplement **83**, 92.

Woodward, E.M.S. and N.J.P. Owens. (1990). Nutrient depletion studies in offshore North Sea areas. *Netherlands J. Sea Res.* **25**: 57-63.

Zee, C. van and L. Chou. (2004). Seasonal cycling of phosphorus in the southern bight of the North Sea. *Biogeosciences,* **2**: 27-42.

Zubkov, M.V., M.A. Sleigh, P.H. Burkill, and R.J.G. Leakey. (2000). Picoplankton community structure on the Atlantic Meridional Transect: a comparison between seasons. *Progr. Oceanogr.* **45**: 369-386.

Zubkov, M.V., B.M. Fuchs, G.A. Tarran, P.H. Burkill, and R. Amann. (2003). High rate of uptake of organic nitrogen compounds by Prochlorococcus cyanobacteria as a key to their dominance in oligotrophic oceanic waters. *Applied Environ. Microbiol.* **69**: 1299-1304.

Zubkov, M.V., G.A. Tarran and B.M. Fuchs. (2004). Depth related amino acid uptake by *Prochlorococcus* cyanobacteria in the Southern Atlantic tropical gyre. *FEMS Microbiol. Ecol.* **50**: 153-161.

Zubkov, M.V. and G.A. Tarran. (2005). Prochlorococcus amino acid uptake in surface waters across the South Atlantic Subtropical Front. *Aquat. Microb. Ecol.* **40**: 241-249.

Zubkov, M.V., M.A. Sleigh, G.A. Tarran, P.H. Burkill, and R.J.G. Leakey. (1998). Picoplanktonic community structure on an Atlantic transect from 50^{o}N to 50^{o}S. *Deep-Sea Res. I* **45**, 1339-1355.

Journal of Automated Methods & Management in Chemistry, **2005** (2005), no. 4, 240–246

Simultaneous Determination of Dissolved Organic Carbon and Total Dissolved Nitrogen on a Coupled High-Temperature Combustion Total Organic Carbon-Nitrogen Chemiluminescence Detection (HTC TOC-NCD) System

Xi Pan,[1] Richard Sanders,[1] Alan D. Tappin,[2] Paul J. Worsfold,[2] and Eric P. Achterberg[1]

[1]*National Oceanography Centre Southampton, University of Southampton, European Way, Southampton SO14 3ZH, UK*
[2]*School of Earth, Ocean and Environmental Science, University of Plymouth, Plymouth PL4 8AA, UK*

Received 20 April 2005; Accepted 12 May 2005

The marine biogeochemistries of carbon and nitrogen have come under increased scrutiny because of their close involvement in climate change and coastal eutrophication. Recent studies have shown that the high-temperature combustion (HTC) technique is suitable for routine analyses of dissolved organic matter due to its good oxidation efficiency, high sensitivity, and precision. In our laboratory, a coupled HTC TOC-NCD system with a sample changer was used for the automated and simultaneous determination of dissolved organic carbon (DOC) and total dissolved nitrogen (TDN) in seawater samples. TOC control software was used for TOC instrument control, DOC data acquisition, and data analysis. TDN data acquisition and manipulation was undertaken under LabVIEW. The combined system allowed simultaneous determination of DOC and TDN in the same sample using a single injection and provided low detection limits and excellent linear ranges for both DOC and TDN. The risk of contamination has been remarkably reduced due to the minimal sample manipulation and automated analyses. The optimised system provided a reliable tool for the routine determination of DOC and TDN in marine waters.

1. INTRODUCTION

Global change and global warming have become dominant issues in environmentalscience. The increased use of fossil fuels in the postindustrial period has resulted in enhanced emissions of greenhouse gases, including CO_2. The oceans form an important sink of atmospheric CO_2 through both the physical and biological pumps [1]. As part of the biological pump, atmospheric CO_2 is fixed by primary producers in the surface ocean and planktonic detritus is transferred to the deep ocean following cell death. This process transfers atmospheric carbon to the deep ocean for medium (1000′ s of years) to long (millions of years) time periods. Both in the surface and deep ocean, particulate planktonic detritus is mineralised by marine heterotrophic organisms and dissolved organic carbon and nutrients are released. Furthermore, DOC is released into the surface waters via phytoplankton exudation and cell lysis [2]. As a consequence of these processes the concentrations of DOC are closely related to primary production and are highest in the surface waters and decrease markedly through the thermocline to low levels in deep oceanic water. The importance of oceanic DOC is indicated by Siegenthaler and Sarmiento [3], who reported that the amounts of carbon in oceanic DOC ($\sim 700 \times 10^{15}$ g C) are similar to those of atmospheric CO_2 ($\sim 750 \times 10^{15}$ g C). Thus, a net oxidation of merely 1% of the oceanic DOC will be sufficient to generate CO_2 fluxes, which are greater than those produced annually by fossil fuel combustion [4]. An improved understanding of the distribution and cycling of marine DOC is therefore important for a global assessment of fluxes and reservoirs of carbon.

Total dissolved nitrogen (TDN) comprises dissolved organic nitrogen (DON) and dissolved inorganic nitrogen (DIN) in the forms of nitrate, nitrite, and ammonium. The DON fractions have historically been ignored because they were considered to be biologically inert [5]. Recent studies, however, indicated that DON concentrations account for as much as 40%–70% of the TDN pool in surface seawater and an important fraction of DON is readily available to the microbial community [2]. Nitrogen compounds are introduced into the marine environment mainly by riverine and atmospheric inputs and nitrogen fixation. In coastal water,

Correspondence and reprint requests to Eric P. Achterberg, National Oceanography Centre Southampton, University of Southampton, European Way, Southampton SO14 3ZH, UK; E-mail: eric@noc.soton.ac.uk.

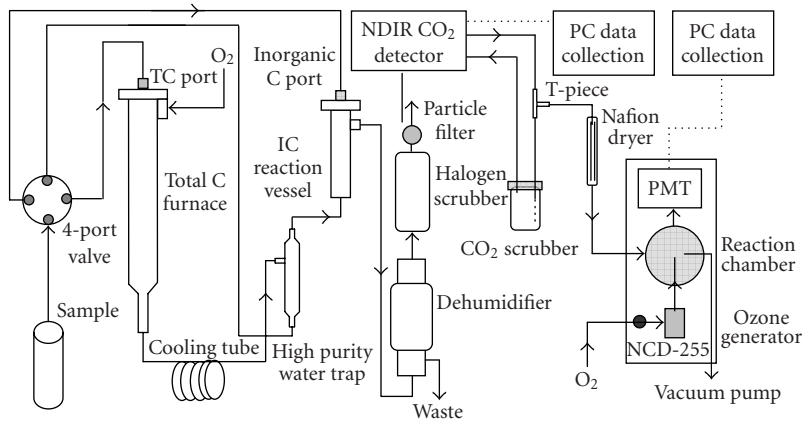

Figure 1: A schematic of the Shimadzu TOC 5000A total carbon analyser coupled with the Sievers NCD 255 nitrogen chemiluminescence detector (adapted from Badr et al, 2003).

excess nitrogen inputs lead to eutrophication and harmful algal blooms. However, in the open ocean the surface waters are typically subject to nitrogen limitation. The majority of studies of nitrogen in the marine environment have only determined DIN (using standard colorimetric techniques), however the omission of the DON fractions may lead to an important underestimation of nitrogen available to the microbial community [2].

Different analytical techniques have been applied for the determination of DOC in marine waters, including UV oxidation [6], wet chemical oxidation using persulphate [7], and high-temperature combustion (HTC [8]). The CO_2 produced in these techniques during the oxidation of organic carbon is quantified using nondispersive infrared detection. The HTC technique is currently the most widely used approach [9] because of its good oxidation efficiency, high sensitivity, and precision.

As no analytical technique exists for direct DON measurements, this variable is determined through separate DIN (using colorimetric techniques) and TDN analyses. A commonly used technique for TDN analyses involves wet chemical oxidation using persulphate digestion and UV oxidation followed by colorimetric nitrate analysis [10]. More recently, high-temperature combustion of TDN followed by chemiluminescence detection of NO has become the dominant technique [10, 11]. In this paper we describe the development of hardware and software, and the application of a coupled analytical system for automated and simultaneous determination of DOC and TDN in marine waters. This coupled online approach allows a high sample throughput and facilitates carbon and nitrogen clean operating procedures, and the detection systems exhibit a high sensitivity, precision, and minimal interference problems.

2. EXPERIMENTAL

2.1. Reagents and samples treatment

Plasticware and glassware were cleaned by soaking in decon solution (2% v/v, Analar grade, VWR Ltd, England) for 24 hours followed by HCl (10% v/v, Analar grade, VWR Ltd, England) for 24 hours. De-ionised water (Milli-Q, Millipore Inc, England) was used for thorough rinsing between each cleaning step. Glassware was then combusted at 450°C for 6 hours to remove remaining organic residues. Samples were collected using glass bottles. In order to minimise the influences of biological degradation, samples were filtered immediately upon collection using ashed glass fibre filters (0.7 μM pore size, 47 mm diameter, Whatman GF/F, England) with an ashed glass filtration unit (Nalgene, US). Flame-sealable glass ampoules (Adelphi Ltd, England) were employed for sample storage. Prior to closing the ampoules, HCl (50% v/v, Analar grade, VWR Ltd, England) was added to acidify the samples to pH 2. A potassium hydrogen phthalate and glycine (both Analar grade, VWR Ltd, England) mixture (C : N atom ratio = 6 : 1) was made up for calibration of the coupled TOC-NCD instrument.

2.2. Coupled TOC-NCD system

In our laboratory, HTC measurements of DOC and TDN were performed using a Shimadzu TOC 5000A total carbon analyser (Shimadzu Corp, Japan) coupled with a Sievers NCD 255 nitrogen chemiluminescence detector (Sievers Instruments, Inc, US). Ancillary instrumentation included an autosampler (ASI 5000A, Shimadzu Corp, Japan) and a two-stage vacuum pump (no 8, Edwards High Vacuum Ltd, England). Carbon-free, high purity (99.999%) oxygen gas (BOC gas, England) was applied as carrier gas. Figure 1 shows a schematic diagram of the coupled HTC TOC-NCD system. A full analytical measurement cycle consists of two steps.

Step 1. Acidified sample was sparged using pure oxygen for a period of 8 minutes (75 mL min^{-1}) to remove inorganic carbon compounds and then injected into the furnace of the TOC instrument. The carrier gas pushed the sample into the combustion column, which was heated to 680°C and filled with a catalyst (aluminium oxide coated by 0.5% of platinum (Shimadzu Corp, Japan)). Organic carbon and nitrogen compounds, and ammonia in the sample were oxidisedto

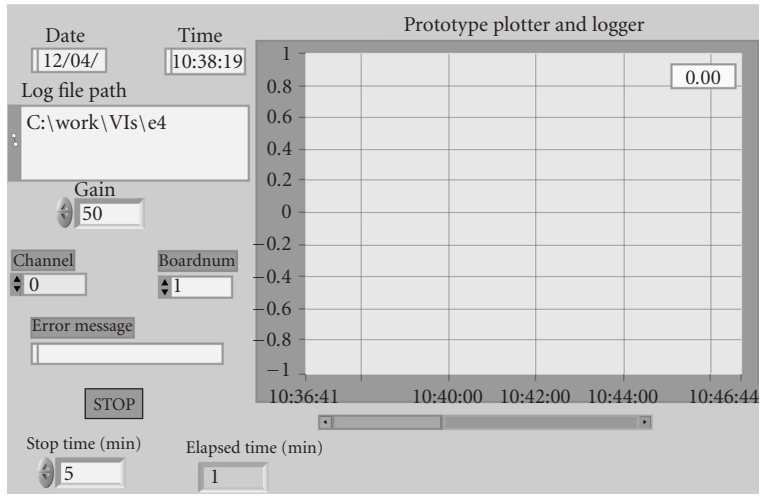

Figure 2: LabVIEW graphical user front panel for the automated virtual NCD instrument.

CO_2, NO, and H_2O, whereas nitrate and nitrite were reduced to NO.The gas stream was pushed in turn through a cooling tube, an electronic dehumidifier to remove water vapour, and a Cu-based halogen scrubber for gas purification. Then, the dried, purified gas stream was drawn into the sample cell housed in a nondispersive infrared (NDIR) gas analyser, where CO_2 in the gas stream was detected by the NDIR detector. The produced analogue signals were amplified by the amplifier and converted to pulse frequency by the V/F converter.

Step 2. The gas stream was drawn out of the TOC instrument with the aid of the vacuum pump, passed through a Nafion membrane dryer (Perma Pure Inc, US) in order to remove any remaining water vapour, and then routed to the NCD reaction chamber. The additional drying step using the Nafion dryer is important as moisture quenches the chemiluminescence reaction and leads to tailing peak [5]. The vacuum pump produced operating pressures of 2–10 torr in the reaction cell. The TDN determination relied on the chemiluminescence reaction of NO and O_3. NO generated from Step 1 reacted with O_3 produced by the ozone generator housed in the NCD instrument to give rise to the radical species $NO_2{}^*$, which emitted quantifiable energy (light) upon decay to its ground state:

$$NO + O_3 \longrightarrow O_2 + NO_2{}^* \longrightarrow NO_2 + h\nu. \quad (1)$$

The reaction of NO and O_3 occurred in front of the photo-multiplier tube (PMT). The emitted light ($h\nu$) was collected by the PMT and converted to a voltage signal stoichiometrically proportional to the total nitrogen concentrations in the sample.

Samples for nitrate and nitrate (DIN) for a North Sea research cruise fieldwork were analysed using standard colourimetric techniques [12]. Salinity was determined using an in situ conductivity probe as part of a standard ship-board CTD system.

2.3. DOC data acquisition and manipulation

TOC instrument control was undertaken using the TOC control (5000/5000A & 5050/5050A) software (version 1.05.01, Shimadzu Corp, Japan) installed in a desktop computer linked to an RS-232 board (PC-15N) (Shimadzu Corp, Japan) placed in the rear of the Shimadzu TOC instrument via an AWM E101344 style 2464 28AWG cable. This software was also capable of data acquisition and manipulation. Pulse frequency was recorded and quantified as peak area by the Shimadzu Model CR6A Chromatopac computing integrator. Following the analyses of calibration standards, the software allowed for automated calculations of DOC concentrations in the samples. The results of the DOC concentration calculations, including statistic analysis are displayed in a real-time window and stored on the computer's hard-disk.

2.4. TDN data acquisition

The analogue signals from the Sievers NCD instrument were collected by a CIO-DAS08/JR/16 A/D card (Talisman Electronic Ltd, England) installed in a desktop computer through a female 37-pin, D-type connector (Talisman Electronic Ltd, England). An interface box was built to link the analogue output of the NCD to the A/D card. A TCIO-MINI37 screw terminal board (Talisman Electronic Ltd, England) was placed in the interface box. A one metre long TC37FF-5 cable (Talisman Electronics Ltd, England) linked the terminal board and the D-type connector on the A/D card.

A LabVIEW graphical programming environment was used to design a virtual instrument (VI) with a flexible user interface for the TDN data acquisition and manipulation. The VI software was developed in collaboration with Ruthern Instruments (Bodmin, UK) and written in LabVIEW version 6 (National Instruments Corp, US). The digital signals from the A/D card were acquired by the VI. The LabVIEW front panel contains ready-to-use switches, buttons, and controls to start the data acquisition, define the signal gain, and stipulate the stop time of the data collection (Figure 2).

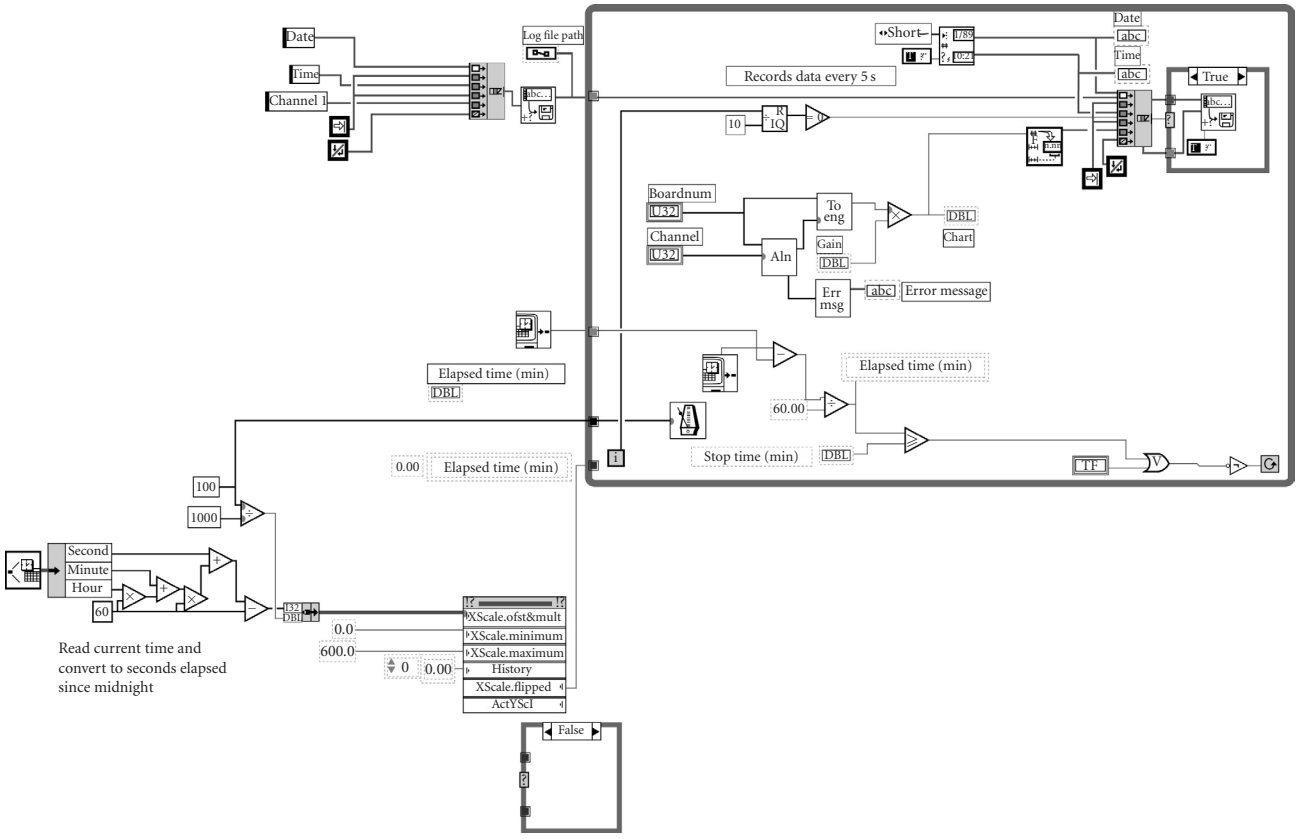

Figure 3: Graphical code for NCD instrument control.

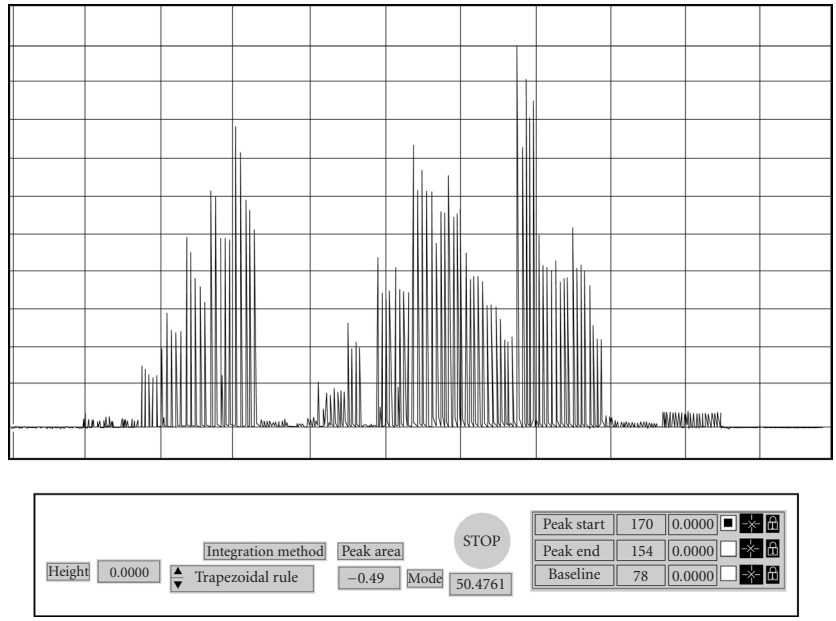

Figure 4: LabVIEW graphical user front panel for data analyses.

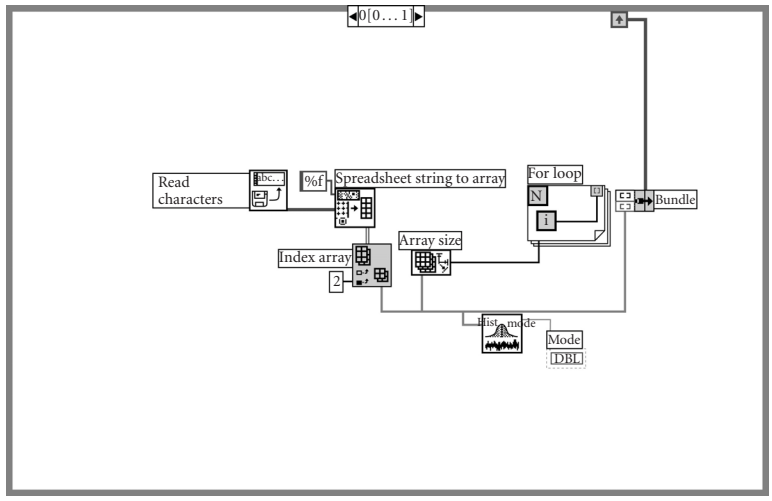

(a)

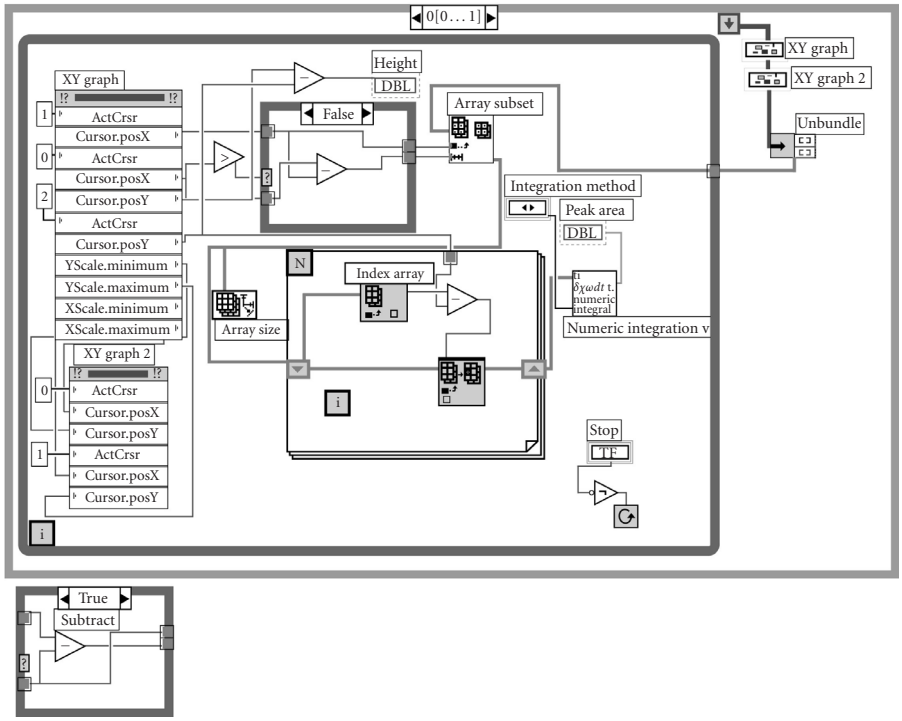

(b)

Figure 5: Graphical code for data analysis.

The nitrogen signals are displayed in real-time in the box on the front panel. The LabVIEW VI wiring diagram for the TDN data acquisition is presented in Figure 3, showing the data entry, analysis definitions, and stop procedure.

Once the coupled TOC-NCD instrument is running, data acquisition can be started instantaneously by depressing the run icon from the LabVIEW environment element bar (Figure 2). The processes can be halted by depressing the abort icon, alternatively the data acquisition is stopped automatically afterthe time period indicated in the "stop time" window on the front panel (Figure 2). A real-time window displayed on the right-hand side of the front panel visualises the data acquisition process. Data is stored on the hard disk of the computer.

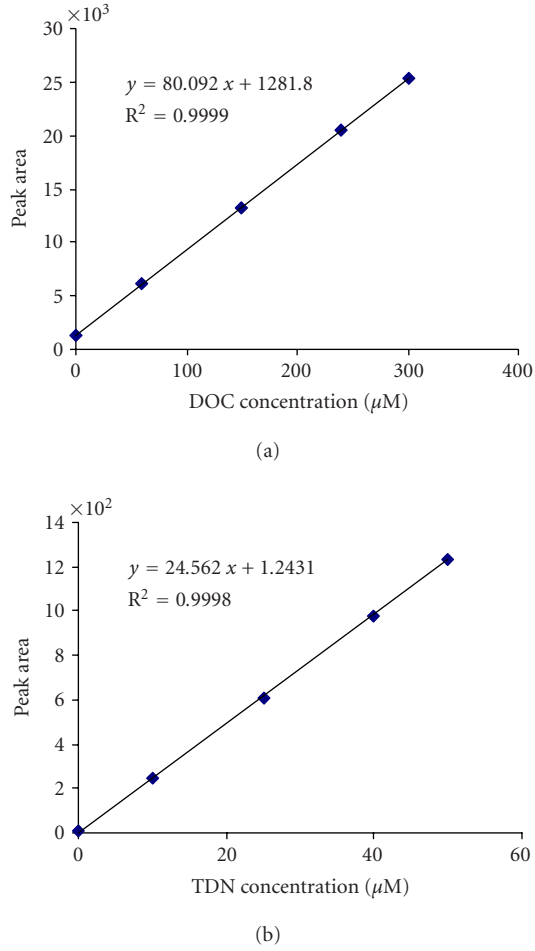

Figure 6: Calibration graphs of DOC and TDN.

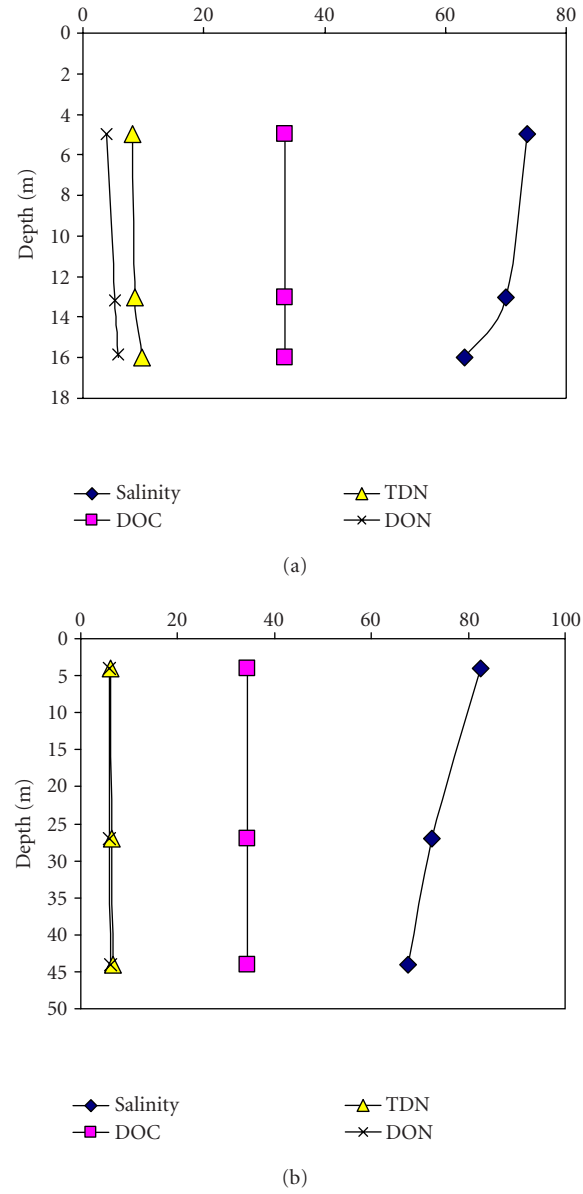

Figure 7: (a) Depth distribution of salinity, and DOC, TDN, and DON (in μM) at near shore station (station 7) in North Sea (53° 32.7′N, 0° 23.5′E), sampled in September 18, 1999. (b) Depth distribution of salinity, and DOC, TDN, and DON (in μM) at offshore station (station 26) in North Sea (54°12.7′N, 1°36.7′E), sampled in September 21, 1999.

2.5. *TDN data manipulation*

An additional LabVIEW VI was designed to allow quantification of TDN peak area. Figure 4 shows the graphical user front panel of the virtual data manipulation instrument. The virtual data manipulation instrument is flexible, and allows positioning of the baseline and a user-controlled definition of the peak start and peak end position. The automated calculation of peak area can be undertaken using a range of different integration methods. The approach typically used for our TDN peak area determinations applies the trapezoidal rule, which is a mathematic method for approximation of a definite integral by evaluating the integrand at finitely many points. The LabVIEW VI wiring diagram for the TDN data manipulation is presented in Figure 5, showing the data entry and integration approach.

3. ENVIRONMENTAL APPLICATION

Examples of standard solution graphs for DOC and TDN determinations are presented in Figure 6, both of which showed excellent linearity. Linear ranges were estimated to be 8–600 μM C and 0.3–100 μM N, respectively. The limit of detection ($3\sigma_{\text{blank}}$) was 8.0 μM Cand 1.0 μM N. For the combined HTC TOC-NCD in our laboratory, the coefficient of variation was less than 1.5% (3–5 repeat injections) and de-ionised water blank was lessthan 10 μM TOC and about 1.0 μM TDN. For the quantitative validation and accreditation of analytical measurements, a deep ocean water supplied by the Hansell Laboratory (University of Miami, US) was used as a certified reference material (CRM). The CRM was analysed with every sample run and the results (44–46 μM DOC and 21.5 μM TDN) obtained using

the combined HTC TOC-NCD system showed an excellent agreement with the certified values (44.3 μM DOC and 21.2 μM TDN).

The combined TOC-NCD system has been used for analysis of samples collected during the IMPACT cruise, conducted on the North Sea in September 1999. Figures 7a and 7b show depth profiles of salinity, DOC, TDN, and DON for inshore (station 7) and offshore waters (station 26) of the North Sea.The DOC concentrations ranged approximately between 65–88 μM at these stations. The highest DOC concentrations were observed in the surface waters, most likely as a result of enhanced primary productivity in these waters. The TDN concentrations were low (below 10 μM), indicating nitrogen uptake by primary producers and dilution of coastal waters with cleaner Atlantic waters flowing into the western North Sea from the north. Dissolved organic nitrogen constituted between 48% and 60% of the TDN at station 7, and between 91% and 94% at station 26. This shows that DON forms the major part of the dissolved nitrogen pool in the North Sea. The inshore station (station 7) is more influenced by DIN inputs from the Humber Estuary, and hence has a lower percentage of DON as part of TDN compared with the offshore station (station 26). The DOC, TDN, and DON concentrations observed in the present study agree well with previous work in other marine waters [2]. However, the DON/TDN ratio at station 26 was higher than the reported average range [2], indicating the high uptake of inorganic nitrogen species by microbial organisms in the highly productive North Sea, with subsequent production of DON.

4. CONCLUSIONS

The combined HTC TOC-NCD system provided excellent linearity and precision. The results of deep oceanic water CRMs for the system showed a good agreement with the certified values. TOC control software was capable of automated peak area recognition and quantification, concentration calculation, and statistical analysis. The developed LabVIEW VIs allowed flexible TDN data acquisition and manipulation. This optimised system allowed simultaneous analysis of DOC and TDN in seawater samples using a single injection of the same sample and hence involved a minimum of sample handling and risk of contamination. The limit of detection makes it feasible to determine DOC and TDN in all marine environments. The optimised methodology will allow the studies of the distribution and behaviours of DOC and TDN/DON in marine ecosystems and improve our understanding of marine biogeochemistry of carbon and nitrogen.

ACKNOWLEDGMENTS

Xi Pan acknowledges the financial support by the University of Southampton. Mr John Woods of Ruthern Instruments is gratefully acknowledged for his hardware and software support. The captain and crew of the *RRS Challenger* are thanked for outstanding support on the North Sea IMPACT cruise.

REFERENCES

[1] J. Houghton, *Global Warming: The Complete Briefing*, Cambridge University Press, Cambridge, UK, 3rd edition, 2004.

[2] D. A. Bronk, "Dynamics of DON," in *Biogeochemistry of Marine Dissolved Organic Matter*, D. A. Hansell and C. A. Carlson, Eds., pp. 153–247, Academic Press, San Diego, Calif, USA, 2002.

[3] U. Siegenthaler and J. L. Sarmiento, "Atmospheric carbon dioxide and the ocean," *Nature*, vol. 365, no. 6442, pp. 119–125, 1993.

[4] J. I. Hedges, "Global biogeochemical cycles:progress and probles," *Marine Chemistry*, vol. 39, pp. 67–93, 1992.

[5] T. W. Walsh, "Total dissolved nitrogen in seawater: a new-high-temperature combustion method and a comparison with photo-oxidation," *Marine Chemistry*, vol. 26, no. 4, pp. 295–311, 1989.

[6] F. A. J. Armstrong, P. M. Williams, and J. D. H. Strickland, "Photooxidation of organic matter in seawater by ultraviolet radiation, analytical and other applications," *Nature*, vol. 211, pp. 481–483, 1966.

[7] N. Ogura, "The relation between dissolved organic carbon and apparent oxygen utilization in the Western North Pacific," *Deep-Sea Research and Oceanographic Abstracts*, vol. 17, no. 2, pp. 221–231, 1970.

[8] Y. Suzuki, Y. Sugimura, and T. Itoh, "A catalytic oxidation method for the determination of total nitrogen dissolved in seawater," *Marine Chemistry*, vol. 16, no. 1, pp. 83–97, 1985.

[9] G. Spyres, M. Nimmo, P. J. Worsfold, E. P. Achterberg, and A. E. J. Miller, "Determination of dissolved organic carbon in seawater using high temperature catalytic oxidation techniques," *TrAC Trends in Analytical Chemistry*, vol. 19, no. 8, pp. 498–506, 2000.

[10] J. H. Sharp, A. Y. Beauregardt, D. Burdidge, et al., "A direct instrument comparison for measurement of total dissolved nitrogen in seawater," *Marine Chemistry*, vol. 84, no. 3-4, pp. 181–193, 2004.

[11] E.-S. A. Badr, E. P. Achterberg, A. D. Tappin, S. J. Hill, and C. B. Braungardt, "Determination of dissolved organic nitrogen in natural waters using high-temperature catalytic oxidation," *TrAC Trends in Analytical Chemistry*, vol. 22, no. 11, pp. 819–827, 2003.

[12] T. R. Parson, *A Manual of Biological and Chemical Methods for Seawater Analysis*, Pergamon Press, Oxford, UK, 1990.

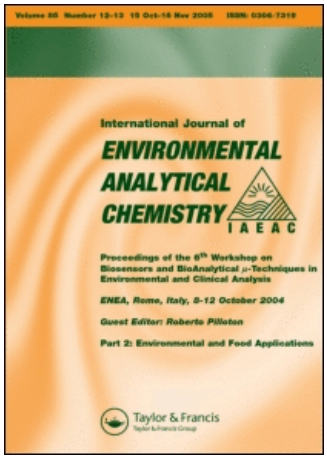

International Journal of Environmental Analytical Chemistry
Publication details, including instructions for authors and subscription information:
http://www.informaworld.com/smpp/title~content=t713640455

Conversion efficiency of the high-temperature combustion technique for dissolved organic carbon and total dissolved nitrogen analysis

To cite this Article: , 'Conversion efficiency of the high-temperature combustion technique for dissolved organic carbon and total dissolved nitrogen analysis', International Journal of Environmental Analytical Chemistry, 87:6, 387 - 399
To link to this article: DOI: 10.1080/03067310701237023
URL: http://dx.doi.org/10.1080/03067310701237023

Intern. J. Environ. Anal. Chem.
Vol. 87, No. 6, 15 May 2007, 387–399

Conversion efficiency of the high-temperature combustion technique for dissolved organic carbon and total dissolved nitrogen analysis

KAORI WATANABE†, EL-SAYED BADR†, XI PAN‡ and ERIC PIETER ACHTERBERG*‡

†School of Earth, Ocean and Environmental Science, University of Plymouth, Plymouth PL4 8AA, UK
‡National Oceanography Centre Southampton, School of Ocean and Earth Science, University of Southampton, European Way, Southampton SO14 3ZH, UK

(*Received 6 September 2006; in final form 22 January 2007*)

The measurements of dissolved organic carbon (DOC) and total dissolved nitrogen (TDN) in seawater are key in global change and coastal eutrophication studies. Nowadays, the high-temperature combustion (HTC) technique is a widely used method for DOC and TDN analysis. However, uncertainties exist about the operation of the catalyst in the conversion process of DOC and TDN in the HTC method. In this study, five different 'catalyst' materials were tested for their blanks, calibration slopes, and conversion efficiency of DOC and TDN using the Shimadzu TOC 5000A total organic carbon analyser coupled to a Sievers NCD 255 nitrogen chemiluminescence detector. The materials included four metallic catalysts (Shimadzu and Johnson 0.5% Pt–alumina, 13% Cu(II)O–alumina, 0.5% Pd–alumina) and quartz beads. The results indicated that DOC blank signals for the HTC approach using metallic catalysts with an alumina support are higher compared with quartz beads, as a result of the amphoteric nature of the alumina. However, the slopes of the standard calibration graphs were lowest for DOC and TDN determinations on the quartz beads. The DOC recoveries for the metallic catalysts were close to 100% for all compounds tested, with the exception of ammonium pyrrolidine dithiocarbamate. Using quartz beads, poor recoveries were obtained for a range of organic compounds, including the commonly used calibration compounds potassium hydrogen phthalate and glycine. The TDN recoveries for all compounds were typically >90%, with the exception of $NaNO_2$. Furthermore, analysis using the CuO–alumina and Pd–alumina catalysts and quartz beads showed low recoveries for NH_4Cl. This study showed that catalyst performance should be verified on a regular basis using model compounds and blank checks made during every run, and that the Shimadzu 0.5% Pt–alumina material was an efficient catalyst for DOC and TDN analyses using the coupled total organic carbon–nitrogen chemiluminescence detector (TOC-NCD) analyser.

Keywords: Dissolved organic carbon; Dissolved organic nitrogen; Total dissolved nitrogen; High-temperature combustion; Catalyst

*Corresponding author. Fax: +44-23-8059-3052. Email: eric@noc.soton.ac.uk

International Journal of Environmental and Analytical Chemistry
ISSN 0306-7319 print/ISSN 1029-0397 online © 2007 Taylor & Francis
DOI: 10.1080/03067310701237023

1. Introduction

Investigations of the marine carbon and nitrogen cycles are key to our understanding of global change and coastal eutrophication. Dissolved organic carbon (DOC) forms the vast majority of the organic matter in seawater [1], and on a global scale its contribution to the carbon pool is of the same order of magnitude as that of atmospheric CO_2. Dissolved organic nitrogen (DON) forms on average 60–69% of the total dissolved nitrogen (TDN) pool in marine waters, with highest contributions in the surface waters (90–100%) and lowest in deep oceanic waters (ca $10 \pm 3\%$) [2]. DOC and TDN studies require high-quality analytical measurements. DOC measurements typically involve a direct analysis, whereas the concentration of DON is determined as the difference between TDN and dissolved inorganic nitrogen (DIN), composed of nitrate, nitrite, and ammonium. The DIN species are independently analysed using colorimetric procedures [3]. For the determination of DOC and TDN, one of two approaches is commonly used. The first relies on wet chemical oxidation (WCO) to convert the DOC to CO_2 and TDN to NO_3^-, which are then measured using infrared gas analyses and colorimetry, respectively. WCO methods include alkaline persulfate digestion and UV photo-oxidation [4–6]. The second approach is based on direct aqueous injection of the sample onto a combustion column, and relies on the conversion of the DOC to CO_2 and TDN to NO [7, 8]. The CO_2 is subsequently measured by infrared gas detection, and NO by chemiluminescence following conversion of NO to radical NO_2^* species using ozonation [9–11]. The aqueous injection techniques make use of high-temperature (680–1100°C) combustion (HTC) of carbon and nitrogen compounds, and this process is typically aided by a metallic catalyst or quartz beads [11–14]. The HTC technique is commonly used and allows the simultaneous determination of DOC and TDN in the same sample in a single injection through coupling of commercial instruments (total organic carbon (TOC) analyser and nitrogen chemiluminescence detector (NCD)). The coupled HTC method minimizes the risk of carbon and nitrogen contamination due to minimal sample handling, and exhibits an excellent linearity, a good precision and reported detection limits of ca 8 μM C and 0.6 μM N [14]. The Shimadzu TOC 5000A analyser coupled to either a Sievers or Antek NCD is the most commonly reported configuration. In a recent instrument comparison exercise for TDN analysis in seawater, these instrument configurations showed a tight agreement over a wide TDN concentration range, an excellent performance in terms of reproducibility and 'user-friendliness', and consequently potentially providing an edge over stand-alone HTC NCD and WCO persulfate methods [15].

The most challenging and controversial step in DOC and DON determination is the complete decomposition of dissolved organic matter (DOM) [11]. There is no consensus in the HTC community concerning the role the catalyst plays in facilitating DOM oxidation during HTC analysis [16]. The reactions involving the DOM and the heterogeneous catalysts employed in HTC analysis are complex, and the rates, kinetics, and mechanisms are difficult to measure. The relevant equations for complete DOC and DON combustion are:

$$\text{Organic C} + O_2 \rightarrow H_2O + CO_2 \tag{1}$$

$$CO + 0.5O_2 \rightarrow CO_2 \tag{2}$$

$$\text{Organic N} + H_2O \rightarrow NO + H_2. \tag{3}$$

Equations (1) and (3) refer to the combustion of the organic carbon and nitrogen fractions, respectively, of DOM. The oxidation of organic nitrogen appears to occur to NO via HCN and NH_x intermediates [17]. Equation (2) refers to the complete combustion of CO, which may be formed during incomplete combustion processes.

While oxygen is understood to be an important oxidant in DOC combustion, recent work has shown that catalytic DOC breakdown can be performed with N_2 as the carrier gas (instead of O_2), inferring that water forms an important source of oxidizing species [18, 19]. The TDN analysis using HTC methods furthermore involves the conversion of ammonium, nitrite, and nitrate to NO. Reduced nitrogen compounds (organic matter and ammonium) must therefore be oxidized from an oxidation state of -3 to $+2$, whereas nitrite and nitrate must be reduced from $+3$ and $+5$, respectively.

D-electron metals are capable of undertaking catalytic functions; these metals include Ag, Au, Co, Cu, Fe, Ir, Ni, Pd, Pt, Re, Rh, Ru, and Os [20]. Pd and Pt are catalysts used in a wide number of applications for the conversion of hydrocarbons and CO to CO_2, and their high catalytic activity is attributed to the activation of O–O, O–H, and C–H bonds [17]. In addition, these noble metals also readily convert organically bound N and inorganic N to NO [17]. Pt coated on alumina is the catalyst used in the Shimadzu TOC analysers, but a range of different metallic catalysts (including CoO, CoCr, CuO, and MnO_2) are used in other HTC instruments [11]. In addition, the successful application of quartz beads has been reported in TOC instruments as an alternative for metallic catalysts and operate by facilitating DOM breakdown through their action as an inert heat exchanger [12, 21].

Overviews of recovery efficiencies for a range of N and organic C compounds using various catalysts in different HTC instruments have been reported by [13, 14, 22, 23]. Furthermore, comparative DOC measurements of seawaters and deionized water blanks have been reported using platinized alumina catalysts with different Pt concentrations and performed on a single HTC instrument [24, 25]. However, no systematic DOC and TDN recovery experiments for different types of catalysts and catalyst-type materials in a single HTC TOC-TDN instrument are available in the literature. The aim of this study therefore is to investigate the efficiencies of various metallic catalysts and quartz for DOC and TDN conversion in a single coupled TOC-NCD (Shimadzu TOC 5000A-Sievers NCD 255) system.

2. Experimental

All glassware was soaked in 2% Decon (VWR Ltd, Lutterworth, UK) for 24 h, rinsed with UV-irradiated, High Wycombe, UK ultra-high-purity (UV-UHP) water ($>18.2\,M\Omega\,cm^{-1}$, Elga Ltd, High Wycombe, UK), soaked in 10% HCl (Aristar grade, VWR Ltd) for 24 h, and subsequently rinsed five times with UV-UHP water. The glassware was then combusted at $\sim$450°C for 4–6 h to remove any remaining organic residues [13, 14]. DOC and TDN analyses were undertaken using a Shimadzu TOC 5000A, (Milton Keynes, UK) coupled with a Sievers NCD 255 (GE Instruments, Boulder, USA). The Shimadzu TOC furnace temperature was operated at 680°C, with a carrier-gas (high-purity (99.999%) oxygen, BOC Ltd, Guilford, UK) flow rate of $150\,mL\,min^{-1}$. The gas flow rate for the NCD 255 was $100\,mL\,min^{-1}$. Prior to analysis, all injected solutions were sparged for a period of 8 min (at $75\,mL\,min^{-1}$ using

high-purity oxygen) in order to remove the majority of the carbon dioxide. As the solutions were not acidified, a minor background carbon signal was detected in the DOC analyses as a consequence of remaining traces of carbon dioxide in the solutions. Replicate injections (three to five in total) of 100 μL were undertaken for each solution. DOC data acquisition and peak area quantification was undertaken using the Shimadzu TOC 5000A software. TDN data acquisition was undertaken using an A/D card (Talisman Electronics Ltd) slotted into a Pentium PC, and the peak area was quantified using LabView software (National Instruments Inc., Newbury, UK). Full details of the TOC-NCD system operations and their coupling can be found in Badr *et al*. [14].

Five different materials were tested for their conversion efficiency, including four metallic catalysts (1) Shimadzu 0.5% Pt on alumina beads (1.5–3 mm diameter; Shimadzu, Milton Keynes, UK), (2) Johnson 0.5% Pt on alumina pellets (3 mm diameter; Johnson Matthey plc., London, UK), (3) 13% Cu(II)O on alumina pellets (−14 + 20 mesh; Aldrich Chemical Company Inc., Milwaukee, USA), (4) 0.5% Pd on alumina pellets (3.2 mm diameter; Aldrich Chemical Company Inc., Milwaukee, USA), and Quartz beads (3 × 3 mm; Quartz Scientific Inc., Fairport Harbor, USA). These materials were chosen because they are used in other HTC systems, or offered a potential as a suitable catalyst (e.g. Pd). In order to support the materials, a Pt gauze and quartz wool were placed at the bottom of the quartz combustion column, and quartz wool was placed at the top of the catalyst.

New catalyst materials were directly placed in the combustion tube (i.e. without prior treatment) to assess their immediate blank performance. After placing the new material in the tube, the blank was determined using UV-UHP water until a low and stable DOC signal was obtained. The nitrogen blank values were monitored in a similar manner. This experiment was not conducted for the Johnson 0.5% Pt–alumina catalyst, as this had been used previously (received approximately 3500 injections).

Carbon and nitrogen calibrations were undertaken using a mixture of potassium hydrogen phthalate (KHP) and glycine (VWR Ltd) in UV-UHP water. The C : N atomic ratio of the mixture was 10 : 1. Calibrations were undertaken at two concentration levels, in order to study the influence of C concentration on catalyst performance. A first set of six standards for DOC was prepared in the concentration range of 100–1500 μM C and determined at sensitivity setting 5 for the TOC software; TDN was not determined on these standards as the top concentrations exceeded the range of the NCD. A second set of four standards was prepared with concentrations of 40–300 μM C and 4–30 μM N, and the DOC calibrations on these standards were undertaken at the most sensitive setting of the TOC instrument (setting 1). The chosen TDN calibration standards were in line with those required for calibration of TDN concentrations observed in marine waters (typical TDN concentrations: 5–200 μM). The DOC standards were somewhat higher than required for calibration of samples from marine waters (typical observed DOC concentrations: 40–150 μM); this approach was taken in order to obtain high-precision DOC measurements of the standards for the sensitivity and recovery experiments. In agreement with findings by Alvarez-Salgado and Miller [22], no significant differences were observed between the slopes of standard calibrations performed in UV-UHP water and filtered seawater for both DOC and TDN. Consequently, standard calibrations and recovery experiments (see below) were undertaken in UV-UHP because of its low carbon and nitrogen concentration and low risk of microbiological degradation and contamination.

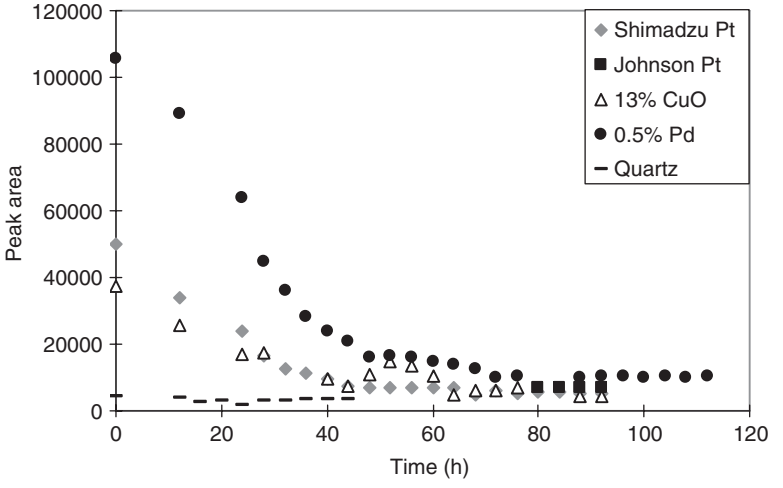

Figure 1. Carbon blank experiments. Peak area *vs.* blank UHP water injection period for the various metallic catalysts and quartz beads.

Recovery experiments were conducted to investigate the combustion efficiency of the various metallic catalysts and quartz beads using a range of organic compounds with different chemical structures: caffeine, thiourea, urea, ethylenediaminetetraacetic acid (EDTA), ammonium pyrrolidine dithiocarbamate (APDC); and inorganic nitrogen salts: ammonium chloride, sodium nitrate, sodium nitrite (all chemicals from VWR Ltd). All solutions were prepared in UV-UHP water.

3. Results and discussion

3.1 *Carbon and nitrogen blank experiments*

Water blank analyses are routine operations on HTC TOC–NCD instruments for conditioning the metallic catalyst, removing salts from the combustion column, reducing memory effects and more generally to obtain an indication of the instrument's operations. The DOC blank value provides an estimate of the combined blank resulting from components of the analytical system (instrument blank) and residual carbon in the UV-UHP water. With the use of low carbon UV-UHP water, the metallic catalyst forms the most important contribution to the DOC water and system blanks [24]. Determination of the DOC system blank using the automated blank checking programme on our Shimadzu TOC 5000A typically resulted in values close to the UV-UHP water blanks (ca 1–3 μM C lower), indicating the low carbon content of our UV-UHP water (which includes a minor contribution from residual carbon dioxide; see section 2). The UV-UHP water blanks hence provided a good indication of the DOC blank caused by the catalyst used in the combustion tube.

Figure 1 shows the results of the DOC blank experiments for the various metallic catalysts and quartz beads investigated using the Shimadzu-Sievers TOC-NCD instrument. The materials showed high initial UV-UHP water DOC blank values, with the exception of the quartz beads. For example, the initial blank values for the first injections of the Shimadzu 0.5% Pt–alumina and 0.5% Pd–alumina catalysts

Table 1. Calibration data, figures of merits, and blank data for DOC measurements of calibration standards in the concentration range 40–300 μM C (instrument sensitivity setting: 1) and 100–1500 μM C (instrument sensitivity setting: 5).

	Slope	*y*-intercept	R^2	LOD[a] (μM)	CV (%)	Blank (μM)
Catalyst/sensitivity setting 1						
Shimadzu 0.5% Pt–alumina	143.9	2643	0.9996	2.4	<1.5	23
13% CuO–alumina	105.8	3383.5	0.9999	1.9	<2.5	30
0.5% Pd–alumina	109.3	8400.1	0.9999	1.7	<2.0	77
Quartz	74.9	1047.7	0.9981	2.7	<3.0	21
Catalyst/sensitivity setting 5						
Shimadzu 0.5% Pt–alumina	22.7	−461	0.9993	50.3	<1.7	<LOD
Johnson 0.5% Pt–alumina	25.6	770	0.9999	13.4	<2.0	38
13% CuO–alumina	20.7	401	0.9998	11	<1.0	5
0.5% Pd–alumina	22	1490	0.9999	5	<0.7	70
Quartz	14.5	−140	0.9998	36.5	<2.0	<LOD

[a]Limit of detection.

were ca 50,000 and 105,000 area units, respectively. A good approach for reduction of the blanks for new catalysts with an alumina support involves combustion (without injections) for at least 24 h in the HTC column at 680°C, or muffle oven (450–550°C), followed by numerous injections of UV-UHP water (>50 h, >750 injections). In case of the Shimadzu 0.5% Pt–alumina catalyst, heating in the TOC instrument for 24 h resulted in a decrease in the blank area from 50,000 to 24,000 area units. Furthermore, following a large number of injections (ca 600) using UV-UHP water for 40 h, the blank value decreased further for this catalyst and reached stable readings (ca 3000 area units, equivalent to ca 29 μM C). Following heat treatment of the 0.5% Pd–alumina catalyst, UV-UHP water injections for >80 h were required to reduce the blank value to 10% of its initial value (10,500 area units).

The UV-UHP water blank signal for the Johnson 0.5% Pt–alumina (pre-used) and 13% CuO–alumina catalysts reached a stable value at about 7000 and 4000 area units, respectively. The blank signals for the quartz beads reached low and stable values (ca 3000 units) within 30 h of injections (450 injections), without prior heating. UV-UHP water analyses undertaken with acidified (pH 2) solutions and utilizing quartz and Shimadzu 0.5% Pt–alumina materials, resulted in even lower blank signals (ca 700–1100 area units; results not presented), as a consequence of a full removal of residual carbon dioxide from the UV-UHP water prior to analysis. Table 1 presents UV-UHP water DOC blank values for the materials, determined after ca 5 days use (>1500 injections). For the high sensitivity setting of the Shimadzu instrument (setting 1), the materials (with the exception of the Johnson 0.5% Pt–alumina and 0.5% Pd–alumina catalysts) provided UV-UHP water blank values close to the instrument blanks of 10–30 μM C and 5–15 μM C reported by Benner and Strom [24] and Alvarez-Salgado and Miller [22], respectively. These workers used the TOC 5000A instruments with Shimadzu 0.5% Pt–alumina catalysts.

The enhanced blank signal values of the metal–alumina catalysts are understood to be caused by the alumina support [11]. The alumina used in the catalysts is an amphoteric oxide and absorbs acid as well as alkaline molecules. The acidic properties of CO_2 result in absorption by the alumina. Consequently, the absorbed CO_2 needs to be removed from a new catalyst, and furthermore the absorption process will result

Table 2. Calibration data, figures of merits, and blank data for TDN measurements of calibration standards in the concentration range 4–30 μM N.

Catalyst	Slope	*y*-intercept	R^2	LOD[a] (μM)	CV (%)	Blank (μM)
Shimadzu 0.5% Pt–alumina	31.8	32.8	0.9999	0.35	<2.0	0.1–1.0
Johnson 0.5% Pt–alumina	41.6	16.2	0.9999	0.37	<3.5	0.4
13% CuO–alumina	32.2	178.4	0.9999	0.32	<3.0	5.6
0.5% Pd–alumina	34.2	27.7	0.999	0.83	<4.0	1.4
Quartz	23.5	76.9	0.998	0.81	<2.0	1.7

[a]Limit of detection.

in a memory effect during DOC analyses which may influence the quality of the measurements. The more rapid conditioning of the quartz beads, and associated low UV-UHP water blank, can be explained by the acidic nature of this material [20], resulting in a low capacity to absorb CO_2.

Table 2 presents the TDN blank values for all the investigated materials. Stable UV-UHP water blank values were obtained for the TDN analysis following only 20–30 injections. The UV-UHP water TDN blanks for the Shimadzu 0.5% Pt–alumina, Johnson 0.5% Pt–alumina, 0.5% Pd–alumina catalysts and quartz beads were 25–45 area units (equivalent to ca 0.25–1.7 μM N). These results compare well with TDN system blanks of <0.3–0.6 μM reported by Alvarez-Salgado and Miller [22]. The blank area of the 13% CuO–alumina catalyst levelled off at a stable value of 140 area units (equivalent to ca 5.6 μM N). This result is possibly caused by N impurities in the catalyst material, and consequently this catalyst is less well suited for low-level TDN analyses.

3.2 *Sensitivity of DOC and TDN analysis*

Instrument sensitivity, as ascertained from the slope of the standard calibrations, forms an important characteristic of the HTC analysis of DOC and TDN. A low instrument sensitivity increases the limit of detection of the analysis, and also provides an indication of poor catalyst or detector performance. The details of the DOC and TDN standard calibrations, obtained using a mixture of KHP and glycine, for the five materials is presented in tables 1 and 2. The DOC calibrations undertaken using standards with concentrations of 100–1500 μM C (sensitivity setting 5 for the TOC instrument) resulted in good linear plots with regression coefficients (R^2) >0.999 for all five materials (table 1). The slope of the linear regression for the DOC standard calibration using the quartz beads was lower (14.5) than for the metallic catalysts (20–25), indicating an incomplete breakdown of the KHP–glycine mixture. The quartz beads furthermore showed the lowest R^2 value (0.998) and slope of linear regression (74.9 compared with 105–110 for the metallic catalysts) for DOC calibrations undertaken using standards with low concentrations (40–300 μM C; instrument sensitivity setting 1). The R^2 values for all TDN calibration graphs obtained using the different materials were >0.998. The slope of the TDN calibration graph for quartz beads was lower (23.5) than for the other catalysts (32–42), a similar observation as for the DOC calibration.

The limits of detection (LODs; determined as 3σ of the blank) for DOC and TDN analyses ranged between 1.7 and 2.7 μM C (instrument sensitivity setting 1) and between 0.32 and 0.83 μM N, respectively, for the materials investigated in this study

(tables 1 and 2). These LODs indicate that the materials would allow the detection of the lowest DOC and TDN concentrations in marine waters. The coefficient of variance (CV) for five replicate DOC analyses of standards and samples was highest for the quartz beads (<3%), and lowest (<1.5%) for the Shimadzu 0.5% Pt–alumina catalyst. In case of TDN measurements, the CVs for analyses using the quartz beads and Shimadzu 0.5% Pt–alumina catalyst were <2%. In comparison, the precision of TDN analyses undertaken using Johnson 0.5% Pt–alumina, 13% CuO–alumina and 0.5% Pd–alumina catalysts was weaker. The CV results for the Shimadzu 0.5% Pt–alumina catalyst are in agreement with values (<1.5% for DOC and TDN analyses) reported by Alvarez-Salgado and Miller [22].

3.3 *Recovery experiments*

DOM in marine waters comprises a spectrum of compounds with different levels of resistance to breakdown by the HTC method. The use of KHP-glycine standards for calibration purposes is therefore not representative of DOC and DON in marine waters. Hence, recovery experiments using organic compounds with different chemical structures and refractivities are undertaken on a regular basis to test the breakdown efficiency of the HTC instrument. In addition, a good recovery for DIN is required in their conversion to NO. Experiments were undertaken in this study to investigate the conversion activities of the different materials. The chosen TDN compound concentrations of 8 μM N and 20 μM N can be considered relevant for marine waters, whereas higher DOC concentrations of 200 and 1000 μM C were chosen to allow small differences in recovery efficiencies to be observed.

Figure 2(a) shows the results of the DOC recovery experiments for the five different materials at compound concentrations of 200 μM C. Using the Shimadzu 0.5% Pt–alumina, Johnson 0.5% Pt–alumina, 13% CuO–alumina and 0.5% Pd–alumina catalysts, the recoveries were approximately 100% for caffeine, thiourea, urea and EDTA. These results are in good agreement with previous findings by Chen and Wangersky [26] and Aiken *et al*. [27]. However, APDC was relatively difficult to oxidize by these catalysts, showing recoveries between 79 and 95%. This observation is thought to result from the adsorption onto the catalyst surface of the heterocyclic structure of APDC, which includes nitrogen and two sulfur groups, causing interference with the catalytic breakdown. Similar observations of a reduced recovery were made for the recalcitrant N,S-containing compound sulfathiazole by Sugimura and Suzuki [7] and Chen and Wangersky [26] (50% and 95%, respectively).

In a number of measurements, recoveries were higher than 100%, which were most likely caused by carbon-rich impurities in the test compounds. For all catalysts, the recovery results for compounds at a higher concentration (1000 μM C; determined using sensitivity setting 5) showed a similar trend (figure 2b) compared with the lower concentration (200 μM C). This indicates that the catalyst efficiency for breakdown of specific organic compounds is determined by the nature of the compounds rather than their concentrations (at 200 and 1000 μM C).

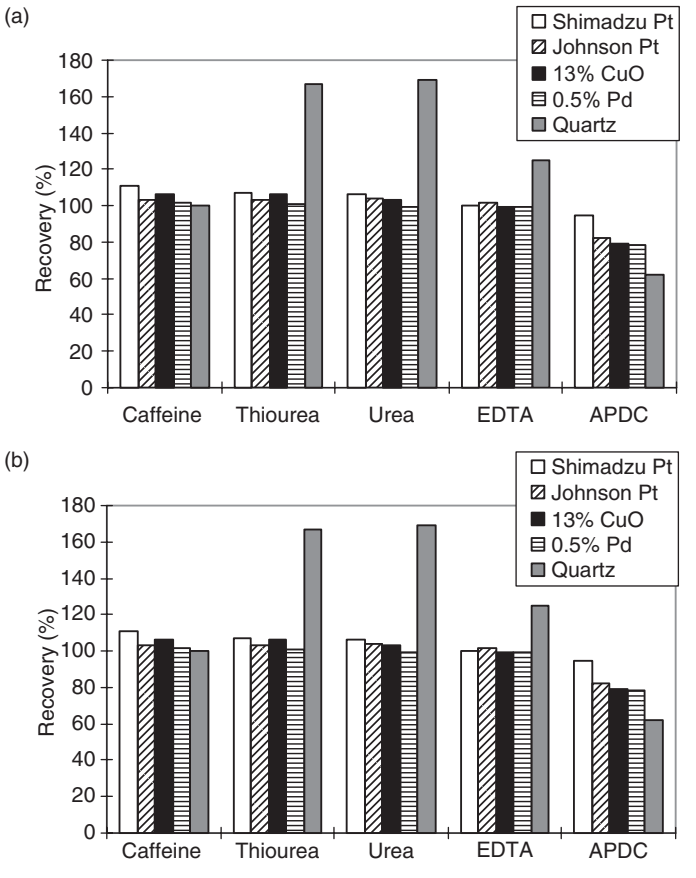

Figure 2. Results of recovery experiments for DOC at 200 μM C (a) and 1000 μM C (b) concentrations of model compounds.

The experiments involving quartz beads showed recoveries of >100% for thiourea, urea and EDTA (at 200 and 1000 μM C). These observations were the result of the incomplete oxidation of the calibration compounds (KHP and glycine) with a consequent overestimation of compound recoveries (see figure 2a and b). The relatively low slope of the calibration graph obtained using the quartz beads (see table 1) underpins this explanation. Further recovery experiments were undertaken using the quartz beads and with thiourea as calibration compound, as this compound showed a high yield in the original recovery experiment. This resulted in recoveries of EDTA (58 and 62%), APDC (44 and 33%), KHP (49 and 39%) and glycine (56 and 59%) at concentrations of 200 and 1000 μM C, respectively. These results indicate that a poor recovery occurred during the HTC combustion of a range of organic compounds using the quartz beads, including the commonly used calibration standards KHP and glycine. Our findings are not in agreement with those by Qian and Mopper [12, 28] who reported ca 100% DOC recoveries for a range of compounds including caffeine, EDTA, thiourea, methanol, antipyrine and sulfathiazole by use of a column with quartz beads

(same type as tested in this study) in a MQ Scientific DOC instrument. Additional sulfix and CuO was added to the quartz beads by Qian and Mopper [12] to enhance oxidation efficiency and remove sulfur and halogens from the gas stream, but the use of sulfix and CuO was not reported by Qian and Mopper [28]. Possible reasons for the observed differences between our results and Qian and Mopper's work involve the operation of their HTC column at higher temperatures of 700–800°C [12, 28] and the addition of sulfix and CuO to the combustion column [12]. The former explanation is supported by the low recoveries these workers observed for EDTA (65%) and phthalate (85%) when operating the combustion column at lower temperatures (600–640°C) [12]. Our findings suggest that the quartz beads may require higher temperatures and/or that the relatively small amounts of sulfix and CuO are required in addition to the quartz beads for optimal DOC recoveries.

Figure 3(a) and (b) show the results of the recovery experiments for TDN at 8 and 20 μM, respectively, using the metallic catalysts and quartz beads. In addition to the new Shimadzu 0.5% Pt–alumina catalyst, a pre-used Shimadzu catalyst (>4000 injections) was used in these experiments (no other pre-used catalysts materials were available). Similar trends in recovery efficiencies for the different nitrogen containing compounds using the metallic catalysts and quartz beads were observed using concentrations of 8 μM N and 20 μM N. The recoveries for all compounds were typically >90%, and the new (less than 500 injections) Shimadzu 0.5% Pt–alumina catalyst yielded the best results, corresponding with findings by Alvarez-Salgado and Miller [22]. $NaNO_2$ and ammonia showed low recoveries in a number of experiments. The recoveries for $NaNO_2$ were <92% for all materials investigated. Furthermore, using the 13% CuO–alumina, 0.5% Pd–alumina catalysts, and quartz beads, the recoveries for NH_4Cl were also low.

The conversion of NO_2^- (oxidation state +3) and NO_3^- (+5) on metallic catalysts to N_2 (0), N_2O (+1) and NO_2 (+4) has been reported by Morrison [29]. These compounds will not be detected by the NCD following the ozonation step. Indeed, the conversion of NO_2^- to NO_2 constitutes an oxidation process, and this process may occur in the combustion column instead of reduction to NO. The observed low recovery of nitrite may therefore be inherent to the HTC method for particular metallic catalysts. The Shimadzu 0.5% Pt–alumina catalyst showed the best recovery for nitrite (92% at 8 μM N and 88% at 20 μM N), which is in reasonable agreement with findings (101% for 25 μM N) by Alvarez-Salgado and Miller [22].

The low recovery for NH_4Cl (77% at 8 μM N and 76% at 20 μM N) using the CuO catalyst can be explained by the oxidation of ammonia to N_2O as well as NO on the surface of the CuO catalyst [30]. In contrast, ammonia is chiefly oxidized to NO at high temperatures on the surface of Pt catalysts [30]. A possible explanation for the low recovery of NH_4Cl using quartz beads (24% at 8 μM N and 28% at 20 μM N) is the production of N_2 and/or N_2O rather than NO during the oxidation of NH_4Cl [30], and the same mechanism may explain the lower NH_4Cl recoveries using the Pd catalyst.

The experiments using the pre-used (>4000 injections) Shimadzu 0.5% Pt–alumina catalyst indicated lower recoveries of NO_2^- and NO_3^- compared with the new Shimadzu catalyst (see figure 3a and b). This indicates that the long-term use of the Shimadzu catalyst did not appear to affect the oxidation efficiency of ammonia and organic nitrogen compounds to NO, but that catalyst de-activation occurred with respect to the reduction efficiency of NO_2^- and NO_3^- to NO. Therefore, it is important to undertake regular DOC and TDN recovery experiments before commencing seawater analysis and to replace the catalyst when recovery efficiencies decrease.

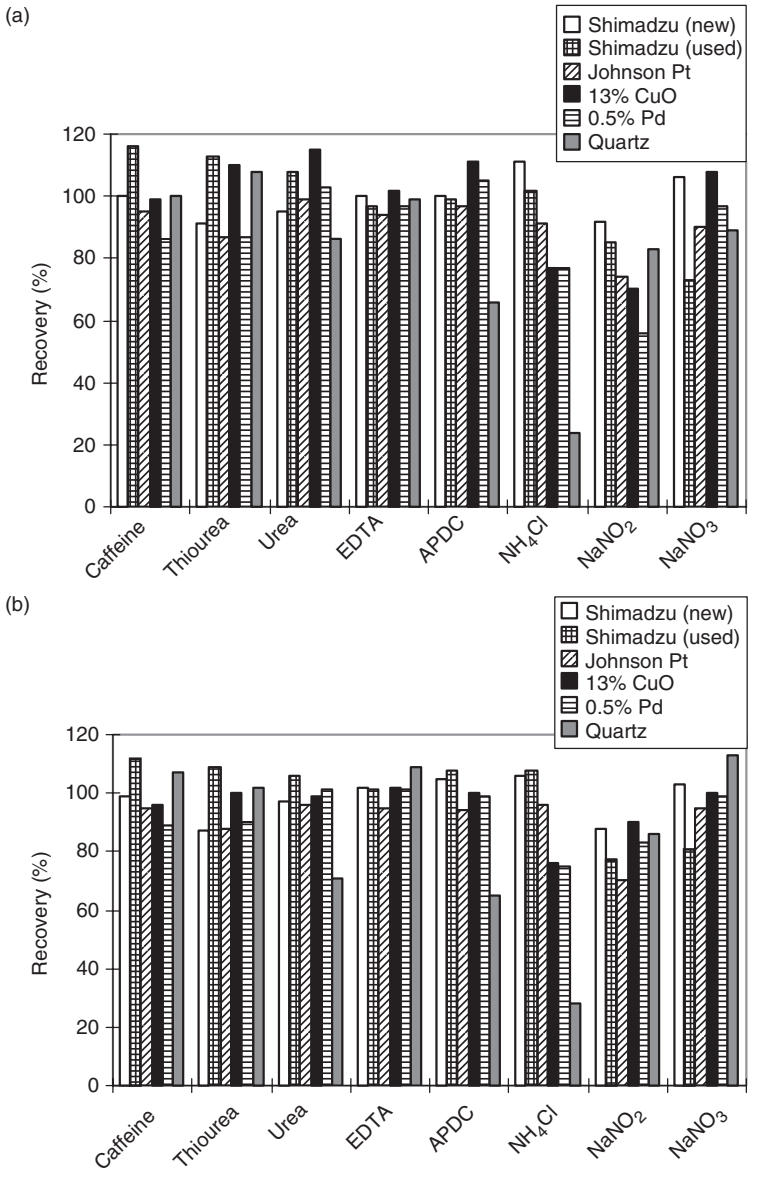

Figure 3. Results of recovery experiments for TDN at 8 μM N (a) and 20 μM N (b) concentrations of model compounds.

4. Conclusions

The HTC technique using a coupled TOC-NCD instrument package is now a widely used approach for DOC and TDN analysis. The coupled TOC-NCD technique allows the simultaneous determination of DOC and TDN in the same sample in a single injection. This approach enhances sample throughput and minimizes the risk of carbon and nitrogen contamination. A range of different materials, including metallic catalysts

and quartz beads, are used in the HTC technique to enhance the conversion efficiency of DOC and TDN to CO_2 and NO, respectively. A systematic investigation into the efficiencies of a range of noble and transition metal catalysts, and quartz beads showed that the 0.5% Pt–alumina beads supplied by Shimadzu constitute the best catalyst for simultaneous DOC-TDN analyses using the Shimadzu TOC 5000A analyser coupled to the Sievers NCD 255. Sub-optimal conversion of NO_2^- to NO by metallic catalysts in general, and NH_4Cl to NO by 13% CuO–alumina and 0.5% Pd–alumina catalysts in particular, can be attributed to alternative reaction pathways on the catalysts surface. Consequently, CuO and Pd are not the most efficient catalysts for DOC-TDN analyses in the Shimadzu-Sievers instrument. The weak performance of the quartz beads in terms of DOC conversion can most likely be attributed to the lower operation temperatures (680°C) of the combustion column in the Shimadzu TOC 5000A, compared with the MQ Scientific instrument. In addition, the quartz beads showed a poor conversion of NH_4Cl which was attributed to the production of N_2 and/or N_2O rather than NO.

Acknowledgements

XP acknowledges support by the University of Southampton, and ESB the support by the University of Mansura.

References

[1] P. Wangersky. *J. Am. Sci.*, **53**, 358 (1965).
[2] D.A. Bronk. In *Biogeochemistry of Marine Dissolved Organic Matter*, D.A. Hansell, C.A. Carlson (Eds), pp. 153–249, Academic Press, Boston, MA (2002).
[3] K. Grasshoff, K. Kremling, M. Ehrhardt (Eds), *Methods of Seawater Analysis*, Wiley-VCH, Weinheim, pp. 632 (1999).
[4] D.W. Menzel, R.F. Vaccaro. *Limnol. Oceanogr.*, **9**, 138 (1964).
[5] M. Pujo-Pay, P. Raimbault. *Mar. Ecol. Progr. Ser.*, **105**, 203 (1994).
[6] P.J. Statham, P.J. le B Williams. In *Methods of Seawater Analysis*, 3rd Edn, K. Grasshoff, K. Kremling, M. Ehrhardt (Eds), pp. 421–436, Wiley-VCH, Weinheim (1999).
[7] Y. Sugimura, Y. Suzuki. *Mar. Chem.*, **24**, 105 (1988).
[8] D.A. Hansell. *Mar. Chem.*, **41**, 195 (1993).
[9] T.W. Walsh. *Mar. Chem.*, **26**, 295 (1989).
[10] J.H. Sharp, K.R. Rinker, K.B. Savidge, J. Abell. *Mar. Chem.*, **78**, 171 (2002).
[11] G. Cauwet. In *Methods of Seawater Analysis*, 3rd Edn, K. Grasshoff, K. Kremling, M. Ehrhardt (Eds), pp. 407–420, Wiley-VCH, Weinheim (1999).
[12] J. Qian, K. Mopper. *Anal. Chem.*, **68**, 3090 (1996).
[13] G. Spyres, M. Nimmo, P.J. Worsfold, E.P. Achterberg, A.E.J. Miller. *Trends Anal. Chem.*, **19**, 498 (2000).
[14] E.A. Badr, E.P. Achterberg, A.D. Tappin, S.J. Hill, C.B. Braungardt. *Trends Anal. Chem.*, **22**, 819 (2003).
[15] J.H. Sharp, A.Y. Beauregardt, D. Burdige, G. Cauwet, S.E. Curless, R. Lauck, K. Nagel, H. Ogawa, A.E. Parker, O. Primm, M. Pujo-Pay, W.B. Savidge, S. Seitzinger, G. Spyres, R. Styles. *Mar. Chem.*, **84**, 181 (2004).
[16] E.V. Dafner, P.J.J. Wangersky. *Environ. Monit.*, **4**, 48 (2002).
[17] R. Prasad, L.A. Kennedy, E. Ruckenstein. *Catal. Rev.-Sci. Eng.*, **26**, 1 (1984).
[18] A. Skoog, D. Thomas, R. Lara, K. Richter. *Mar. Chem.*, **56**, 39 (1997).
[19] W. Chen, Z. Zhao, J. Koprivnjak, E.M. Perdue. *Mar. Chem.*, **78**, 185 (2002).
[20] J.E. Bauer, M.L. Occelli, P.M. Williams, P.C. McCaslin. *Mar. Chem.*, **42**, 95 (1993).

[21] M.L. Peterson, S.Q. Lang, A.K. Aufdenkampe, J.I. Hedges. *Mar. Chem.*, **81**, 89 (2003).
[22] X.A. Alvarez-Salgado, A.E.J. Miller. *Mar. Chem.*, **62**, 325 (1998).
[23] A.A. Amman, T.B. Ruttimann, F. Burgi. *Wat. Res.*, **34**, 3573 (2000).
[24] R. Benner, M. Strom. *Mar. Chem.*, **41**, 153 (1993).
[25] Y. Suzuki, E. Tanque, T. Ito. *Deep Sea Res.*, **39**, 185 (1992).
[26] W. Chen, P.J. Wangersky. *Mar. Chem.*, **42**, 95 (1993).
[27] G. Aiken, L.A. Kaplan, J. Weishaar. *J. Environ. Monit.*, **4**, 70 (2002).
[28] J. Qian, K. Mopper. 2000. Automated, high precision total inorganic carbon (TIC) and volatile organic carbon (VOC) measurement using a commercial TOC analyzer with a built-in FID. Available from http://mqscientific.com/mqpost00.htm (accessed 3 February 2003).
[29] S.R. Morrison (Ed.). *The Chemical Physics of Surfaces*, Plenum Press, New York (1977).
[30] P.G. Ashmore (Ed.). *Catalysis and Inhibition of Chemical Reactions*, Butterworth, London (1963).